

Title of thesis

**Dynamic analysis for normal and inclined tether Tension
Leg Platforms**

I, MOHAMMED ABUELGASIM ABBASS MOHIELDEEN

Hereby allow my thesis to be placed at the Information Resources Center (IRC) of Universiti Teknologi PETRONAS (UTP) with the following conditions:

1. The thesis becomes the property of UTP.
2. The IRC of UTP may make copies of the thesis for academic purposes only.
3. This thesis is classified as

Confidential

Non – confidential

If this thesis is confidential, please state the reason:

The contents of this thesis will remain confidential for _____ years.

Remarks on disclosure:

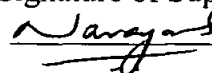
Endorsed by



Signature of Author
Permanent Address:
Home No.599, Salalab North,
Port-Sudan, Red Sea State,
Sudan.



Signature of Supervisor



Signature of Co-Supervisor

Date: 23-10-2008

Date: 23-10-2008

UNIVERSITI TEKNOLOGI PETRONAS

Approval by supervisor(s)

The under signed certify that they have read, and recommend to the postgraduate studies programme for acceptance, a thesis entitled

Dynamic analysis for normal and inclined tether Tension
Leg Platforms

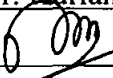
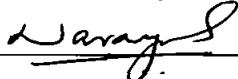
Submitted by

Mohammed Abuelgasim Abbass Mohieldeen

For the fulfillment of the requirements for the degree of
Masters of Science in Civil Engineering

22-10-2008

Date

Main supervisor : AP. Dr. Kurian V. John
Signature : 
Co-Supervisor : AP. Dr. Narayanan Sambu Potty
Signature : 
Date : 22-10-2008

UNIVERSITI TEKNOLOGI PETRONAS

Dynamic analysis for normal and inclined tether Tension

Leg Platforms

By

Mohammed Abuelgasim Abbass Mohieldeen

A THESIS

SUBMITTED TO THE POSTGRADUATE STUDIES PROGRAMME

AS A REQUIREMENT FOR THE

DEGREE OF MASTERS OF SCIENCE IN CIVIL

ENGINEERING

Civil Engineering

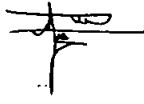
BANDAR SERI ISKANDAR,

PERAK

September, 2008

DECLARATION

I hereby declare that the thesis is based on my original work except for quotations and citations which have been duly acknowledged. I also declare that it has not been previously or concurrently submitted for any other degree at UTP or other institutions.

Signature:  _____

Name : Mohammed Abuelgasim Abbass Mohieldeen

Date : 22 - 10 - 2008

ACKNOWLEDGEMENT

- ✎ All thanks and praises for GOD first, under whose provision and blessing this work was carried out.
- ✎ To my supervisor Assoc. Prof. Dr. Kurian V. John for his expert guidance, valuable advice, help and encouragement.
- ✎ To Assoc. Prof. Dr. Narayanan Sambu Potty for his help and advice.
- ✎ To my parents and family members for their support and encouragement.
- ✎ To all members of Civil Engineering Department and Post graduate office for their valuable help.
- ✎ To my friends and colleagues for their support, help and for the joyful environment that they continuously provided.
- ✎ For others who helped directly or indirectly.

ABSTRACT

Tension leg platform (TLP) is a type of compliant offshore structure where its excess buoyancy over the weight produces pretension in the tethers connecting the hull to the seabed. TLP technology preserves many of the operational advantages of a fixed platform at the same time reducing the cost of production in deep water. Its production and maintenance operations are similar to those of fixed platforms. TLP combines the initial cost-saving benefits associated with floating production system with the operational benefits attributed to the fixed platforms.

The dynamic responses of TLP such as the motions and the tether tensions when it is subjected to wave forces are needed for the design and maintenance of the structure. The amplitudes of motion responses must be within permissible limits to prevent flexural yielding of the drilling risers which connect the platform to the sea bed completion template. Limiting these responses leads to better stability and safe drilling operations.

In this study, a MATLAB computer program was developed for determining the dynamic responses of rectangular, triangular and inclined-tether TLPs subjected to random waves. The platform was considered as a rigid body and all the six motions were determined. The hydrodynamic drag and inertia coefficients at each point on the platform were revised after each time step. Second order wave theory and Modified Morison equation were used for wave force calculations. Newmark Beta Method of time domain analysis was used for the dynamic analysis. The response amplitude operators (RAO) for typical square TLPs were compared with available theoretical results. The inclined-tether stiffness matrix was developed, using which the responses of inclined tether square TLP under regular and random waves were determined. Also, parametric studies were made varying parameters such as water depth, pretension, wave angle and position of CG. The inclined-tether square TLP results were compared with the results for the square and triangular TLPs. The results proved the capability of the developed programme in predicting the responses. The results also indicated that the square TLPs performed much better compared to triangular TLPs under random waves. The parametric studies

highlighted the remarkable change in platform responses caused by changing the above mentioned parameters. It was also shown that the inclined-tether square TLP had better performance compared with vertical-tethered rectangular and triangular TLPs.

ABSTRAK

Pelantar Kaki Tegang atau lebih dikenali sebagai *Tension Leg Platform (TLP)* adalah sejenis struktur pelantar luar pantai yang berhemah dimana apungan lebih berbanding berat menghasilkan daya pra-tegangan pada kabel sokongnya (*tether*) yang menghubungkan pelantar ke permukaan tanah dasar laut. Teknologi *TLP* menyimpan kebanyakan kelebihan operasi pelantar tetap pada masa yang sama mengurangkan kos pengeluaran dilaut dalam. Operasi pengeluaran dan penyelenggaraannya sama dengan pelantar tetap. *TLP* menggabungkan keuntungan penjimatan kos permulaan yang berkaitan dengan sistem pengeluaran apungan dengan keuntungan operasi yang diberikan oleh pelantar tetap.

Tindakbalas Dinamik *TLP* seperti pergerakan dan tegangan pada *tether* bila dikenakan daya ombak adalah diperlukan untuk rekabentuk dan penyelenggaraan struktur ini. Amplitud tindakbalas pergerakan mestilah didalam had yang dibenarkan untuk mengelakkan alahan fleksur (*flexural yielding*) pada paip gerudi yang menegak yang menghubungkan pelantar dengan struktur tetap didasar laut. Menghadkan tindakbalas ini meningkatkan kestabilan dan operasi gerudian yang selamat.

Dalam kajian ini, perisian komputer *MATLAB* telah diusahakan untuk menentukan tindakbalas dinamik bagi *TLP* yang berbentuk segiempat, segitiga dan yang mempunyai *tether* yang condong; yang dikenakan ombak tidak menentu (*random waves*). Andaian telah dibuat bahawa pelantar sebagai sebuah jasad tegar dan kesemua enam jenis pergerakan adalah telah ditentukan. Geseran dinamik hidro dan pemalar momen sifat tekun jasad disetiap titik pada pelantar telah dikaji semula selepas setiap langkah masa. Teori Ombak Peringkat Kedua dan Persamaan Morison yang diubahsuai digunakan untuk mengira daya ombak. Kaedah Beta Newmark dari analisa domain masa telah digunakan untuk analisa dinamik. Operator Amplitud Tindakbalas (RAO) untuk *TLP* segiempat sama dan segitiga telah dibandingkan dengan keputusan teori yang sedia ada. Matrik kekukuhan *tether* condong dapat dihasilkan. Dengan menggunakan hasil keputusan, tindakbalas *tether* condong *TLP* segiempat sama dengan menggunakan ombak biasa dan ombak tidak menentu diperolehi. Juga, kajian parametrik telah dibuat dengan mengubah parameter

seperti kedalaman air, pra-tegangan, sudut ombak, dan kedudukan pusat gravitasi. Keputusan *TLP* segiempat sama bagi tether condong telah dibandingkan dengan keputusan bagi *TLP* segiempat sama dan segitiga. Keputusannya menunjukkan kemampuan program yang dihasilkan dalam menjangkakan tindakbalasnya. Keputusan juga telah menunjukkan bahawa *TLP* segiempat sama berfungsi dengan lebih baik berbanding *TLP* segitiga dibawah ombak yang tidak menentu. Kajian parametrik menjelaskan perubahan yang ketara di dalam tindakbalas pelantar apabila parameter-parameter seperti di atas diubah. Jelas juga bahawa *TLP* segiempat sama dengan *tether* condong berfungsi dengan lebih baik berbanding *TLP* segiempat tepat dan segitiga dengan *tether* menegak.

TABLE OF CONTENT

STATUS OF THESIS.....	i
APPROVAL PAGE.....	ii
TITLE PAGE.....	iii
DECLARATION.....	iv
ACKNOWLEDGEMENT.....	v
ABSTRACT.....	vi
ABSTRAK.....	viii
TABLE OF CONTENT.....	x
LIST OF TABLES.....	xiii
LIST OF FIGURES.....	xiv
NOMENCLATURE.....	xviii
CHAPTER ONE.....	1
1 INTRODUCTION.....	1
1.1 Background.....	1
1.2 Offshore platform development.....	1
1.3 Offshore Structure Configurations.....	2
1.4 Tension Leg Platform (TLP).....	2
1.4.1 TLP origin and growth.....	3
1.4.2 Basic features of TLPs.....	4
1.4.3 Hull Requirements.....	5
1.4.4 Deck support functional requirements.....	5
1.4.5 Mooring system.....	5
1.4.6 Construction of platform.....	6
1.4.7 TLP designs for different water depths.....	6
1.4.8 Installation of TLPs.....	6
1.5 Problem statement.....	7
1.6 Objectives of the study.....	8
1.7 Scope of study.....	8
CHAPTER TWO.....	9
2 LITERATURE REVIEW.....	9
2.1 Introduction.....	9
2.2 TLP Types and Configurations.....	9

2.3	Behavior of TLPs.....	12
2.4	Wave theories.....	13
2.4.1	Airy’s linear wave theory.....	13
2.4.2	Stokes Second-Order theory	14
2.5	Wave spectrum.....	15
2.6	Frequency domain analysis.....	16
2.7	Review of the literature.....	17
2.7.1	Platform behaviour.....	17
2.7.2	Environmental forces on the platform	20
2.7.3	Parameters affecting TLPs behavior	21
2.7.4	Different shapes of TLP	23
2.7.5	TLPs tethers system	25
2.8	Summary of the literature	28
CHAPTER THREE		30
3	RESEARCH METHODOLOGY.....	30
3.1	Introduction.....	30
3.2	Wave Force calculations	30
3.2.1	Morison equation	31
3.3	Mass matrix.....	41
3.4	Stiffness matrix	42
3.4.1	Rectangular TLP	43
3.4.2	Triangular TLP.....	46
3.4.3	Inclined tether square TLP.....	50
3.5	Equation of motion	61
3.6	Newmark beta method	62
3.7	Solution procedure	63
CHAPTER FOUR.....		65
4	RESULTS AND DISCUSSIONS.....	65
4.1	Introduction.....	65
4.2	Selected data	65
4.3	Discussion of the results	66
4.3.1	Square TLPs.....	66

4.3.2	Triangular TLP.....	81
4.3.3	Inclined tether TLP	94
CHAPTER FIVE		106
5	CONCLUSIONS AND FURTHER STUDIES	106
5.1	Introduction.....	106
5.2	Conclusions.....	106
5.3	Further studies.....	108
REFERENSES.....		109
Publications from the work.....		115
Appendices.....		116

LIST OF TABLES

Table 1.1: Existing Tension leg platforms.....	4
Table 2.1: Linear wave theory formulae.....	16
Table 2.2: Second-order wave theory formulae.....	17
Table 4.1: Platforms details	66
Table 4.2: RAOs for various Tension leg Platform	105
Table A-1: RAOs for square TLP.....	117
Table A-2: RAOs for triangular TLP.....	117
Table A-3. RAOs for inclined tether TLP.....	118

LIST OF FIGURES

Figure 1.1: Cost effectiveness comparison for deep water platforms.....	3
Figure 2.1 : Components of TLP	10
Figure 2.2: Square and Triangular TLPs.....	11
Figure 2.3: Sea Star and Moses TLP	11
Figure 2.4: Rectangular and Triangular ETLT	12
Figure 2.5: Parameters of wave	14
Figure 2.6: Range of suitability of various wave theories [?]......	15
Figure 3.1: Square TLP pontoon elements	33
Figure 3.2: Triangular TLP pontoon elements.....	36
Figure 3.3: Inclined tethers TLP	51
Figure 3.4: Surge motion	55
Figure 3.5: Heave motion	56
Figure 3.6: Roll motion.....	58
Figure 3.7: Yaw motion.....	60
Figure 3.8: Program flow chart.....	64
Figure 4.1: P-M spectrum	67
Figure 4.2: RAO surg.....	68
Figure 4.3: RAO heave.....	68
Figure 4.4: RAO pitch.....	68
Figure 4.5: RAO tether tension.....	68
Figure 4.6: Surge spectrum.....	69
Figure 4.7: Heave spectrum	69
Figure 4.8: Pitch spectrum.....	69
Figure 4.9: Tension spectrum	69
Figure 4.10: Surge response.....	71
Figure 4.11: Heave response.....	71
Figure 4.12: Pitch response.....	71
Figure 4.13: Tether tension	71
Figure 4.14: Surge responses in regular wave	72
Figure 4.15: Sway responses in regular wave.....	72

Figure 4.16: Heave responses in regular wave	72
Figure 4.17: Roll responses in regular wave.....	73
Figure 4.18: Pitch responses in regular wave	73
Figure 4.19: Yaw responses in regular wave	73
Figure 4.20: RAO Surge in time domain for TLP ₂	75
Figure 4.21: RAO Heave in time domain for TLP ₂	75
Figure 4.22: RAO Pitch in time domain for TLP ₂	75
Figure 4.23: RAO tension in time domain for TLP ₂	75
Figure 4.24: Surge response in time domain for TLP ₂	76
Figure 4.25: Heave response in time domain for TLP ₂	76
Figure 4.26: Pitch response in time domain for TLP ₂	76
Figure 4.27: Tether tension in time domain for TLP	76
Figure 4.28: Results validation for surge and tether tension	77
Figure 4.29: RAO surge for TD and FD.....	79
Figure 4.30: RAO heave for TD and FD	79
Figure 4.31: RAO pitch for TD and FD.....	79
Figure 4.32: RAO tension for TD and FD	79
Figure 4.33: RAO surge for different depths	82
Figure 4.34: RAO heave for different depths	82
Figure 4.35: RAO pitch for different depths.....	82
Figure 4.36: RAO surge for different pretension.....	83
Figure 4.37: RAO heave for different pretension	83
Figure 4.38: RAO pitch for different pretension	83
Figure 4.39: RAO surge for different CG position.....	84
Figure 4.40: RAO heave for different CG position	84
Figure 4.41: RAO pitch for different CG position.....	84
Figure 4.42: RAO surge for different wave angle	85
Figure 4.43: RAO sway for different wave angle.....	85
Figure 4.44: RAO heave for different wave angle.....	85
Figure 4.45: RAO roll for different wave angle	86
Figure 4.46: RAO pitch for different wave angle.....	86
Figure 4.47: RAO yaw for different wave angle	86

Figure 4.48: RAO surge for different hydrodynamic approximations	87
Figure 4.49: RAO heave for different hydrodynamic approximations.....	87
Figure 4.50: RAO pitch for different hydrodynamic approximations	87
Figure 4.51: RAO surge for triangular TLP.....	89
Figure 4.52: RAO heave for triangular TLP.....	89
Figure 4.53: RAO pitch for triangular TLP.....	89
Figure 4.54: RAO tension for triangular TLP.....	89
Figure 4.55: Triangular surge response.....	90
Figure 4.56: Triangular heave response.....	90
Figure 4.57: Triangular pitch response.....	90
Figure 4.58: Triangular tether tension	90
Figure 4.59: RAO surge for TLP ₂ and TLP ₃	93
Figure 4.60: RAO heave for TLP ₂ and TLP ₃	93
Figure 4.61: RAO pitch for TLP ₂ and TLP ₃	93
Figure 4.62: RAO tension for TLP ₂ and TLP ₃	93
Figure 4.63: Triangular RAO surge for different depths	95
Figure 4.64: Triangular RAO heave for different depths	95
Figure 4.65: Triangular RAO pitch for different depths.....	95
Figure 4.66: Triangular RAO surge for different pretension.....	96
Figure 4.67: Triangular RAO heave for different pretension	96
Figure 4.68: Triangular RAO pitch for different pretension.....	96
Figure 4.69: Triangular RAO surge for different CG position	97
Figure 4.70: Triangular RAO heave for different CG position	97
Figure 4.71: Triangular RAO pitch for different CG position.....	97
Figure 4.72: Triangular RAO surge for different wave angle	98
Figure 4.73: Triangular RAO sway for different wave angle.....	98
Figure 4.74: Triangular RAO heave for different wave angle.....	98
Figure 4.75: Triangular RAO roll for different wave angle.....	99
Figure 4.76: Triangular RAO pitch for different wave angle	99
Figure 4.77: Triangular RAO yaw for different wave angle	99
Figure 4.78: RAO surge for inclined TLP.....	101
Figure 4.79: RAO heave for inclined TLP.....	101

Figure 4.80: RAO pitch for inclined TLP.....	101
Figure 4.81: RAO tension for inclined TLP	101
Figure 4.82: Surge response for TLP ₄	102
Figure 4.83: Heave response for TLP ₄	102
Figure 4.84: Pitch response for TLP ₄	102
Figure 4.85: Tether tension for TLP ₄	102
Figure 4.86: RAO surge for various types of TLPs	103
Figure 4.87: RAO heave for various types of TLPs	103
Figure 4.88: RAO pitch for various types of TLPs.....	104
Figure 4.89: RAO tension for various types of TLPs.....	105
Figure A-1: KC and Drag coefficient relationship.....	116
Figure A-2: KC and Inertia coefficient relationship.....	116

NOMENCLATURE

A	cross sectional area of tethers.
A_D	area of drag.
A_I	area of inertia.
a, b	half the center to center distance between columns in surge and sway directions.
a_{sx}	structure acceleration in x direction.
a_{sy}	structure acceleration in y direction.
a_{sz}	structure acceleration in z direction.
a_x	wave acceleration in horizontal direction.
a_z	wave acceleration in vertical direction.
C	total damping matrix, structural + hydrodynamic damping.
C_D	drag coefficient.
C_h	hydrodynamic damping matrix.
C_M	inertia coefficient.
C_{MP}	pontoon inertia coefficient.
C_s	structural damping matrix.
C_x, C_y, C_z	direction cosines of the element axis.
d	water depth.
D_c	column diameter.
D_p	equivalent pontoon diameter.
d_r	platform draught.
e	eccentricity of buoyancy force position from the center of gravity.
\tilde{F}	effective loading matrix.
$F(t)_i$	total wave force in i th column or pontoon.
F_b	buoyancy force.
F_i	inertia force.
f	wave frequency.
f_x, f_y, f_z	force per unit length of the cylinder in x, y and z direction.
F_{xn}	total force on a column along x axis.
F_{yn}	total force on a column along y axis.
F_{zn}	total force on a column along z axis.
ΔF_b	change in buoyancy force.
g	gravity acceleration.
G_i	axial stiffness per tether = AE/l .
H	wave height.
H_s	significant wave height.
h	time step duration.
h_c	distance from center of gravity (CG) to keel.
H_s	significant wave height.
I_{44}, I_{55}, I_{66}	mass moment of inertia in roll, pitch and yaw degrees of freedom.
\tilde{K}	effective stiffness matrix.
K	stiffness matrix.
k	wave number.
L	wave length.
l	distance from the seabed to the bottom end of the platform (tether length).

l_o	original length of inclined tether.
L_o	deep water wave length.
M	mass matrix.
M_a	added mass matrix.
N	number of pontoon elements.
n	pontoon element's number.
P_1 to P_6	change in pretension due to the displacement in the six degrees of freedom x_1 to x_6 respectively.
P_l	length of the triangular platform.
P_o	initial pretension per tether.
P_{ot}	total pretension.
r_x, r_y, r_z	radius of gyration about x, y, z axes.
s	vertical distance from the seabed.
s_p	height of pontoon axis from the seabed.
t	the time.
T	wave period.
u	wave velocity in horizontal direction.
u_{rel}	real velocity which is equal wave velocity minus structure velocity.
u_s	structure velocity.
u_{sx}	structure velocity in x direction.
u_{sz}	structure velocity in z direction.
u_{zy}	structure velocity in y direction.
v	wave velocity in vertical direction.
W	platform weight.
w_i	normal water particle velocity.
x_1 to x_6	arbitrary displacements in the six degrees of freedom.
x_i	the distance between element and wave propagation line.
x_{so}, u_{so}, a_{so}	initial structure motion, velocity and acceleration.

GREEK SYMBOLS

α	wave angle with x axis.
γ_1, γ_2	the angle between inclined tethers with the vertical z axis for back and front tethers respectively.
γ_{ij}	the inclination of tether in i group due to displacement in j degree of freedom.
η	wave profile.
ξ	damping ratio.
ρ	water density.
ω	wave frequency.

CHAPTER ONE

INTRODUCTION

1.1 Background

The last three decades showed tremendous increase in the demand of hydrocarbon products, which necessitated increased efforts in exploring and producing oil, especially in deep water. As there is about 72 % water and 28 % of the dry land on the earth, therefore the future of the hydrocarbon is going to be in offshore, especially in deep water. Deep water reservoirs present new challenges for the structures due to its harsh environment, therefore innovative structures and modifications have to be proposed to optimize the stability of the structures, safety of the drilling operation and cost effectiveness of the project.

1.2 Offshore platform development

The offshore exploration of oil dates back to the nineteenth century. The first offshore oil wells were drilled from piers extending into the water at Summerland, California during the 1890's. However, the first offshore oil platform was built in Louisiana in 1947 that stood 7 m water depth in the Gulf of Mexico. Since the installation of the first platform in the Gulf of Mexico about 61 years ago, the offshore industry has seen many innovative structures placed in deeper waters and more hostile environments [1]. The depth of water extended to 2133 m in 2005 with BP Atlantis project. Lately in 2007, Independence Hub production platform was installed in the Mississippi canyon area in the eastern Gulf of Mexico in more than 2439 m deep water. There will undoubtedly be a progression into further deeper waters in the future.

An offshore structure (OS) may be defined as one which has no fixed access to dry land and which is required to stay in position in all weather conditions. While major offshore structures support the exploration and production of oil and gas from beneath the sea floor, other major structures such as structures designed to derive power from the sea are also developed. Offshore structures are typically built of steel, concrete or combination of them, commonly referred to as hybrid construction. There are two general classes of (OS), fixed and compliant. A structure is considered fixed if it withstands the environmental force on it without substantial displacement or deformation. Compliant structures have two types: one is rigid and floating but connected to the sea floor by some mechanical means, while the other allows large deformation of its members when subjected to waves, wind and current loads [1].

The structures with compliant nature have more advantages in deep water than the fixed platform. Tension leg platform became one of the most important choices for deep-water production in the Gulf of Mexico in the last ten years [2].

1.3 Offshore Structure Configurations

Offshore structure may be defined as being either bottom-supported or floating. Bottom supported structures are either fixed such as jackets and gravity base structures, or compliant such as the guyed tower and the compliant tower. Floating structures are compliant by nature. They can be viewed either as “neutrally buoyant”, such as the semi-submersible-based, ship-shaped and Mono-column spar, or “positively buoyant”, such as the tension leg platform (TLP).

1.4 Tension Leg Platform (TLP)

The tension leg platform is one of the most promising compliant structural concepts among different structural systems being considered for deep water applications. Unlike conventional platforms which resist environmental loads by their

stiffness, the TLP is compliant in nature and has lower natural frequency in the horizontal plane that precludes resonance at the dominant wave frequency [3]. However, this particular character presents new problems because the compliant structures become more sensitive to the low frequency component of hydrodynamic loads. The cost curves for fixed offshore structures will raise more rapidly than the TLP in deep water reservoir, because for a TLP, only the cost of mooring system and its installation increases as the water depth increase. Figure 1.1 depicts the relation between the cost and the water depth for various offshore structures. It clearly shows that the cost of TLP is less in deep water [4].

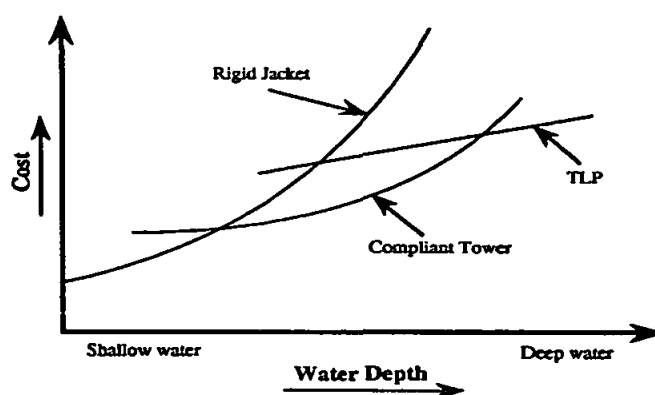


Figure 1.1: Cost effectiveness comparison for deep water platforms

1.4.1 TLP origin and growth

The first TLP, Conoco's Hutton platform in the UK North Sea, was installed in 1984 in approximately 150 m of water. Since that date about two decades ago, the TLP has seen many developed structures placed in deeper water and more hostile environments up to third quarter of 2004 when ABB has designed a TLP for nearly 1500 m of water for Conoco's Magnolia project in the Gulf of Mexico (GOM). This is considered as deepest TLP so far. Table 1.1 shows some of the existing TLPs in deep water. The accelerating rate of industry acceptance of the TLP is very much linked to the concept's rapid growth in technology. For example, specific design enhancements have allowed the concept to carry heavier payloads into deeper water [5].

Table 1.1: Existing Tension leg platforms

S.N.	TLP Name	Location	Water depth	Year	Notes
1	Hutton	North sea, UK	148 m	1984	First TLP removed in 2001
2	Jolliet	Green Canyon, GOM	335 m	1989	First deep water well head TLP
3	Snorre	Norwegian North sea	310 m	1992	
4	Auger	Garden Banks, GOM	872 m	1994	
5	Heidrun	Norwegian North sea	350 m	1995	First concrete TLP
6	Maras	Mississippi Canyon	894 m	1996	
7	Ram/Powell	Viosca Knoll, GOM	980 m	1997	
8	Morpeth	Gulf of Mexico	532 m	1998	
9	Uras	Mississippi Canyon	1204 m	1999	Largest TLP in GOM
10	Marlin	Gulf of Mexico	1012 m	1999	
11	Allegheny	Gulf of Mexico	1030 m	1999	
12	Brutus	Green Canyon, GOM	914 m	2001	
13	Prince	Gulf of Mexico	469 m	2001	
14	Typhoon	Gulf of Mexico	659 m	2001	
15	Matterhorn	Gulf of Mexico	891 m	2003	
16	Marco Polo	Gulf of Mexico	1350 m	2004	
17	Magnolia	ABB, Gulf of Mexico	1500 m	2004	Deepest TLP

1.4.2 Basic features of TLPs

TLP is a type of compliant platform since it carries a lot of similarities in concepts except for tether system and foundation techniques. The platform is supported by extra buoyancy which provide a positive tension in the tether system and produce a tension in the pile foundation system. This positive tension restricts the motion of the platform in the vertical direction (heave, roll and pitch) and minimizes the horizontal motion (surge, sway and yaw) by its horizontal component. Amplitudes of motion are kept sufficiently small to prevent flexural yielding of the drilling risers which connect the platform to the sea bed completion template [6].

1.4.3 Hull Requirements

The principal function of the hull is to provide the buoyancy to support the weight, most of which is in the deck load. A considerable amount of the buoyancy is devoted for developing tendon tension. It should be noted that the hull is also required to support the deck above the highest wave. In addition to providing buoyancy, the principal function of the pontoons is to provide a vertical hydrodynamic force (heave) to balance the hydrodynamic force on the column bottoms. For multi-column TLPs, the pontoons also have a structural function as part of a space frame consisting of the deck, columns and the pontoons. The height of the columns should be sufficient to support the deck with adequate clearance above the highest waves taking into account maximum set-down [1].

1.4.4 Deck support functional requirements

The deck supports the functional requirements. It has to provide space for accommodation, working area, processing equipments, derricks, cranes, pumps, helideck, control room, etc. Like all other compliant platforms, TLP's deck provide the above requirements but with different layout and hook-up procedure. It should be kept in mind that the TLP is sensitive to payload increase, directly affecting its displacement requirements [6]. Other factors that can influence the displacement and leg spacing of TLPs are the platform response characteristics, tow-out stability and barge size carrying the deck for mating.

1.4.5 Mooring system

Mooring system design is to make the system compliant enough to avoid excessive forces on the platform, and making it stiff enough to avoid difficulties, such as damage to drilling or production risers, caused by excessive offsets. Unlike other compliant platforms TLPs mooring system is subjected to a considerable pretension that necessitates special design considerations. High-strength materials or composites could also be used as tendons in addition to solid or hollow pipes or wire ropes, especially in

deep waters. Risers and their relevant structural components as vertical tension members can contribute to the station-keeping capability of the mooring system. Both tendon and riser analysis make the proper design of the platform complex [1,6].

1.4.6 Construction of platform

Construction of the platform is done in onshore fabrication yard. The weight and volume of the platform play a major role in the construction procedure and hence optimizing these parameters very much required for saving cost of the platform hull, foundation and mooring system. Heavy weight and large volume could be a hindrance for the platform during the tow-out and delivery operation. As the TLP move into deeper water, these two factors can impose restrictions on the mooring and foundation design. It is significant to note that the platform design is not affected by the field location and water depth [6].

1.4.7 TLP designs for different water depths

TLP design for different water depths is almost same except for tethers whose length increases in deep waters. Increasing water depth decreases tether stiffness which leads to the vertical response frequencies entering the wave frequency range. In this case high modulus material should be used to balance that condition. These and other installation issues make TLP mooring system the most important criteria in the design of TLP in deep waters.

1.4.8 Installation of TLPs

A method and system for attaching a TLP to its tendons use pull-down lines to rapidly submerge the hull to installation draft. This compensates for inherent hull instability during submergence, provides motion arrest and aids in station keeping. The system includes tensioning devices mounted on the TLP, usually one for each tendon. Each tensioning device is equipped with a pull-down line which is connected to the

corresponding tendon. The TLP hull is submerged to lock-off draft by applying tensions to the pull-down lines connected to the top of the tensions, or by a combination of applying tensions to the pull-down lines and ballasting the hull. As the tensioners take in pull-down line, the hull submerges, i.e. the draft increases. After lock-off, high levels of tension in the pull-down lines can be rapidly transferred to the connection sleeves by slacking the pull-down lines, thus allowing the TLP to be made storm-safe much faster than by prior art methods which require de-ballasting to tension the tendons. Along with TLP installation, this method may be used to attach the mooring tendons to the seabed by suspending and lowering the tendons into their foundation receptacle in the seabed [1,6].

1.5 Problem statement

Although the earlier investigations have covered many aspects of the TLP behavior, TLP needs more studies to reach the best possible configuration.

- 1- The calculation of the maximum surge and sway responses are very important as they should be limited to prevent flexural yielding of the drilling risers which connect the platform to the sea bed completion template. Also large values of surge and sway would change water line location on the buoyancy hull which permits waves to strike the deck structure.
- 2- The weight and volume of the platform play a major role in the construction procedure and hence optimization of these parameters is very much required for saving cost of the platform hull, foundation and mooring system.
- 3- In the earlier studies, the hydrodynamic coefficients in the platform were considered either as constant values for the platform or separate constants for columns and pontoons. Variation of the hydrodynamic coefficient at every point of the TLP has not been considered.
- 4- Due to limited literature about the comparisons between frequency and time domain analyses, it is important to conduct this comparison to know the degree of accuracy of the frequency domain compared to the time domain analysis.

- 5- The responses of triangular TLP have been compared with the responses of rectangular TLP under regular waves. The same comparisons have not been done for random waves.

1.6 Objectives of the study

A comprehensive study on triangular, square and inclined tether tension leg platform will be conducted to satisfy the following objectives;

1. To study the effect of varying hydrodynamic coefficients in the behavior of tension leg platform.
2. To improve the behavior of the Tension Leg Platforms by applying the concept of inclined tether TLP after formulating its stiffness matrix.
3. To study the effect of varying parameters like water depth, pretension, position of center of gravity and wave angle on the responses of TLPs.
4. To conduct a dynamic analysis for normal square, triangular and inclined tether TLPs and to find out the difference between their responses.

1.7 Scope of study

1. To develop a computer program (using MATLAB programming) for conducting dynamic analysis in time domain to determine the responses of TLP subjected to regular and random waves
2. To evaluate the degree of accuracy of the frequency domain analysis compared with the time domain analysis.
3. To formulate the wave force equations for the elements of column and pontoons of the square and triangular TLPs.

CHAPTER TWO

LITERATURE REVIEW

2.1 Introduction

Although the Tension Leg Platform is not a new concept, the variations incorporated in the analysis and design of the tension leg platforms have produced great innovative studies and achievements. The estimation of hydrodynamic forces on structural members of TLP is vital for its economic and safe design. Several studies were carried out in last two decades to gain understanding of the TLP structural behavior and determine the effect of several parameters on the dynamic responses and average life time of the structure. In this chapter some of the recorded studies were reported to explain the considerable progress in the TLP behavior and to highlight the significant issues and modifications, which represent most of the researchers' concern. The most important wave theories those are commonly used in the design of offshore structures, have been illustrated in this chapter with their applicability conditions. Finally, summarizing the literature was necessary to support the objectives and approaches of the current study.

2.2 TLP Types and Configurations

A typical TLP hull configuration consists of four vertical columns that can be cylindrical or square in cross section. Rectangular pontoons connect the columns below the water surface. On top of the columns, and integral to the hull, is the structural deck that supports the topsides production facilities, drilling system, production risers, living quarters, etc. Figure 2.1 shows the main components of TLP.

Tension leg platform takes a lot of shapes such as square, triangular, sea star, Moses and Extended Tension Leg Platform (ETLP).

- The classic square TLP consists of a square deck supported on four cylindrical columns, which are provided at each corner and are interconnected at their bottom by four cylindrical pontoons (Figure 2.2 a). The columns are anchored to the seabed by cylindrical steel tendons and fixed in place with templates.

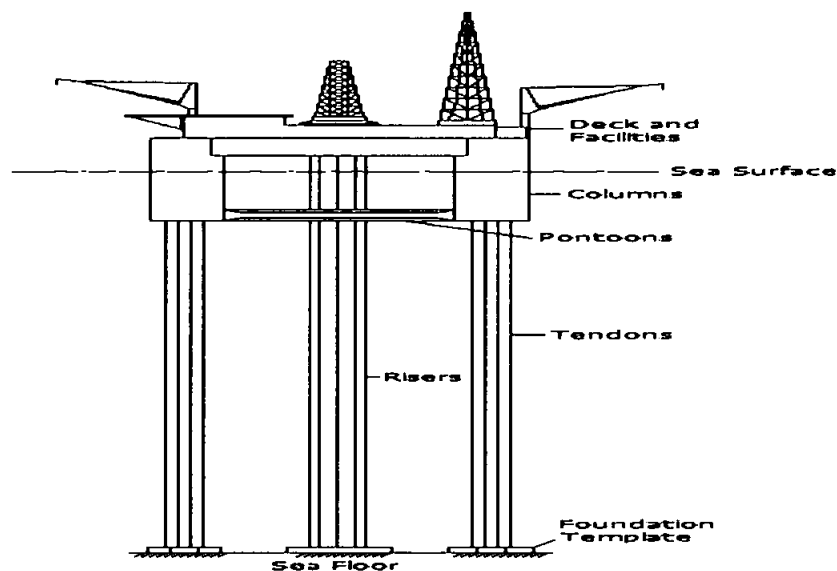


Figure 2.1 : Components of TLP

- The Triangular TLP consists of a triangular deck supported on three cylindrical columns, which are provided at each corner and are interconnected at their bottom by three cylindrical pontoons (Figure 2.2 b). The columns are anchored to the seabed by cylindrical steel tendons and fixed in place with templates.
- Sea star (Mini TLP) is a small TLP with a single surface piercing column. The column is necked down near the sea surface to reduce surface loads on the structure. The submerged hull spreads into three structural members at the bottom in a triangular fashion which are used to support and separate taut tubular steel tendons (Figure 2.3 a). The hull provides sufficient buoyancy to support the

deck, facilities and flexible risers. The excess buoyancy provides tendon pretension.

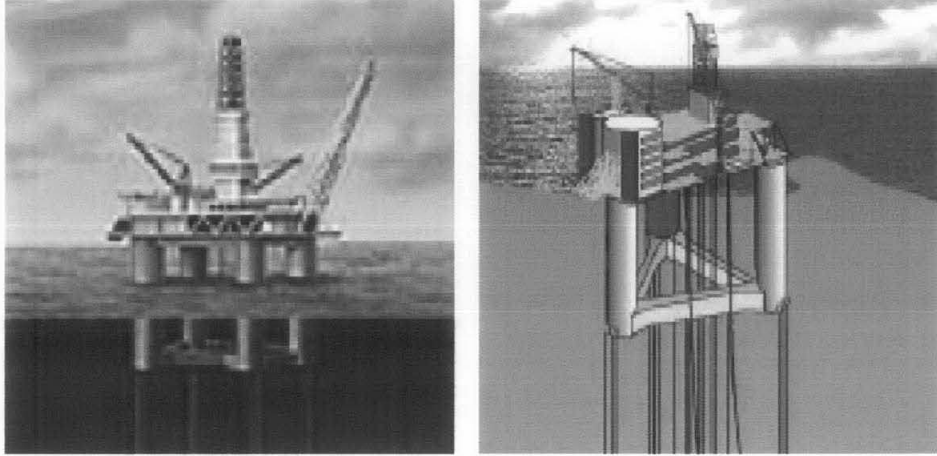


Figure 2.2: Square and Triangular TLPs

- Moses TLP appears to be a miniaturized TLP as the deck structure is supported by four rectangular columns and the columns are connected by pontoons (Figure 2.3 b). Motion characteristics of Moses are similar to that of the sea star [1].



Figure 2.3: Sea Star and Moses TLP

- Extended tension leg platform (ETLP) is a modern configuration of TLPs. The primary difference between a classic TLP and the new ETLP platform is the hull,

form. Previously, tendons were connected to the lowermost outboard portion of the hull on the columns [5]. For the ETLP concept, the columns have been moved inboard allowing a more favorable support condition for the deck and its associated riser and drilling related loads (Figure 2.4). Pontoon extensions on the outboard edge of the column are used as tendon connection points.

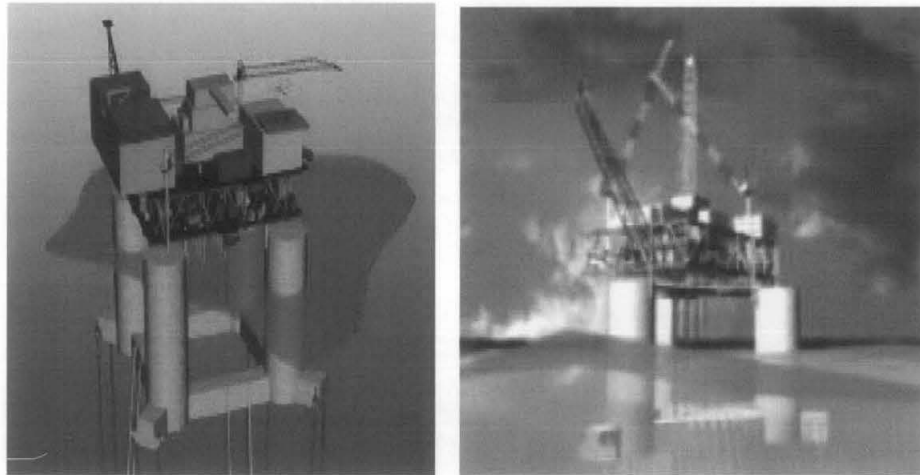


Figure 2.4: Rectangular and Triangular ETLP

2.3 Behavior of TLPs

TLPs can be considered as hybrid structures. The surge, sway and yaw degrees of freedom have very high natural periods of about 80 to 120 second which are well above the periods of dominant waves. On the other hand, TLPs are stiff in the heave, pitch and roll motions with natural periods of about 2 to 5 seconds which are below the periods of the exciting waves. Therefore, TLPs act as compliant structures in the low frequency degrees of freedom [4]. These features, which allow the TLPs to avoid the exciting wave frequency zone, are mainly achieved by the buoyancy exceeding the hull weight. The difference between these forces imposes initial tension forces in the tendons. Such forces ensure that, the tendons are always kept in tension. Also, the tensions in tethers limit the horizontal motion and preclude vertical motion.

2.4 Wave theories

Many wave theories have been developed and applied to evaluate the sea environment for the different sea conditions dependent upon the specific environmental parameters, e.g., water depth, wave height and wave period (Figure 2.5). Each theory has its own assumptions and is applicable only under certain conditions. Airy's linear wave theory and Stokes second-order theory are applicable in the current study. According to the classification in Figure 2.6 which was developed by Dean (1968) and LeMehaute (1970) [7],. In this chapter, only the above mentioned theories and its applications are presented.

2.4.1 Airy's linear wave theory

This wave theory is also known as sinusoidal wave theory or small amplitude wave theory. It is based on the assumption that the wave height is small compared to the wave length or water depth. For the linear wave theory, the wave has the form of a sine curve and the free surface profile is represented by the Equation 2.1:

$$\eta = \frac{H}{2} \cos(kx - \omega t) \quad (2.1)$$

Where, H is the wave height. While the symbol k is the wave number and ω is the wave frequency.

The Equations for Airy's wave theory are listed in Table 2.1 [1,7-9]. The Table includes the kinematics properties of wave like horizontal and vertical particle velocity u and v as well as horizontal and vertical particle acceleration a_x and a_z respectively.

2.4.2 Stokes Second-Order theory

Stokes second-order wave provides two components for the wave kinematics, the first one is the linear part and the second one is the second-order contribution. The second order-component is smaller than the first-order contribution. The two components provide a steeper crest and shallower trough. Steeper waves in the ocean will have a similar form. Therefore, in selecting a regular wave theory in the calculation of response of an offshore structure, the higher wave resulting from large storms require application of second-order theory or higher [1,7]. Table 2.2 shows the relevant formula for the two components

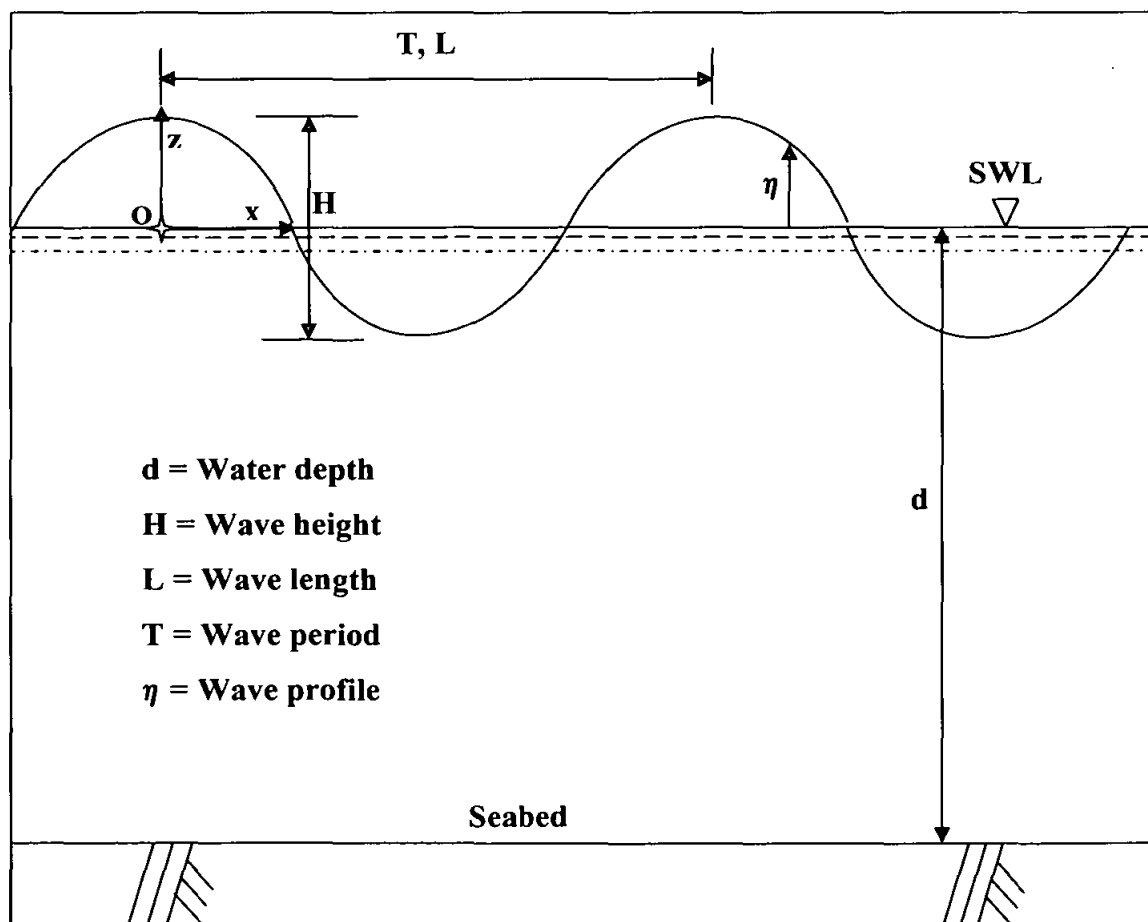


Figure 2.5: Parameters of wave

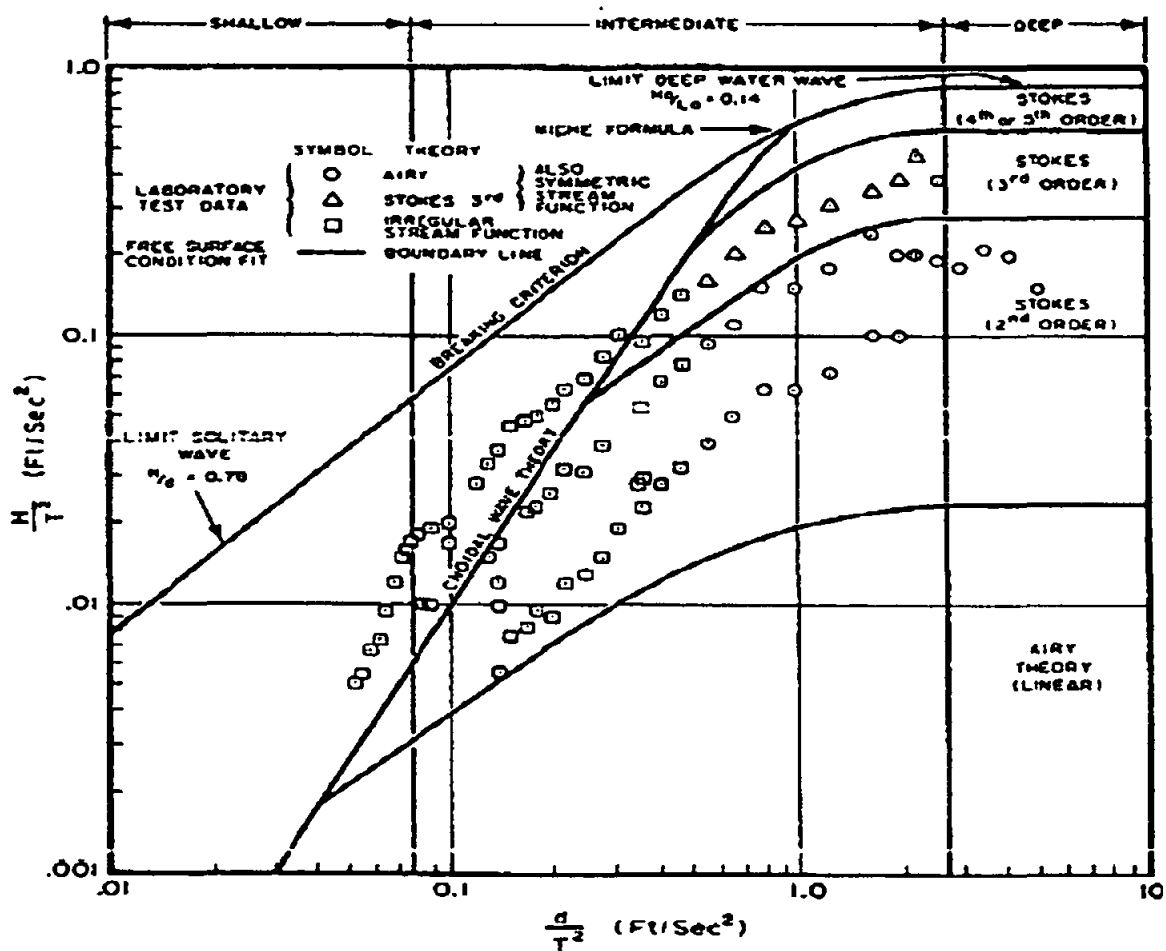


Figure 2.6: Range of suitability of various wave theories [7]

2.5 Wave spectrum

There are two basic approaches in choosing the design wave environment for an offshore structure. One of this uses a single design wave method which considers the platform subjected to regular wave. The other approach takes into consideration an appropriate density distribution of the sea waves at the site by choosing a suitable wave spectrum.

There are many types of wave spectrums used, the most common one is Pierson-Moskowitz (P-M) Spectrum which describes a fully-developed sea condition. The P-M spectrum model (Equation 2.2) has been found to be useful in representing a sever storm wave in offshore structure design [7].

Table 2.1: Linear wave theory formulae

Quantity	Formula
Wave profile	$\eta = \frac{H}{2} \cos(kx - \omega t)$
Horizontal velocity	$u = \frac{\pi H}{T} \frac{\cosh ks}{\sinh kd} \cos(kx - \omega t)$
Vertical velocity	$v = \frac{\pi H}{T} \frac{\sinh ks}{\sinh kd} \sin(kx - \omega t)$
Horizontal acceleration	$a_x = \frac{2\pi^2 H}{T^2} \frac{\cosh ks}{\sinh kd} \sin(kx - \omega t)$
Vertical acceleration	$a_z = -\frac{2\pi^2 H}{T^2} \frac{\sinh ks}{\sinh kd} \cos(kx - \omega t)$

$$S(f) = \frac{\alpha g^2}{(2\pi)^4} f^{-5} \exp\left(-1.25\left(\frac{f}{f_o}\right)^{-4}\right) \quad (2.2)$$

Where $\alpha = 0.0081$, $f_o = \omega_o / 2\pi$ and $\omega_o^2 = 0.161g/H$,

2.6 Frequency domain analysis

The frequency domain is a general approach for evaluating the dynamic responses of the structures, and the amplitude coefficients corresponding to each frequency are determined. The main equations were used to determine the responses in the frequency domain analyses are given as below;

$$RAO_x = \frac{F_i / (H/2)}{\left[(K_i - m_i \omega^2)^2 + (C_i \omega)^2\right]^{1/2}} \quad (2.3)$$

Where RAO_x is the Response Amplitude Operator in a particular direction (x), F_i is the inertia force amplitude which is linear with wave height. K_i is the stiffness where m_i is the

total mass of the system and C_i is the damping coefficient. The subscript i is the particular direction of motion.

$$S_x(f) = RAO_x^2 S(f) \quad (2.4)$$

When $S_x(f)$ response spectral density and $S(f)$ is wave spectral density.

Table 2.2: Second-order wave theory formulae

Quantity	Formula
Wave profile	$\eta = \frac{H}{2} \cos(kx - \omega t) + \frac{\pi H^2}{4L_o} \cos(2(kx - \omega t))$
Horizontal velocity	$u = \frac{\pi H}{T} \frac{\cosh ks}{\sinh kd} \cos(kx - \omega t) + \frac{3}{4} \left(\frac{\pi H}{L} \right) \frac{\pi H}{T} \frac{\cosh 2ks}{\sinh^4 kd} \cos(2(kx - \omega t))$
Vertical velocity	$v = \frac{\pi H}{T} \frac{\sinh ks}{\sinh kd} \sin(kx - \omega t) + \frac{3}{4} \left(\frac{\pi H}{L} \right) \frac{\pi H}{T} \frac{\sinh 2ks}{\sinh^4 kd} \sin(2(kx - \omega t))$
Horizontal acceleration	$a_x = \frac{2\pi^2 H}{T^2} \frac{\cosh ks}{\sinh kd} \sin(kx - \omega t) + \frac{3\pi^2 H}{T^2} \left(\frac{\pi H}{L} \right) \frac{\cosh 2ks}{\sinh^4 kd} \sin(2(kx - \omega t))$
Vertical acceleration	$a_z = -\frac{2\pi^2 H}{T^2} \frac{\sinh ks}{\sinh kd} \cos(kx - \omega t) - \frac{3\pi^2 H}{T^2} \left(\frac{\pi H}{L} \right) \frac{\sinh 2ks}{\sinh^4 kd} \cos(2(kx - \omega t))$

2.7 Review of the literature

There are many factors affecting the design of tension leg platforms. In this review the main concentration was on the behavior of the TLP and its dynamic analysis (time and frequency domain analysis). The hydrodynamic coefficients and some parameters were also presented.

2.7.1 Platform behaviour

The nonlinear coupled response of TLPs to regular wave, presented in Jain (1995) [10], considered the coupling between the degrees of freedom and the nonlinearities produced

due to change in cable tension and drag term. The results showed that the coupling effect leads to sway and yaw motion of the TLP even when the wave force acts in the surge direction due to the coupling of the heave motion with surge, sway and yaw. The author also found that the fluctuations in the tension of the tethers of the TLP could be large due to a possible resonance effect with heave frequency since the heave period of the TLP is normally close to frequently occurring wave periods. Finally he observed that the heave response will be highly underestimated if the coupling effect between various degrees-of-freedom is ignored in the analysis of TLP.

Hsien H. et al (1999) [11] presented the dynamic behavior of both the platform and tether tension in the tension leg platform system when the platform system was subjected to the wave-induced surge motion and the flow-induced drag motion. The study took into account the material property and the dimensional effect for the tether which was incorporated in the tension leg platform in analysis. The scattering problem and radiation problem were first solved separately and then combined together to resolve for all unknowns. The dynamic behavior of the platform and tethers was further solved based on these solutions. It was found that, the dynamic behavior of both the tethers and the platform itself was closely related to the material property and the dimensions of the tethers since the traditional analysis on the tension leg platform system without considering these factors tended to underestimate the vibration amplitude for both the platform and tethers.

M. S. Turnbull et al (2003) [12], presented the wave–structure interaction using coupled structured–unstructured finite element meshes. The interaction of inviscid gravity waves with submerged fixed horizontal structures was modeled in two dimensions using a finite element numerical wave tank. They also conducted a validation test including free and forced sloshing in a rectangular tank, regular progressive wave propagation in a flume, and regular wave loading on a horizontal cylinder. They stated that the experimental results closely agreed with the analytical solutions for waves of small amplitudes. TLPs have to safely withstand frequently occurring environmental forces arising due to wave,

wind, water current, and also those forces arising due to collision of ships with icebergs or any other huge sea creature. Because these forces are less probable in nature, the literature does not address response behavior of TLPs due to these small duration impulsive forces.

Zeng Xiao-hui et al (2007) [13] developed a theoretical model for analyzing the nonlinear behavior of TLP with finite displacement, in which a lot of nonlinearities like finite displacement, coupling of the six degrees of freedom, instantaneous position, instantaneous wet surface, free surface effects and viscous drag force, were taken into account. The comprehensive nonlinear equations were formulated and the nonlinear dynamic analysis of TLP in regular waves was conducted in time domain analysis. The result illustrated that the nonlinearities exerted a significant influence on the dynamic responses of the TLP.

Y.M. Low, R.S. Langley, 2007 [14], conducted a study in time and frequency domain coupled analysis for deepwater floating systems and their aim was to develop and validate a more efficient linearized frequency domain approach. Both time and frequency domain models of a coupled system were developed, which incorporated both first and second order motions. Although their study reflected a good compatibility between the frequency and time domain analysis in the responses prediction, they still preferred using time domain coupled analysis to verify the results at the final design stage.

A Monte Carlo simulation was conducted by A. Naessa *et al* in 2007 [15], to predict the extreme response for nonlinear floating offshore structures subjected to random seas. The first and second order wave frequencies were taken in to account to predict horizontal surge response of a tension leg platform. The study revealed that the commonly assumed obstacle against using the Monte Carlo method for estimating

extreme responses could be circumvented, bringing the computation time down to quite acceptable levels.

2.7.2 Environmental forces on the platform

Ahmad (1996) [16] studied the stochastic TLP response under long crested random sea. The response analysis was based on simulation technique which duly considered various nonlinear effects. Time histories for various results were developed until steady state was achieved. Segments of time histories were statistically analyzed and the salient characteristics such as maximum, minimum, mean and standard deviation were determined for important parametric combination. He stated that, when the sea-state was simulated as long crested, there was no effect of directionality. All the harmonics simulating the random sea were at random phase with respect to time, but not with respect to the direction. The variable submergence was found to be a source of major nonlinearity and significantly enhanced the surge and heave responses, which, in turn introduced tether tension fluctuations.

J.L.B. Carvalho and C.E. Parente (2000) [17], described a directional wave measuring system using a slope array system. The directional wave spectra were determined from direct measurements of sea surface elevation and slopes using resistive wave-staffs were disposed in a square array. The wave meter performance was successfully compared with a pitch-and-roll buoy. Their results showed that the use of resistive wave staffs to determine time series of surface elevation and slope was a promising technique since could develop a good estimation for the directional spectral functions, particularly the angular spreading function, which was difficult to determine in many other systems. More over they considered these equipments as low cost which allowed them to be used for several structures. Finally they recommended some useful improvements and tests for more accurate results.

Tabeshpour et al (2006) [18] studied the nonlinear dynamic analysis of TLP in random sea in both frequency and time domains. The main objective of this work was to develop a comprehensive interpretation of the responses of the structure related to wave excitation and structural characteristics. The hydrodynamic forces were calculated using the modified Morison equation according to Airy's linear wave theory and based on Pierson-Moskowitz spectrum. The power spectral densities (PSDs) of displacements, velocities and accelerations were calculated from nonlinear responses. This kind of analysis was necessary for checking the response of a designed TLP under environmental loads.

The response behavior of triangular TLPs under impact loading was investigated by Chandrasekaran et al (2007) [19]. Two triangular TLP models were selected at different water depths 1200 and 528m. A dynamic analysis was performed under regular wave along with impulse load acting at angle of 45 degrees at the column. Modified Morison equation based on Stokes' fifth order wave theory was used in this work. They stated that impulsive loading acting on corner column of TLP significantly affected its response while that acting on pontoons did not affect TLP behavior. Although the impulsive load was less probable in nature, its effect was significant and should be considered in response analysis.

2.7.3 Parameters affecting TLPs behavior

Chakrabarti (1987) [7] explained that for computing the wave load on the components of offshore structures, a suitable wave theory must be selected based on the wave parameters. The basic parameters that are important in describing wave theories are water depth (d), wave height (H), and wave period (T). The linearity of waves was determined by the wave height or by the wave slope. The structural response calculated based on Airy's theory which is linear with the wave height is quite often straightforward even though the response may not be necessarily linear. He also presented the expressions for the water particle kinematics of the Airy's linear theory for structures located at free surface.

A. Ertas and S. Ekwando-Osire (1991) [20] presented the effect of damping and wave parameters on offshore structure under random excitation. The main target of their study was to investigate the effect of the structural damping and wave parameter on both nonlinear and linear dynamic response of the TLP, then two analysis procedures were applied in this work namely nonlinear time domain and linear frequency domain analysis. For the nonlinear time domain analysis the wave properties were simulated for a given wave spectrum and the responses were obtained by integrating the equation of motion. For the linear frequency domain analysis the nonlinear drag term was linearized by introduction of linearization coefficients. Their results showed that varying the damping ratio did not have any effect on the TLP mean response. They also observed that using linear frequency domain analysis resulted an inaccurate response in case of high damping and low wave energy.

V. Vengatesan *et al*, 2000 [21], performed an experimental study of hydrodynamic coefficients for a vertical truncated rectangular cylinder subjected to regular and random waves. The experiments were conducted in 2.2 m water depth for regular and random waves with low KC number up to 6. The rectangular cylinder was of 2 m length, 0.2 m breadth and 0.4 m width with draft of 1.45 m from still water level. The relationship between drag and inertia coefficient were evaluated and expressed as a function of KC number for various values of frequency. Drag and inertia coefficients obtained through regular wave tests were used for the random wave analysis to compute the force spectrum. The results of their study showed that the hydrodynamic coefficients were very sensitive to the variation in the aspect ratios of the cylinder. The drag coefficient decreased and inertia coefficient increased with increase in KC number.

Chandrasekaran *et al* (2004) [22], presented the influence of hydrodynamic coefficients in the response behaviour of triangular TLP in regular waves. Two triangular TLP models namely TLP₁ and TLP₂ were taken for the study at 600 and 1200 m water depths, respectively. The time domain analysis approach was applied using Newmark beta

method to solve the equation of motion. The forces in this work were evaluated using Morison equation since the diffraction effect was ignored. They found that for compliant structure like TLP, application of Morison equation without correctly estimated C_D and C_M values would result in a response behaviour significantly higher compared with that of the expected real behaviour. They also showed that responses in horizontal degrees-of-freedom were highly influenced by the variation of the C_D and C_M values throughout the water depth.

Chandrasekaran et al. (2007) [23] studied the influence of wave approach angle and its influence on the coupled dynamic response of triangular TLPs. The hydrodynamic loading was modeled using Stokes fifth-order nonlinear wave theory with various other nonlinearities. Low frequency surge oscillations and high frequency tension oscillations of tethers were ignored in their analysis. They showed that wave approach angle influenced the coupled dynamic response of triangular TLP in all degrees of freedom except heave. Responses in roll and sway degrees of freedom were activated which otherwise were not present in TLPs response to unidirectional waves. It was also concluded that the heave response in TLP with lesser water depth is more due to its lesser buoyancy.

2.7.4 Different shapes of TLP

Chandrasekaran and Jain (2002) [24] presented the dynamic behavior of square and triangular offshore TLPs under regular wave loads considering the coupling between all the degrees-of-freedom. A unique equilateral triangular TLP model was proposed and its response was compared with that of an equivalent four legged (square) TLP on the basis of two considerations. i) Total initial pretension (T_0) and total weight were kept same for both the triangular and four legged (square) TLP. Therefore, the initial pretension per leg in triangular TLP was more. ii) Initial pretension per tether and the buoyancy were kept same for both triangular and four legged (square) TLP and hence weight of triangular

TLP model was more than that of four legged (square) TLP model. They stated that triangular TLPs exhibited a lower response in the surge and heave degree-of-freedom than that of four-legged TLP considered for comparing the response under regular waves. However, their study showed that pitch response was more than that of a square TLP due to wave forces attracted on inclined pontoons.

Their study also investigated the behavior of triangular TLP subjected to random waves (2002) [25]. The surge power spectral density function (PSDF) indicated that the mean square response was affected by the amplification at the natural frequency of the surge degree of freedom and also the peak frequency of the wave loading. The PSDF of the heave response showed higher peak values near the surge frequency and near the peak frequency of the wave loading. Surge response, therefore, influenced heave response to the maximum. Variable submergence seemed to be a major source of the nonlinearity.

Reddy and Mani (2004) performed a numerical model study to evaluate wave field transmission and wave forces on a single structure of arbitrary shape. After testing different structure shapes they considered that the deflection coefficient reduced considerably in the front side of the structure and increased at the rear side of the structure. Finally, the sequence of deflection profiles was also presented [19].

John et al (2004) [5] studied the advantages of Extended Tension Leg Platform (ETLP) compared with the classic TLP. He discussed the main principals of the tension leg platform like its configuration, behavior and components. Then the development and applications of the new Extended Tension Leg Platform technology were presented. He found that the ETLP had less cost and more stability than classic TLP. Moreover, a low risk installation operation that minimized offshore exposure time was also possible with the ETLP platform.

Xiaohong Chen *et al* (2006) [26], performed a couple dynamic analysis for a Mini TLP. Their study focused on the importance of the coupled dynamic interaction and the effectiveness of different approaches for their prediction. An experimental work was achieved to measure the motion of the selected platform and validate the numerical code (COUPLE) which was developed to compute the behavior of the platform. The developed code was able to predict the dynamic interaction between the hull and its tendon and riser systems while the related quasi-static analysis failed. The comparisons showed that wave loads on the mini-TLP could be accurately predicted using the Morison equation, provided that the wavelength of incident waves was much longer than the diameters of the columns and pontoons. This result was obtained for a mini-TLP only but the authors expected this result to be relevant to a wide range of deep water structures.

2.7.5 TLPs tethers system

Lotsbuge (1991) studied the probabilistic design of tethers of tension leg platform. He discussed various aspects of dynamic and reliability assessments of TLPs under conventional environmental forces. He concluded that the angle of loading had remarkable effects on the dynamic stability of TLP [19].

N.A. Siddiqui, S. Ahmad 2000 [27], performed a study in the reliability analysis against progressive failure of TLP tethers in extreme tension. The limit state function was derived for maximum and minimum tension and von-mises failure criterion was applied to evaluate the failure of tether against maximum tension. It was noted that the minimum tension failure occurred when the tethers were slack due to loss of tension. The probabilities of failure were also obtained for different sea states to assess the annual life time probability of failures. Finally they compared the case of missing one tether with that of intact TLP. They found that in case of missing one tether due to maximum tension the probable life time for the other tethers were different in magnitude and same

in order with that of intact TLP. However, they recommended an immediate replacement for the damaged tether to avoid further failures. They also investigated that in minimum tension case for both regular and long crested sea, the probable life time was less compared to intact TLP.

N.A. Siddiqui and Suhail Ahmad 2001 [28], studied a non-linear dynamic analysis of the TLP to assess the reliability of the TLP tethers against fatigue and fracture due to long crested random wave loading. Palmgren-Miner's rule and fracture mechanics approaches were used to estimate the fatigue damage while first order reliability method and Monte Carlo simulation technique were employed for reliability estimation. This study highlighted that the partial safety factor, an essential requirement of reliability based probabilistic design, was quite sensitive to the idealization of sea environment. A typical value of the reliability index of the system, as in the present study, was about 30% less than that for a joint. The study also showed that if the number of joints in the tether system increased, the fatigue failure also increased and vice versa.

A technical note in stability analysis of TLP tethers was written by S. Chandrasekaran *et al* 2006 [29], on which the dynamic analysis of TLP's tethers was carried out. The cable equation for the tether modeling subjected to tension was considered as linear equation and varying along the length. The study considered the end conditions as simply supported, there were no current effects and the flexural rigidity of the tether was neglected. Different water depths and different TLP shapes were tested using Mathieu stability analysis to obtain the amplitudes of tether vibrations. From the results, the authors concluded that increasing tether tension increased the stability of the platform and improved the equilibrium by increasing hydrodynamic loading contributing to added mass. The results also revealed that the triangular TLPs with increased pretension performed better than the rectangular TLPs in the first vibration mode.

A Dynamic response of an axially loaded tendon of a tension leg platform was studied by Mangala M. Gadagi and Haym Benaroya 2006 [30], they derived a set of nonlinear equations of motion for the tested model using Hamilton's principle. The finite difference method was used to analyze the dynamic response of the tower for various end tension and Morison equation was used for fluid force calculations. In their work they considered the tower as an elastic beam subjected to end tension in plane motion due to random wave excitation. They also studied the effects of some parameters such as significant wave height, increase in the constant end tension and harmonically varying end tension. From the numerical study it was seen that at low tension, the axial motion was mainly induced by geometry while at higher tension, the axial motion was mainly due to elongation. The study also showed that changing the above mentioned parameters had significant effects in the tendons behavior.

Khan et al (2006) [31] presented the reliability assessment of TLP tethers against maximum tension under combined action of extreme wave and impulsive loads. A limit state function for maximum tension was applied using Von-Mises theory of failure. The responses were obtained under sinusoidal, half-triangular and triangular impulsive forces. Effects of some parameters like load angle, variable submergence and material yield strength on tether reliability were also studied. They found in their study that there was less safety in tether tension under sinusoidal and triangular impulsive loads if they act at any one of the TLP columns. That meant, if a TLP tether was safe for impulse load acted at one angle of impact, it would become completely unsafe for the same impulse but acting at different angle of impact. It was also observed that the effects of impulsive loads on TLP tethers were very severe when they acted on TLP columns. However, there was no significant effect on TLP tethers if impulsive loads acted on TLP pontoons.

Claes-Goran Gustafson and Andreas Echtermeyer (2007) [32] studied the properties of carbon fiber composite tethers. An extensive test program was done to characterize the performance of the strand end fitting. Static and fatigue tests were carried out. The

studied tether was based on pultruded carbon fiber composite rods assembled into strands of 31 and 85 rods. Single pultruded rods with 6 mm diameter were tested first to establish the fatigue performance of the basic building block. Fatigue testing was extended to strands built of 85 rods and terminated in a special metallic end-fitting. The results were drawn in SN-diagrams. It was evident from the diagrams that there was a lower fatigue strength associated with the strand compared to that of the single rod. The failure mechanism was always shear failure inside the end-fitting. Performance of the strand with its end-fitting was slightly lower than the performance of the individual rods.

F. Barranco-Cicilia et al 2008 [33], studied the reliability-based design criterion for TLP tendons. They presented the procedures to perform a load and resistance Factor Design criterion for the design of the TLPs tendons in their intact condition. The design criterion considered the ultimate limit state condition for tendon sections, taking into account both dynamic interactions of load effects and the statistics of associated extreme response. The partial safety factors were calibrated for the storm environmental conditions in deep waters of Mexico. They observed that the partial safety factors reflected both the uncertainty content and the importance of the random variables. Finally, it was seen that the target reliability value had a strong influence over the safety factor values and thus over the final size of the structural elements.

2.8 Summary of the literature

The literature survey showed the need for more studies on the dynamic behavior of the TLP varying shapes, hydrodynamic coefficients and other parameters like water depth, wave angle, center of gravity position and tether pretension. The following points were highlighted from the above literature.

- 1- The natural frequencies in all the degrees of freedom in TLP system must not come close to the wave frequency, thus avoiding the occurrence of resonance and reducing the horizontal motion and hence loading on the tether platform system. Handling the responses of the platform represented the main factor to control the resonance phenomena.
- 2- Most of the analysis reported rigid body uncoupled analysis in frequency or time domain using Airy's linear wave theory or Stokes theories to calculate wave properties. Morison equation and its modified version were commonly used in force calculation after adapting them to that particular case.
- 3- Main TLP responses for practical interest are surge, sway motion and tether tension. Surge and sway play vital role in the behavior of the TLP since they affected the offset and sit-down of the platform. An accurate prediction of the surge and sway responses and limiting them represent the major concern of the current study. The reliability assessments of the TLP mooring system and their behavior under all load conditions necessitated more efforts and analysis on the behavior of the platform tether system.

CHAPTER THREE

RESEARCH METHODOLOGY

3.1 Introduction

The methodology adopted for this study is explained in this chapter. A time domain analysis treating the platform as a rigid body was formulated. The wave forces and the dynamic responses of the square and triangular TLPs were presented. Linear and second order wave theories were presented first, and then Morison's Equation was formulated for TLP columns and pontoons. The stiffness matrices for square and triangular TLPs were introduced while the stiffness matrix for the inclined tether TLP was formulated. The Newmark integration scheme with constant-average-acceleration method was used. Finally, a computer program was written and its flowchart was drawn and highlighted.

3.2 Wave Force calculations

An offshore structure in an ocean environment is subjected to loading due to wind, current and wave. The wave force is the most important load acting on the platforms. In general, there are three theories to calculate wave forces on the cylindrical members namely Morison Equation, Froude-Krylov theory and the diffraction theory.

If the diameter of the structure is small compared to the wave length ($D/L < 0.2$), the Morison Equation is applicable [7-9]. If the structure is not small compared to the wave length, then the diffraction theory must be used. In this case, the inertia force is predominant. If the inertia force is still predominant and the drag force is small, but the structure is still small compared with the wave length, Froude-Krylov theory is applied.

In this study, the Morison Equation is applied according to the above mentioned classification.

3.2.1 Morison equation

When a rigid structure is free to move in waves, the Modified Morison Equation can be used (Equation 3.1), which takes relative velocity and acceleration between the structure and water particles into account [7,34-38]. While calculating the wave forces, water particle kinematics for each member are determined with respect to the position of the elements after dividing the columns and pontoons into small elements.

$$F(t)_i = C_{mi} A_I (a_{wi} - a_s) + A_I a_s + C_{Di} A_D |u_{wi} - u_s| (u_{wi} - u_s) \quad (3.1)$$

In which $F(t)$ = wave force per unit length of the cylinder, u_{wi} , a_{wi} , were the wave particle velocity and acceleration at the particular position respectively (given in Tables 2.1-2.2), while u_s , a_s were the structure velocity and acceleration respectively. Inertia and Drag coefficients were presented by C_{mi} and C_{Di} , where (i) term represent the specific element of the cylinder. $A_I = \rho \pi D^2/4$ and $A_D = \rho D/2$. The nonlinear drag term was linearised in Equation 3.2 [39].

$$\begin{aligned} C_D A_D |u_{rel}| u_{rel} &= \frac{8}{3\pi} C_D A_D |u_{rel}|_{\max} u_{rel} \\ &= C_{LD} A_D u_{rel}, \text{ where } C_{LD} = \frac{8}{3\pi} C_D |u_{rel}|_{\max} \\ u_{rel} &= u_{wi} - u_s \end{aligned} \quad (3.2)$$

3.2.1.1 Forces on columns

The total force on a column along x axis was given by summation of the forces of the column's elements as shown in Equation (3.3) [39].

$$F_{x_n} = \cos \alpha \sum_{s=1}^d C_M A_I a_{wi_x} + u_{wi_x} A_{Dx} - \sum_{s=1}^d A_I a_{sx} (C_M - 1) - A_{Dx} u_{sx} \quad (3.3)$$

$$\text{Where } A_{Dx} = \rho \frac{D_c}{2} C_{LDx}$$

$$A_I = \rho \frac{\pi D_c^2}{4}$$

$$C_{LDx} = C_{DC} \frac{8}{3\pi} (u_{wi_x} - u_{sx})_{\max}$$

Where $x_n = x$ coordinate of n^{th} column and α represents the wave angle with x axis.

A similar expression was applied for the total forces on the column along y axis, which is expressed in Equation (3.4).

$$F_{y_n} = \sin \alpha \sum_{s=1}^d C_M A_I a_{wi_y} + u_{wi_y} A_{Dy} - \sum_{s=1}^d A_I a_{sy} (C_M - 1) - A_{Dy} u_{sy} \quad (3.4)$$

$$\text{Where } A_{Dy} = \rho \frac{D_c}{2} C_{LDy}$$

$$C_{LDy} = C_{DC} \frac{8}{3\pi} (u_{wi_y} - u_{sy})_{\max}$$

The total force on the column along z axis is given in Equation (3.5).

$$F_{z_n} = \rho g \frac{\cosh kl}{\cosh kd} \frac{\pi D_c^2}{4} \eta_n \quad (3.5)$$

3.2.1.2 Forces on pontoon

The pontoon was divided into small elements (Figure 3.1 and Figure 3.2). The position of each element from wave reference line along the wave length (x_i) was calculated for Square and Triangular TLPs. Then the forces in pontoon were applied [39], according to the element position. The values of x_i for square and triangular TLPs were derived as below

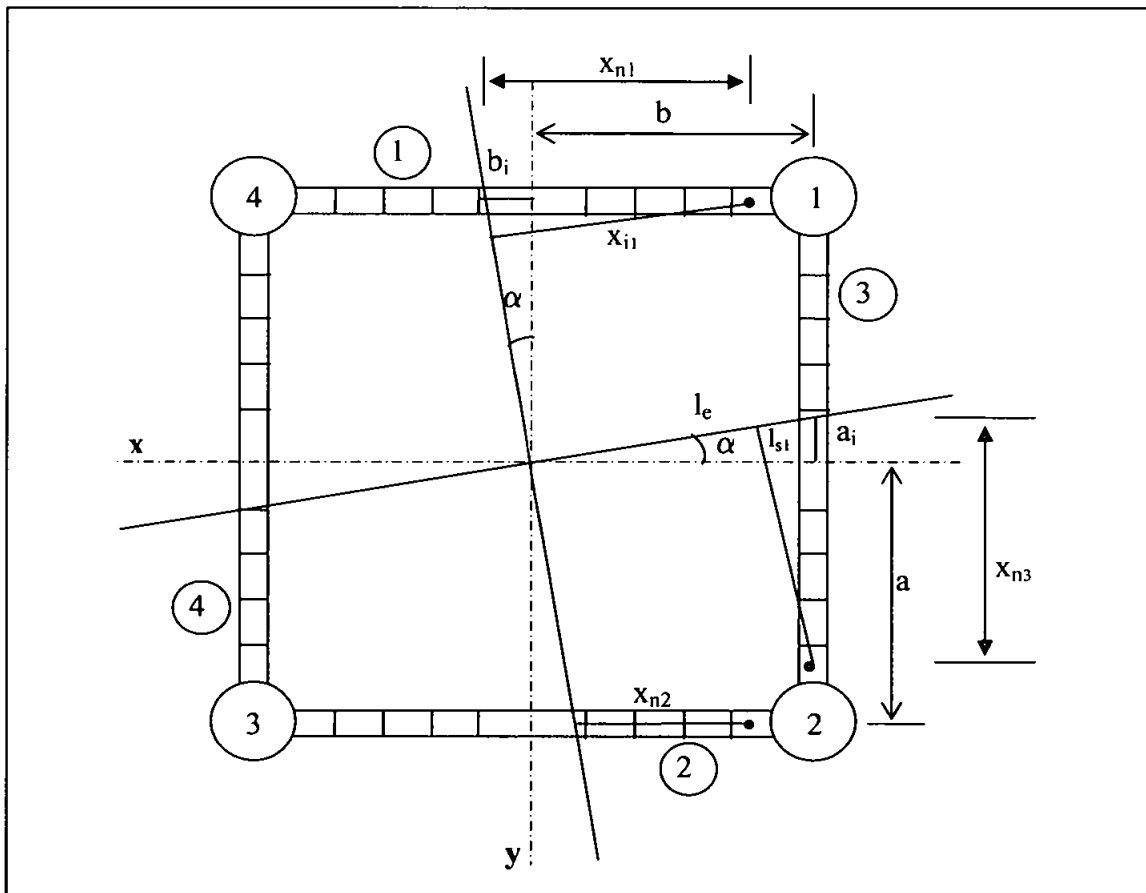


Figure 3.1: Square TLP pontoon elements

a. Square TLP pontoons:

- Pontoon 1 and 2, elements positions;

$$b_i = a \tan \alpha \tag{3.6}$$

$$x_{n1} = \left((b + b_i) - \left(\frac{D_c}{2} + \frac{2b - D_c}{N} (0.5 + (n - 1)) \right) \right) \quad (3.7)$$

$$x_{n2} = \left((b - b_i) - \left(\frac{D_c}{2} + \frac{2b - D_c}{N} (0.5 + (n - 1)) \right) \right) \quad (3.8)$$

Where N was the total number of pontoon elements and n was the element's number. The elements positions for pontoon 1 and 2 were

$$x_{i1} = x_{n1} \cos \alpha \quad (3.9)$$

$$x_{i2} = x_{n2} \cos \alpha \quad (3.10)$$

- Pontoon 3 and 4, elements positions;

$$a_i = b \tan \alpha \quad (3.11)$$

$$l_e = \sqrt{b^2 + a_i^2} \quad (3.12)$$

And

$$x_{n3} = \left((a + a_i) - \left(\frac{D_c}{2} + \frac{2a - D_c}{N} (0.5 + (n - 1)) \right) \right) \quad (3.13)$$

$$x_{n4} = \left((a - a_i) - \left(\frac{D_c}{2} + \frac{2a - D_c}{N} (0.5 + (n - 1)) \right) \right) \quad (3.14)$$

The values of l_{s1} and l_{s2} was calculated as

$$l_{s1} = x_{n3} \sin \alpha \quad (3.15)$$

$$l_{s2} = x_{n4} \sin \alpha \quad (3.16)$$

Then, the elements positions for pontoon 3 and 4 were written as

$$x_{i3} = l_e - l_{s1} \quad (3.17)$$

$$x_{i4} = -(l_e + l_{s2}) \quad (3.18)$$

b. Triangular TLP pontoons:

- Pontoon 1, elements positions;

$$a_{i1} = \frac{2 a \sin \alpha}{3 \sin (\xi - \alpha)} \quad (3.19)$$

$$a_{i2} = \frac{2 a \sin \alpha}{3 \sin (120^\circ - \alpha)} \quad (3.20)$$

$$a_{i3} = \frac{P_1}{3} \tan \alpha \quad (3.21)$$

The values of x_n were written as

$$x_{n1} = \left(\left(\frac{4a}{3} + a_{i1} \right) - \left(\frac{D_c}{2} + \frac{2a - D_c}{N} (0.5 + (n - 1)) \right) \right) \quad (3.22)$$

$$x_{n2} = \left(\left(\frac{4a}{3} - a_{i2} \right) - \left(\frac{D_c}{2} + \frac{2a - D_c}{N} (0.5 + (n - 1)) \right) \right) \quad (3.23)$$

$$x_{n3} = \left((a - a_{i3}) - \left(\frac{D_c}{2} + \frac{2a - D_c}{N} (0.5 + (n - 1)) \right) \right) \quad (3.24)$$

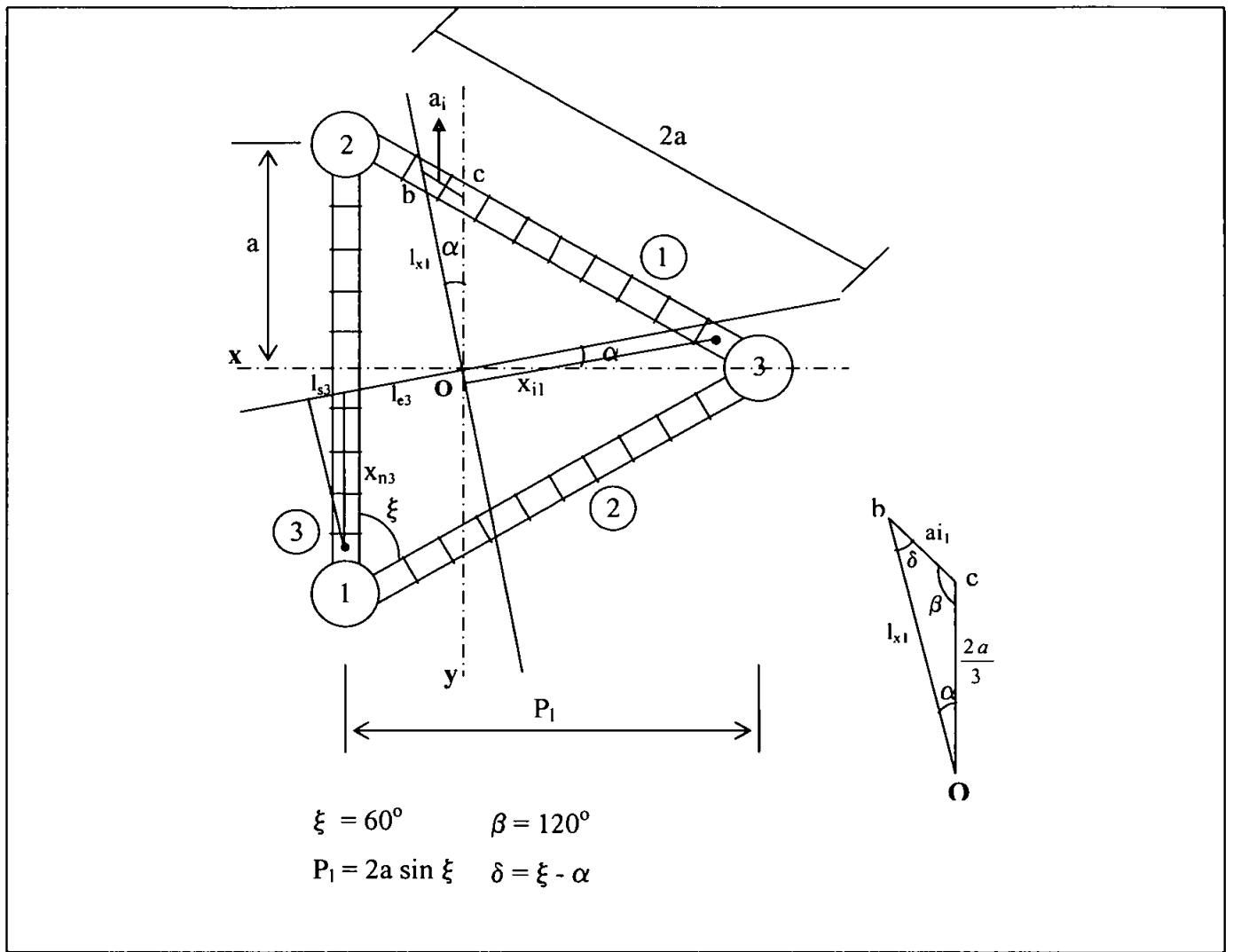


Figure 3.2: Triangular TLP pontoon elements

The positions of elements x_i were calculated by

$$x_{i1} = x_{n1} \cos \left(\alpha + \frac{\xi}{2} \right) \tag{3.25}$$

$$x_{i2} = x_{n2} \cos \left(\alpha - \frac{\xi}{2} \right) \tag{3.26}$$

$$x_{i3} = -(l_{e3} + l_{s3}) \tag{3.27}$$

Where

$$l_{e3} = \sqrt{\left(\left(\frac{P_l}{3}\right)^2 + a_{i3}^2\right)} \quad (3.28)$$

And

$$l_{s3} = x_{n3} \sin \alpha \quad (3.29)$$

After locating the position of the pontoon elements, Modified Morison Equation for inclined cylinder was used to find out the total force in the pontoons taking into account the wave inclination. The inclined cylinder's Equations were as given below [7,39].

$$f_x = C_M A_I a_x + C_D A_D |w| u_x \quad (3.30)$$

$$f_y = C_M A_I a_y + C_D A_D |w| u_y \quad (3.31)$$

$$f_z = C_M A_I a_z + C_D A_D |w| u_z \quad (3.32)$$

The local x axis was taken along direction of wave propagation. Since the pontoons were horizontal, the angle of the cylinder axis to the vertical axis (ζ) was 90° . The values of the unit vectors C_x , C_y and C_z were substituted as

$$C_x = \sin \zeta \cos \alpha = \cos \alpha \quad C_y = \cos \zeta = 0 \quad C_z = \sin \zeta \sin \alpha = \sin \alpha$$

Where

$$\begin{aligned} u_{xi} &= u_i (1 - C_x) \\ u_{yi} &= v_i \\ u_{zi} &= -u_i C_x C_z \end{aligned} \quad (3.33)$$

$$\begin{aligned}
a_{xi} &= u_i (1 - C_x) \\
a_{yi} &= v_i \\
a_{zi} &= -u_i C_x C_z
\end{aligned} \tag{3.34}$$

And

$$|w_i| = \sqrt{(u_{i_{\max}})^2 (1 - C_x^2) + v_{i_{\max}}^2 + u_{i_{\max}}^2 C_x^2 C_z^2} \tag{3.35}$$

$$C_{LDi} = \frac{8}{3\pi} C_{DP} |w_i|_{\max}$$

$$A_{Di} = \frac{\rho D_P}{2} C_{LDi}$$

$$A_{IP} = \rho \frac{\pi D_P^2}{4}$$

The expressions for forces on each pontoon element (F_{xi} , F_{yi} , and F_{zi}) after transforming the coordinate to the global system were as given in Equation (3.36-3.38) [39].

$$\begin{aligned}
F_{xi} &= \cos \alpha (A_{Di} u_{xi} + A_{IP} C_{MP} a_{xi}) + \\
&\sin \alpha (A_{Di} u_{zi} + A_{IP} C_{MP} a_{zi}) - A_{Di} u_{sx} - A_{IP} (C_{MP} - 1) a_{sx}
\end{aligned} \tag{3.36}$$

$$\begin{aligned}
F_{yi} &= \sin \alpha (A_{Di} u_{yi} + A_{IP} C_{MP} a_{yi}) - \\
&\cos \alpha (A_{Di} u_{zi} + A_{IP} C_{MP} a_{zi}) - A_{Di} u_{sy} - A_{IP} (C_{MP} - 1) a_{sy}
\end{aligned} \tag{3.37}$$

$$F_{zi} = A_{Di} u_{yi} + A_{IP} C_{MP} a_{yi} - A_{Di} u_{sz} - A_{IP} (C_{MP} - 1) a_{sz} \tag{3.38}$$

3.2.1.3 Moments due to columns forces at Center of Gravity

The total moment on the platform about a particular axis due to columns was equal to summation of each column force multiplied by the distance of that column from the platform center of gravity.

a. Square TLP

The moments about x axis of forces in y direction was given by the following equations and similar expression for y axis.

$$M_{xy} = \sum_{n=1}^{n=4} \sum_{a_z = -h_c}^{a_z = (dr - h_c)} F_{y_n} a_z \quad (3.39)$$

$$M_{yx} = \sum_{n=1}^{n=4} \sum_{a_z = -h_c}^{a_z = (dr - h_c)} F_{x_n} a_z \quad (3.40)$$

Where, a_z was a moment arm measured vertically from the center of gravity to that particular point. The symbol n was the column number, dr was the column draft and h_c was the center of gravity height.

The moments about x and y axis for column forces in z direction was given as by

$$M_{xz} = \sum_{n=1,4} F_{z_n} a_{r_n} - \sum_{n=2,3} F_{z_n} a_{r_n} \quad (3.41)$$

$$M_{yz} = \sum_{n=3,4} F_{z_n} a_{r_n} - \sum_{n=1,2} F_{z_n} a_{r_n} \quad (3.42)$$

The moments about z axis due to forces in x and y direction were given by

$$M_{zx} = \sum_{n=2,3} F_{z_n} a_{r_n} - \sum_{n=1,4} F_{z_n} a_{r_n} \quad (3.43)$$

$$M_{zy} = \sum_{n=1,2} F_{y_n} a_{r_n} - \sum_{n=3,4} F_{y_n} a_{r_n} \quad (3.44)$$

Where, a_r represented the moment arm measured horizontally from the platform center of gravity to column center. The suffix n was the column number.

b. Triangular TLP

The moments about x axis of forces in the y direction was given by the following Equations and similar expression for moments about y axis.

$$M_{xy} = \sum_{n=1}^{n=3} \begin{matrix} a_z = (dr - h_c) \\ a_z = -h_c \end{matrix} \sum F_{y_n} a_z \quad (3.45)$$

$$M_{yx} = \sum_{n=1}^{n=3} \begin{matrix} a_z = (dr - h_c) \\ a_z = -h_c \end{matrix} \sum F_{x_n} a_z \quad (3.46)$$

The moments about x and y axis of column forces in z direction were given as below

$$M_{xz} = \sum_{n=1,3} F_{z_n} a_{r_n} - \sum_{n=2} F_{z_n} a_{r_n} \quad (3.47)$$

$$M_{yz} = \sum_{n=1,2} F_{z_n} a_{r_n} - \sum_{n=3} F_{z_n} a_{r_n} \quad (3.48)$$

The moments about z axis due to forces in x and y axis were given by

$$M_{zx} = \sum_{n=1,3} F_{z_n} a_{r_n} - \sum_{n=2} F_{z_n} a_{r_n} \quad (3.49)$$

$$M_{zy} = \sum_{n=3} F_{y_n} a_{r_n} - \sum_{n=1,2} F_{y_n} a_{r_n} \quad (3.50)$$

3.2.1.4 Moments due to pontoons forces at center of gravity.

The moment in the pontoons could be calculated similar to column moments, but instead of substituting column force time its distance from the CG position, the values of the forces at each pontoon element time its distance from the CG position have been taken.

3.3 Mass matrix

The mass matrix included the mass at each degree of freedom into account, so it was diagonal in nature. The added mass, M_a , due to the water surrounding the structural members and arising from the Modified Morison Equation has been considered up to the mean sea level (MSL). The presence of off-diagonal terms in the total mass matrix indicated a contribution of the added mass due to the hydrodynamic loading [24,40-42]. The mass matrix was as given below;

$$[M_i] = \begin{bmatrix} M_{11} & 0 & 0 & 0 & 0 & 0 \\ 0 & M_{22} & 0 & 0 & 0 & 0 \\ 0 & 0 & M_{33} & 0 & 0 & 0 \\ 0 & 0 & 0 & I_{44} & 0 & 0 \\ 0 & 0 & 0 & 0 & I_{55} & 0 \\ 0 & 0 & 0 & 0 & 0 & I_{66} \end{bmatrix} \quad (3.51)$$

Where

$M_{11}=M_{22}=M_{33}=M$ = Mass in surge, sway and heave degrees of freedom.

M is the total mass of the entire structure

I_{44} is the total mass moment of inertia about the X axis $=Mr_x^2$

I_{55} is the total mass moment of inertia about the Y axis $=Mr_y^2$

I_{66} is the total mass moment of inertia about the Z axis $=Mr_z^2$

The added mass term was time dependent and was obtained by transferring the inertia terms from the right hand side of the Equation of motion. This indicated that, the total mass matrix $[M]$ changed at each time step according to variation of added mass matrix. Finally the total mass matrix at each time step were written as

$$[M] = [M_i] + [M_a] \quad (3.52)$$

3.4 Stiffness matrix

The stiffness matrix $[K]$ of the TLPs in general was formed as below

$$[K] = \begin{bmatrix} K_{11} & 0 & 0 & 0 & 0 & 0 \\ 0 & K_{22} & 0 & 0 & 0 & 0 \\ K_{31} & K_{32} & K_{33} & K_{34} & K_{35} & K_{36} \\ 0 & K_{42} & 0 & K_{44} & 0 & 0 \\ K_{51} & 0 & 0 & 0 & K_{55} & 0 \\ 0 & 0 & 0 & 0 & 0 & K_{66} \end{bmatrix} \quad (3.53)$$

Where K_{ij} represented the reaction in i degree of freedom due to a unit displacement in j degree of freedom [39-40,43]. The formulae for K_{ij} were different in the different types of the tension leg platform, like triangular, square and inclined tethers TLPs. The stiffness matrix formulation for the above mentioned types were as explained below.

3.4.1 Rectangular TLP

The values of rectangular TLP matrix components were as below [16,39-40].

3.4.1.1 Stiffness in surge direction

By giving an arbitrary displacement x_1 in the x direction the equilibrium of forces in the surge direction gave

$$k_{11} = \frac{4(P_o + P_1)}{\sqrt{(x_1^2 + l^2)}} \quad (3.54)$$

The equilibrium in z direction gave

$$K_{31} = \frac{4P_o}{x_1}(\cos \gamma_x - 1) + \frac{4P_1}{x_1} \cos \gamma_x \quad (3.55)$$

Summation of moment about y axis gave

$$k_{51} = -h_c k_{11} \quad (3.56)$$

3.4.1.2 Stiffness in sway direction

By giving an arbitrary displacement x_2 in the y direction the equilibrium of forces in the sway direction gave

$$k_{22} = \frac{4(P_o + P_2)}{\sqrt{(x_2^2 + l^2)}} \quad (3.57)$$

The equilibrium in z direction gave

$$K_{32} = \frac{4P_o}{x_2} (\cos \gamma_y - 1) + \frac{4P_2}{x_2} \cos \gamma_y \quad (3.58)$$

Summation of moment about y axis gave

$$k_{42} = -h_c k_{22} \quad (3.59)$$

3.4.1.3 Stiffness in heave direction

By giving an arbitrary displacement x_3 in the z direction the equilibrium of forces in the heave direction gave

$$K_{33} = \frac{4AE}{l} + \pi D_c^2 \rho g \quad (3.60)$$

3.4.1.4 Stiffness in roll direction

By giving an arbitrary rotation x_4 in the roll direction the summation of moments along roll direction gave

$$K_{44} = \pi D_c^2 \rho b^2 g + 4 \left(\frac{P_o h_c \sin x_4}{x_4} + \frac{AEb^2 \cos x_4}{l} \right) \quad (3.61)$$

The equilibrium in z direction gave

$$K_{34} = \frac{2}{x_4} (P_4 + P'_4) \quad (3.62)$$

Where

$$P_4 = \frac{AE}{l} bx_4 \cos x_4 \quad (3.63)$$

And $P'_4 = -P_4$ in symmetric structure

3.4.1.5 Stiffness in pitch direction

By giving an arbitrary rotation x_5 in the pitch direction the summation of moments along pitch direction gave

$$K_{55} = \pi D_c^2 \rho b^2 g + 4 \left(\frac{P_o h_c \sin x_5}{x_5} + \frac{AEb^2 \cos x_5}{l} \right) \quad (3.64)$$

The equilibrium in z direction gave

$$K_{35} = \frac{2}{x_5} (P_5 + P'_5) \quad (3.65)$$

Where

$$P_5 = \frac{AE}{l} bx_5 \cos x_5 \quad (3.66)$$

And $P'_5 = -P_5$ in symmetric structures

3.4.1.6 Stiffness in yaw direction

By giving an arbitrary rotation x_6 in the yaw direction, the increase in the initial pre-tension, in each leg gave:

$$P_6 = \frac{AE}{l} (l_6 - l) \quad (3.67)$$

While

$$K_{36} = \frac{4P}{x_6} \left[\frac{l}{l_6} - 1 \right] + \frac{4P_6}{x_6} \frac{l}{l_6} \quad (3.68)$$

And

$$K_{66} = \frac{4(P + P_6)(a^2 + b^2)}{l_6} \quad (3.69)$$

3.4.2 Triangular TLP

The values of triangular TLP matrix components were as given below [24].

3.4.2.1 Stiffness in Surge direction

By giving an arbitrary displacement x_1 in the surge direction, the increase in the initial pre-tension, in each leg, was given by:

$$P_1 = \frac{AE}{l} \left(\sqrt{(x_1^2 + l^2)} - l \right) \quad (3.70)$$

Equilibrium of forces in the surge direction gave

$$k_{11} = \frac{3(P_o + P_1)}{\sqrt{(x_1^2 + l^2)}} \quad (3.71)$$

Equilibrium of forces in the heave direction gave

$$k_{31} = \frac{(3P_o(\cos \gamma_x - 1) + 3P_1 \cos \gamma_x)}{x_1} \quad (3.72)$$

When

$$\cos \gamma_x = \frac{l}{\sqrt{(x_1^2 + l^2)}} \quad (3.73)$$

And Summation of moments along the pitch direction gave:

$$k_{51} = -hck_{11} \quad (3.74)$$

3.4.2.2 Stiffness in sway direction

By giving an arbitrary displacement x_2 in the sway direction, the increase in the initial pre-tension, in each leg, was given by:

$$P_2 = \frac{AE}{l} \left(\sqrt{(x_2^2 + l^2)} - l \right) \quad (3.75)$$

Equilibrium of forces in the sway direction gave

$$k_{22} = \frac{3(P_o + P_2)}{\sqrt{(x_2^2 + l^2)}} \quad (3.76)$$

Equilibrium of forces in the heave direction gave

$$k_{32} = \frac{(3P_o(\cos \gamma_y - 1) + 3P_2 \cos \gamma_y)}{x_2} \quad (3.77)$$

When

$$\cos \gamma_y = \frac{l}{\sqrt{(x_1^2 + l^2)}} \quad (3.78)$$

And Summation of moments along the roll direction gave:

$$k_{42} = -h c k_{22} \quad (3.79)$$

3.4.2.3 Stiffness in heave direction

The displacement in heave direction x_3 affected heave direction alone. By taking Equilibrium of forces in the heave direction

$$k_{33} = 3 \frac{AE}{l} + \frac{3}{4} \pi \rho D_c^2 g \quad (3.80)$$

3.4.2.4 Stiffness in roll direction

By giving an arbitrary rotation x_4 in the roll direction, the increase in the initial pre-tension, in each leg, was given by:

$$P_4 = a \frac{AE}{l} x_4 \cos x_4 = P'_4 \quad (3.81)$$

Equilibrium of forces in the heave direction gave:

$$k_{34} = \frac{P_4}{x_4} \quad (3.82)$$

Summation of moments along the roll direction gave:

$$k_{44} = \frac{(F_b + P_o + P_4)e_4}{x_4} \quad (3.83)$$

Where

$$F_b = \frac{3}{4} \pi \rho D_c^2 g \quad (3.84)$$

3.4.2.5 Stiffness in pitch direction

By giving an arbitrary rotation x_5 in the pitch direction, the increase in the initial pre-tension, in each leg, was given by:

$$P_5 = \frac{AE}{l} x_5 \left(\frac{2}{3} P_l \cos x_5 \right) - 2x_5 \frac{AE}{l} \left(\frac{1}{3} P_l \cos x_5 \right) \quad (3.85)$$

Equilibrium of forces in the heave direction gave:

$$k_{35} = \frac{P_5}{x_5} \quad (3.86)$$

Summation of moments along the pitch direction gave:

$$k_{55} = \frac{F_b h_c \sin x_5}{x_5} \quad (3.87)$$

3.4.2.6 Stiffness in yaw direction

By giving an arbitrary rotation x_6 in the yaw direction, the increase in the initial pre-tension, in each leg, was given by:

$$P_6 = \frac{AE}{l}(l_6 - l) \quad (3.88)$$

Where

$$l_6 = \sqrt{(l^2 + x_6^2(2a^2))} \quad (3.89)$$

Equilibrium of forces in the heave direction gave:

$$k_{36} = \frac{3P_o}{x_6} \left(\frac{l}{l_6} - 1 \right) + \frac{3P_6}{x_6} \left(\frac{l}{l_6} \right) \quad (3.90)$$

Summation of moments along the yaw direction gave:

$$k_{66} = 3 \frac{(P_o + P_6)(2a^2)}{l_6} \quad (3.91)$$

3.4.3 Inclined tether square TLP

The inclined tether TLP is a new concept for the square TLP (Figure 3.3). The tethers formed angle (γ) with the vertical axis and the platform Equation of equilibrium was modified as

$$F_b = W + P_{ot} \cos \gamma \quad (3.92)$$

Instead of equation (3.93) for normal TLP tethers

$$F_b = W + P_{ot} \quad (3.93)$$

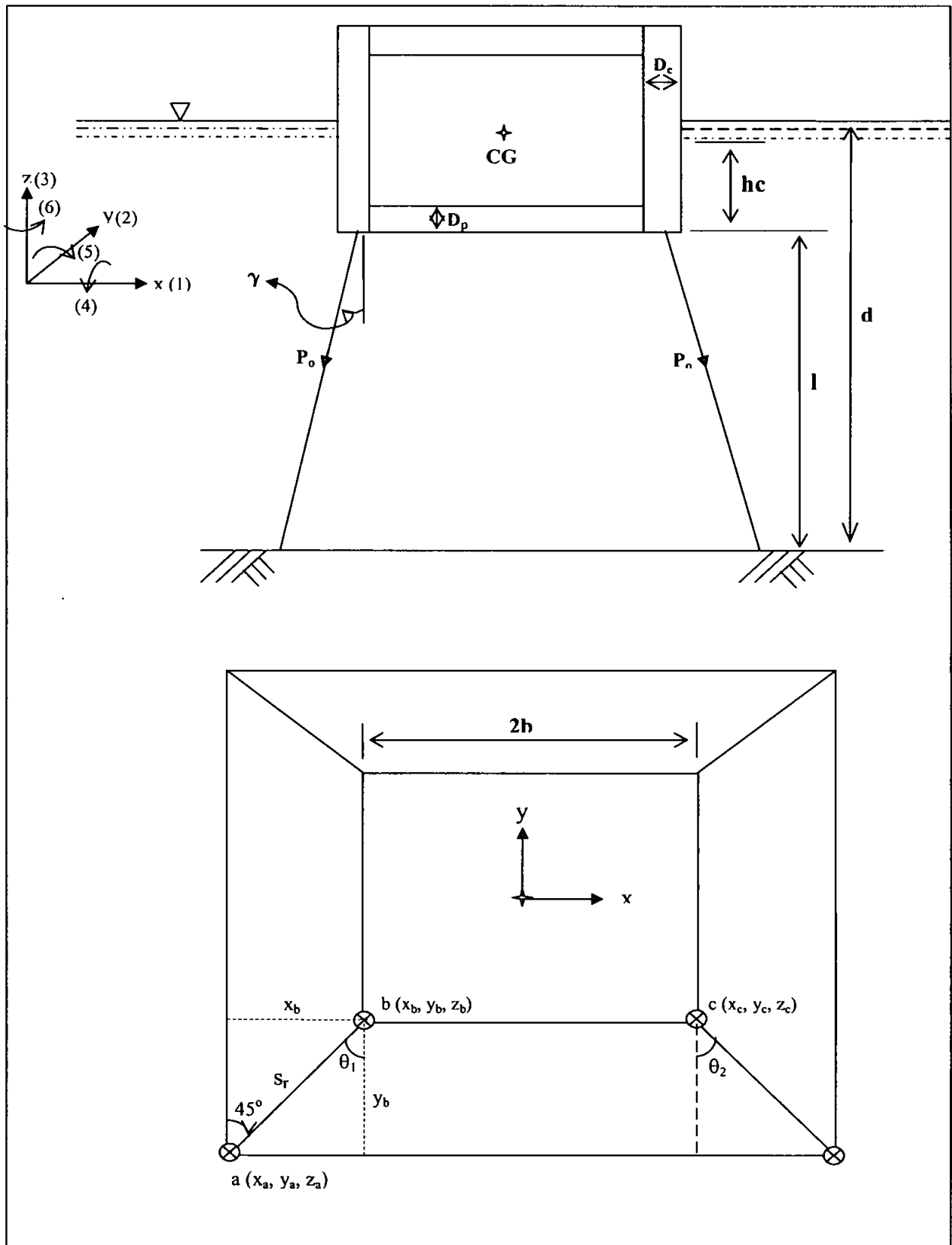


Figure 3.3: Inclined tethers TLP

3.4.3.1 Stiffness in surge direction

A displacement x_1 in surge direction was assumed, Figure 3.4 showed the effect of the displacement.

The length of tethers could be taken as

$$l_o = \frac{l}{\cos(\gamma)} \quad (3.94)$$

When horizontal distances between the platform column and its foundations could be located by

$$sr = \sqrt{l_o^2 - l^2} \quad (3.95)$$

$$xb = yb = sr \cos 45 \quad (3.96)$$

The increase in tension could be determined by the following expressions

$$l_{11} = \sqrt{((x_b + x_1) - x_a)^2 + (y_b - y_a)^2 + (l - z_a)^2} \quad (3.97)$$

$$l_{12} = \sqrt{((x_b + 2b + x_1) - (2x_b + 2b))^2 + (y_b - y_d)^2 + (l - z_d)^2} \quad (3.98)$$

$$\Delta l_{11} = l_{11} - l_o \quad (3.99)$$

$$P_{11} = \frac{AE}{l} \Delta l_{11} \quad (3.100)$$

$$\Delta l_{12} = l_{12} - l_o \quad (3.101)$$

$$P_{12} = \frac{AE}{l} \Delta l_{12} \quad (3.102)$$

The positions of the points after the displacement were

$$\gamma_{11} = \cos^{-1} \left(\frac{l}{l_{11}} \right) \quad (3.103)$$

$$\gamma_{12} = \cos^{-1} \left(\frac{l}{l_{12}} \right) \quad (3.104)$$

$$sr_1 = \sqrt{l_{11}^2 - l^2} \quad (3.105)$$

$$sr_2 = \sqrt{l_{12}^2 - l^2} \quad (3.106)$$

$$\theta_{11} = \cos^{-1} \left(\frac{y_b}{sr_1} \right) \quad (3.107)$$

$$\theta_{12} = \cos^{-1} \left(\frac{y_b}{sr_2} \right) \quad (3.108)$$

Where, the angles θ_{11} and θ_{12} were the deformed shape of angles θ_1 and θ_2 (in Figure 3.3) caused by displacement in surge direction. The symbol sr_1 and sr_2 were the displacement of the column along sr direction caused by displacement in surge direction.

The equilibrium in x directions gave

$$k_{11} = \frac{2}{x_1} [(P_o + P_{11}) \sin(\gamma_{11}) \sin(\theta_{11}) - (P_o + P_{12}) \sin(\gamma_{12}) \sin(\theta_{12})] \quad (3.109)$$

And the equilibrium in z directions gave

$$k_{31} = \frac{1}{x_1} (2((P_o + P_{11}) \cos(\gamma_{11}) + (P_o + P_{12}) \cos(\gamma_{12})) - 4P_o \cos(\gamma)) \quad (3.110)$$

Summation of moments in pitch direction gave

$$k_{51} = -k_{11} h_c \quad (3.111)$$

3.4.3.2 Stiffness in Sway direction

Using same procedure for the sway direction and taking the equilibrium in sway, heave and roll, the following expressions were obtained

$$k_{22} = \frac{2}{x_2} [(P_o + P_{21}) \sin(\gamma_{21}) \sin(\theta_{21}) - (P_o + P_{22}) \sin(\gamma_{22}) \sin(\theta_{22})] \quad (3.112)$$

$$k_{32} = \frac{1}{x_2} (2((P_o + P_{21}) \cos(\gamma_{21}) + (P_o + P_{22}) \cos(\gamma_{22})) - 4P_o \cos(\gamma)) \quad (3.113)$$

$$k_{42} = k_{22} h_c \quad (3.114)$$

3.4.3.3 Stiffness in heave direction

A displacement x_3 in heave direction was assumed. Figure 3.5 showed the effect of the displacement.

$$\Delta F_b = \pi D_c^2 \rho g x_3 \quad (3.115)$$

$$l_3 = \sqrt{(l + x_3)^2 + sr^2} \quad (3.116)$$

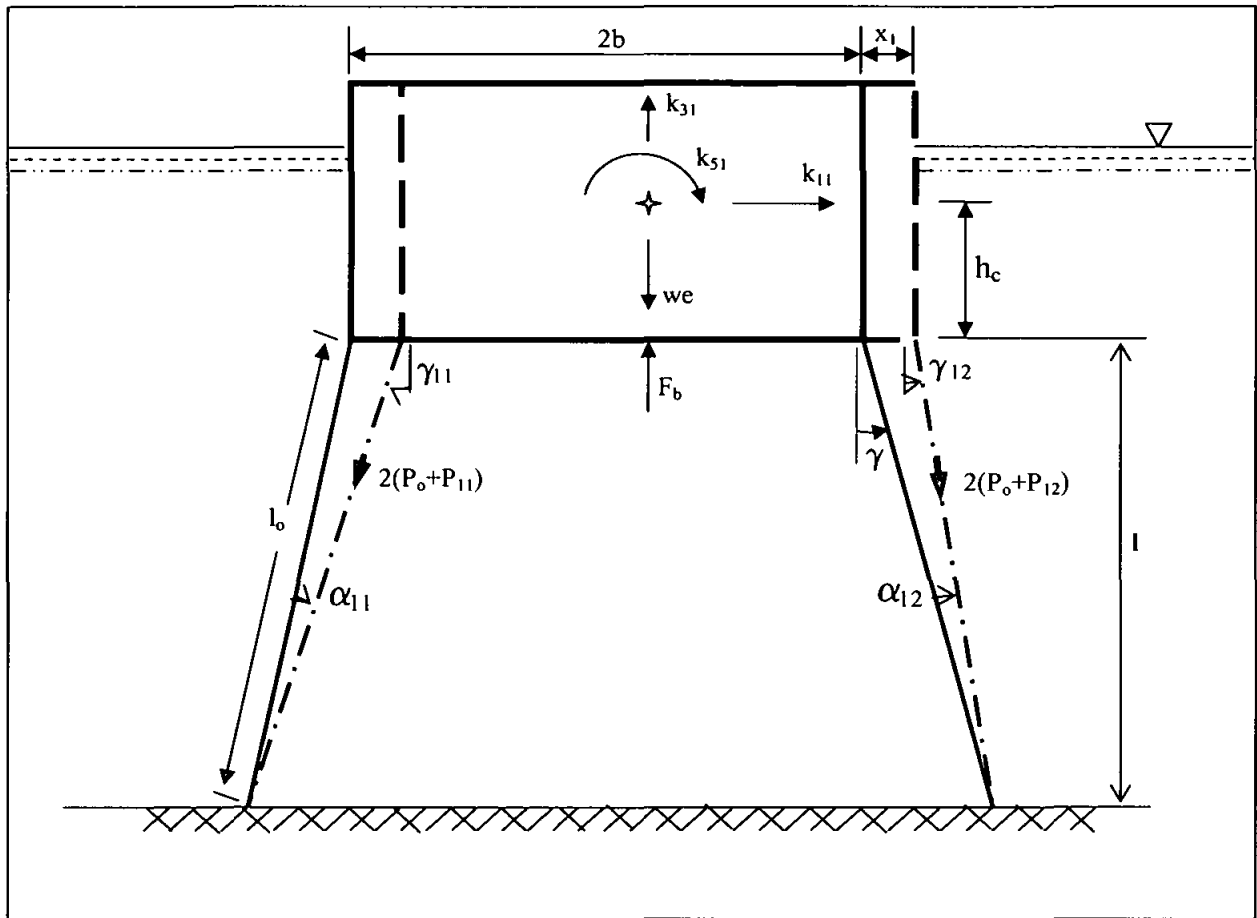


Figure 3.4: Surge motion

$$\Delta l_3 = l_3 - l_o \quad (3.117)$$

$$P_3 = \frac{AE}{l} \Delta l_3 \quad (3.118)$$

$$\gamma_3 = \cos^{-1} \left(\frac{(l + x_3)}{l_3} \right) \quad (3.119)$$

$$k_{33} = \frac{1}{x_3} \left(\frac{AE}{l} 4 \Delta l_3 \cos \gamma_3 + \Delta F_b \right) \quad (3.120)$$

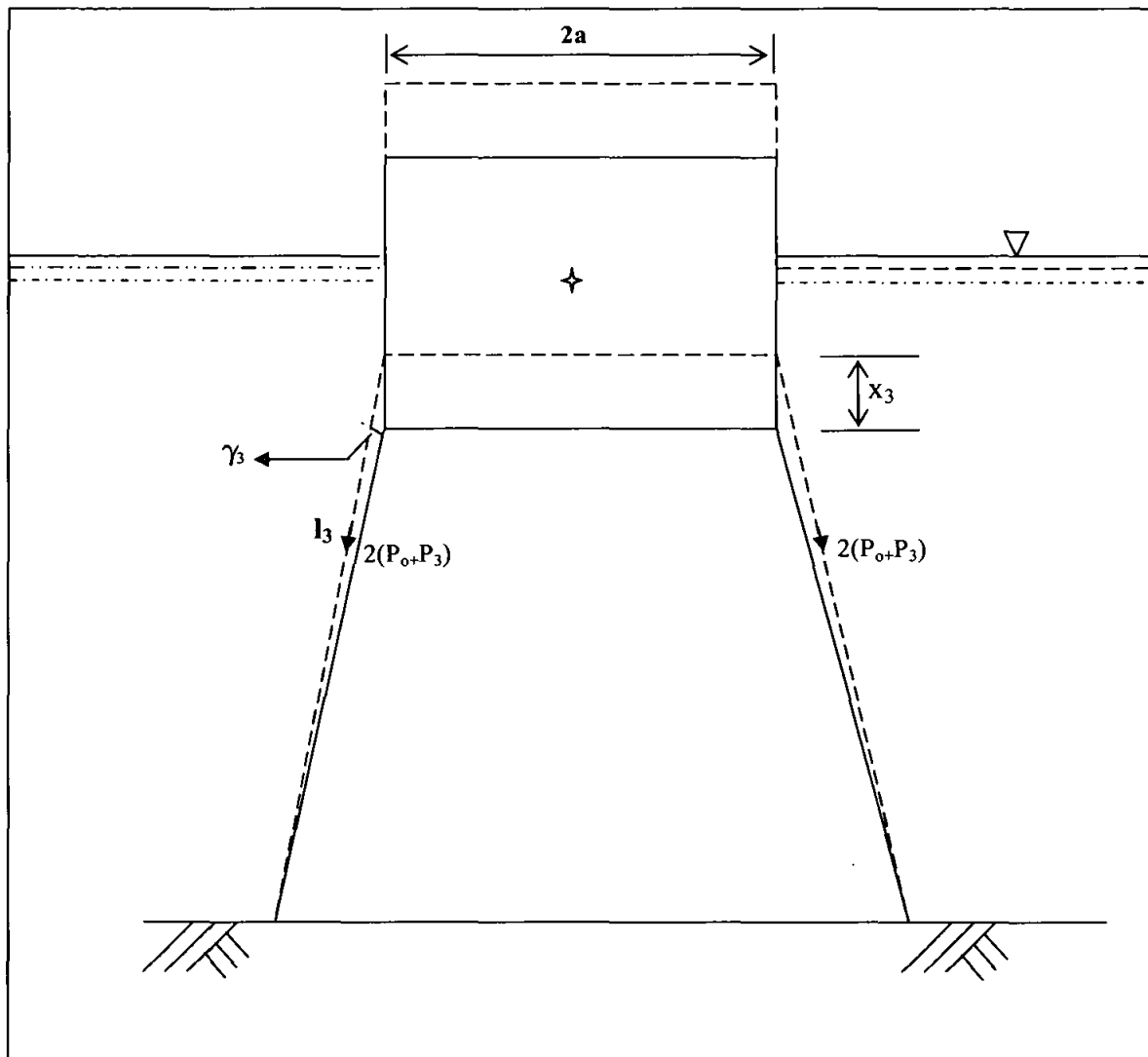


Figure 3.5: Heave motion

3.4.3.4 Stiffness in roll direction

An arbitrary rotation x_4 in roll direction was assumed. Figure 3.6 showed the effect of the displacement. The roll Equations were derived as follows

$$e_4 = h_c \sin x_4 \quad (3.121)$$

$$S_{41} = b + e_4 \quad (3.122)$$

$$S_{42} = b - e_4 \quad (3.123)$$

$$\Delta sr_4 = \frac{hc_x r}{\cos \theta} \quad (3.124)$$

The elongation in the tethers were expressed as

$$l_{41} = \sqrt{(l + bx_r)^2 + (sr - \Delta sr_4)^2} \quad (3.125)$$

$$l_{42} = \sqrt{(l - bx_r)^2 + (sr + \Delta sr_4)^2} \quad (3.126)$$

$$\Delta l_{41} = l_{41} - l_o \quad (3.127)$$

$$\Delta l_{42} = l_{42} - l_o \quad (3.128)$$

The tether tension increased by amounts as below

$$P_{41} = \frac{AE}{l} \Delta l_{41} \quad (3.129)$$

$$\gamma_{41} = \cos^{-1} \left(\frac{l + bx_4}{l_{41}} \right) \quad (3.130)$$

$$P_{42} = \frac{AE}{l} \Delta l_{42} \quad (3.131)$$

$$\gamma_{42} = \cos^{-1} \left(\frac{l - bx_4}{l_{42}} \right) \quad (3.132)$$

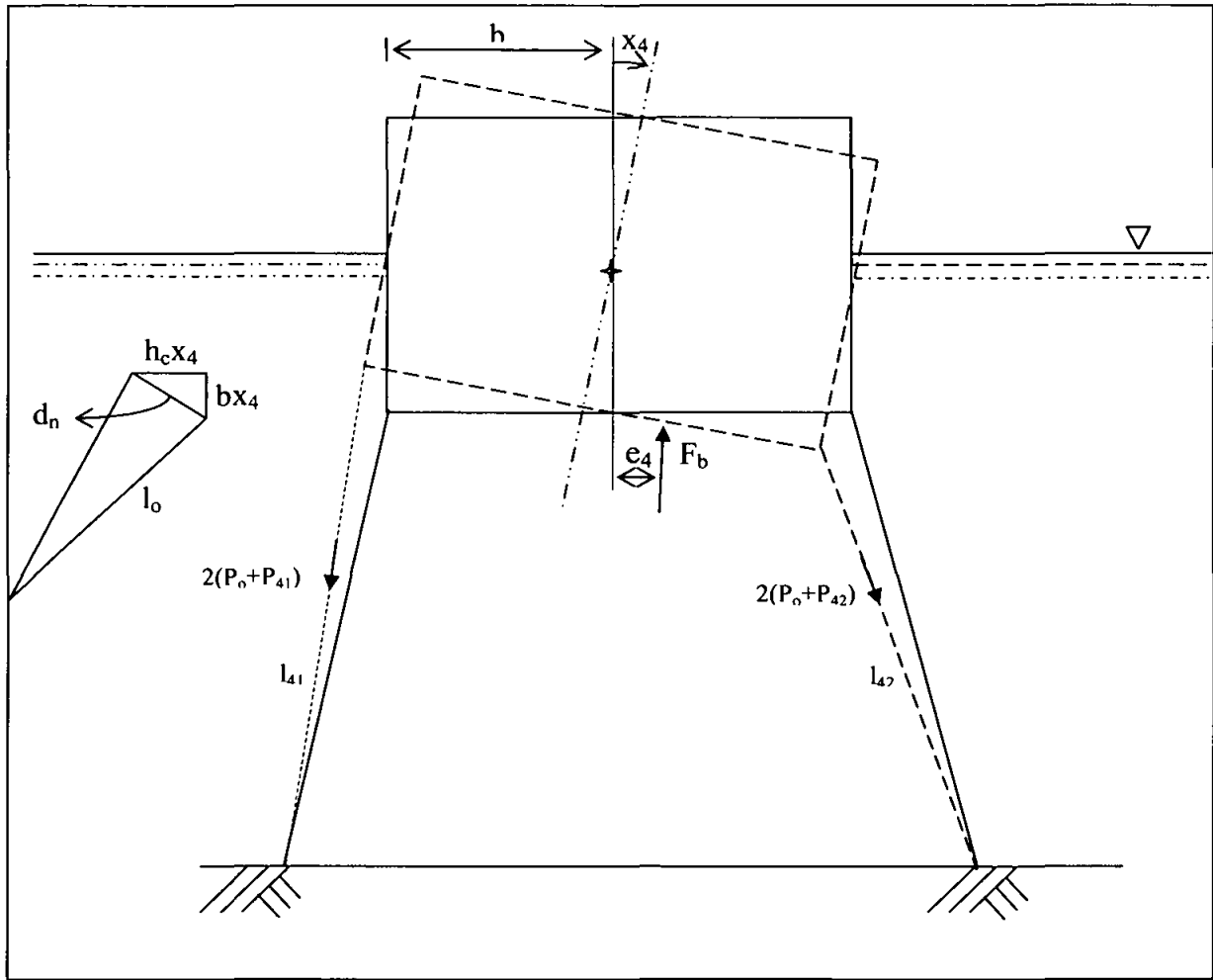


Figure 3.6: Roll motion

$$F_{b4}e_4 = (\pi D_c^2 \rho g b^2 x_4) \quad (3.133)$$

Then

$$k_{44} = \frac{F_{b4}e}{x_4} + \frac{2b}{x_4} (\cos \gamma_{41}(P_o + P_{41}) - \cos \gamma_{42}(P_o + P_{41})) + \frac{2 \cos \theta}{x_4} ((P_o + P_{42})(h_c + b x_4) \sin \gamma_{42} - (P_o + P_{41})(h_c - b x_4) \sin \gamma_{41}) \quad (3.134)$$

$$k_{34} = \frac{2}{x_4} (P_{41} \cos \gamma_{41} + P_{42} \cos \gamma_{42}) \quad (3.135)$$

3.4.3.5 Stiffness in pitch direction

Using same procedure for the roll direction and taking the equilibrium in pitch and heave, the following expressions were obtained.

$$k_{55} = \frac{F_{b5e}}{x_5} + \frac{2b}{x_5} (\cos \gamma_{51}(P_o + P_{51}) - \cos \gamma_{52}(P_o + P_{51})) + \frac{2 \cos \theta}{x_5} \left((P_o + P_{52})(h_c + ax_5) \sin \gamma_{52} - (P_o + P_{51})(h_c - ax_5) \sin \gamma_{51} \right) \quad (3.136)$$

$$k_{35} = \frac{2}{x_5} (P_{51} \cos \gamma_{51} + P_{52} \cos \gamma_{52}) \quad (3.137)$$

3.4.3.6 Stiffness in yaw direction

By giving an arbitrary rotation x_6 in the yaw direction (see Figure 3.7), the increase in the initial pre-tension, in each leg, was given by

$$d_6 = x_6 \sqrt{a^2 + b^2} \quad (3.138)$$

$$l_6 = \sqrt{l_o^2 + d_6^2} \quad (3.139)$$

$$P_6 = \frac{AE}{l} (l_6 - l_o) \quad (3.140)$$

$$\gamma_6 = \cos^{-1} \left(\frac{l}{l_6} \right) \quad (3.141)$$

While

$$k_{36} = \left[\frac{4P_o}{x_6} (\cos \gamma_6 - \cos \gamma) + \frac{4P_6}{x_6} \cos \gamma_6 \right] \quad (3.142)$$

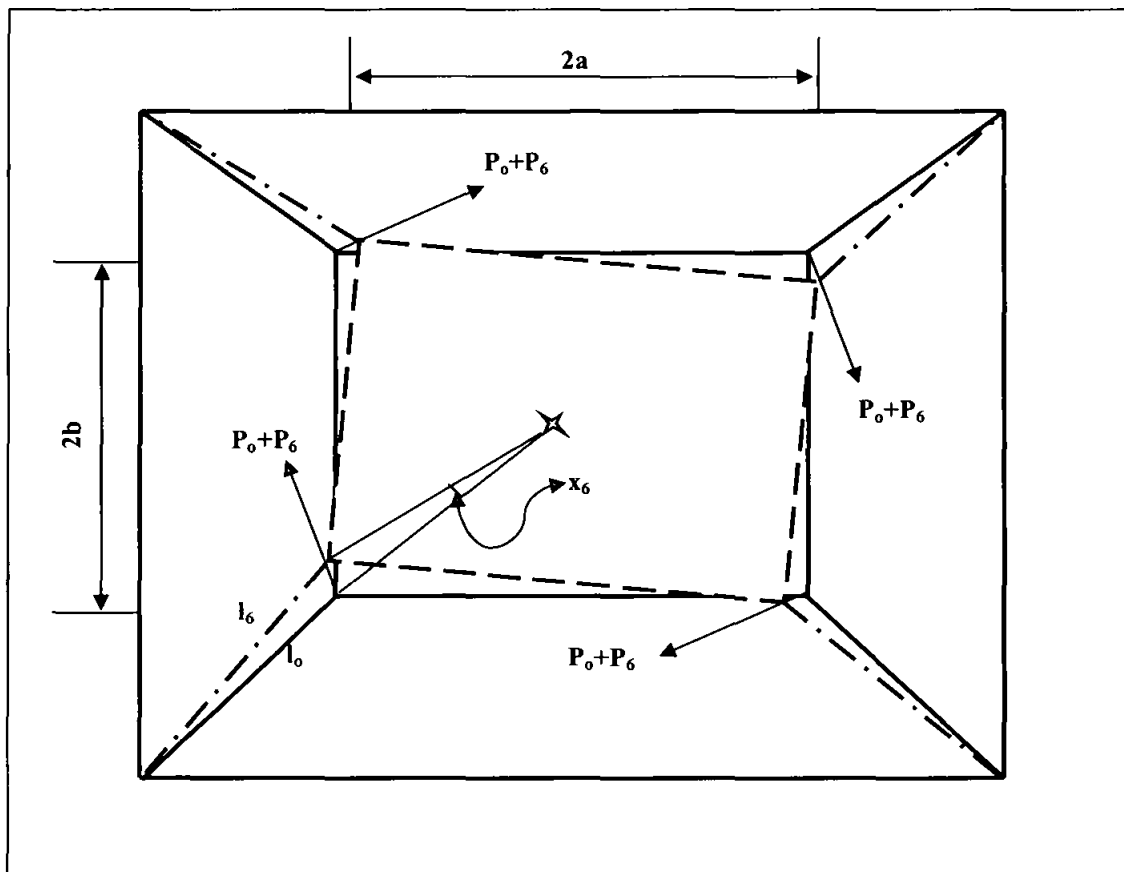


Figure 3.7: Yaw motion

$$k_{66} = \frac{4(P_o + P_6)(a^2 + b^2) \sin \gamma_6}{l_6} \quad (3.143)$$

3.1 Damping matrix

The damping matrix had two parts namely structural damping (C_s) and hydrodynamic damping (C_h). Structural damping was calculated based on a damping ratio (ξ) which was the ratio of the given damping to the critical damping. The hydrodynamic damping was due to hydrodynamic parameters. The structural damping matrix was given below [44-46].

$$[C_s] = \begin{bmatrix} c_{11} & 0 & 0 & 0 & 0 & 0 \\ 0 & c_{22} & 0 & 0 & 0 & 0 \\ 0 & 0 & c_{33} & 0 & 0 & 0 \\ 0 & 0 & 0 & c_{44} & 0 & 0 \\ 0 & 0 & 0 & 0 & c_{55} & 0 \\ 0 & 0 & 0 & 0 & 0 & c_{66} \end{bmatrix} \quad (3.144)$$

While

$$c_{ij} = 2\xi m_i \omega_i$$

The hydrodynamic damping term was time dependent and was obtained by transferring the drag terms from the right hand side of the Equation of motion. This indicated that, the total damping matrix $[C]$ changed at each time step according to variation of structural and hydrodynamic damping matrix. The total damping matrix at each time step were written as

$$[C] = [C_s] + [C_h] \quad (3.145)$$

3.5 Equation of motion

After calculating the wave forces in the structure and formulating the stiffness, mass and damping matrixes, all the components of the Equation of motion were ready. Then Equation of motion could be written as below [39,47-49];

$$[M] \{a_s\} + [C] \{u_s\} + [K] \{x\} = \{F(t, x, u_s, a_s)\} \quad (3.146)$$

Where x , u and a were the displacement, velocity and acceleration of the platform respectively.

3.6 Newmark beta method

The Newmark with constant-average-acceleration method was used to solve the Equation of motion [50-51]. The displacement of the structure at end of the time step was given by Equation (3.147)

$$[\tilde{K}_1] x_1 = [\tilde{F}_1] \quad (3.147)$$

This had the form of a static equilibrium equation involving the effective stiffness matrix $[\tilde{K}_1]$ which was equal

$$[\tilde{K}_1] = K_1 + \frac{2}{h}[C_1] + \frac{4}{h^2}[M_1] \quad (3.148)$$

The effective loading matrix $[\tilde{F}_1]$ is given as below

$$[\tilde{F}_1] = F_1 + \left(\frac{2x_o}{h} + u_{s_o} \right) [C_1] + \left(\frac{4x_o}{h^2} + \frac{4}{h}u_{s_o} + a_{s_o} \right) [M_1] \quad (3.149)$$

Where, the terms M_1 , C_1 , and K_1 referred to mass, damping and stiffness matrices for the first time step respectively.

Using this formulation, the displacement at the end of the time step (x_1) were calculated directly by solving Equation (3.147), using only data that was available at the beginning of the time step. Then, the velocity at that time step (u_{s1}) could be calculated using Equation (3.150). Finally the acceleration at the end of the step (a_{s1}) was derived by solving the dynamic equilibrium Equation at that time, as in Equation (3.151) [51].

$$u_{s1} = \frac{2}{h}(x_1 - x_o) - u_{s_o} \quad (3.150)$$

While

$$a_{s1} = \frac{1}{[M_1]} (F_1 - [C_1]u_{s1} - [K_1]x_1) \quad (3.151)$$

3.7 Solution procedure

The following steps were used in the program to find out the responses of the platform.

1. The wave properties (wave length (L), wave frequency (ω) and wave number (k)) were calculated.
2. Displacement x_0 , velocity u_0 and acceleration a_0 of the platform at first time step were initialized.
3. Stiffness matrix K, mass matrix M and structural damping matrix C were formulated.
4. The wave forces acting on columns were evaluated.
5. The added mass matrix M_a and the hydrodynamic damping matrix C_h due to column effects were determined.
6. The wave forces acting on the pontoons were evaluated.
7. The added mass matrix M_a and the hydrodynamic damping matrix C_h due to pontoon effects were determined.
8. By using Newmark method to solve equation of motion, the displacement, velocity and acceleration for the second time step x_1 , u_1 and a_1 were calculated.
9. Steps 3 to 8 were repeated till time steps are over.

10. The responses, velocity and acceleration were drawn in time series.

According to the above steps a computer program was written using MATLAB programming and its flow chart is shown in Figure (3.8).

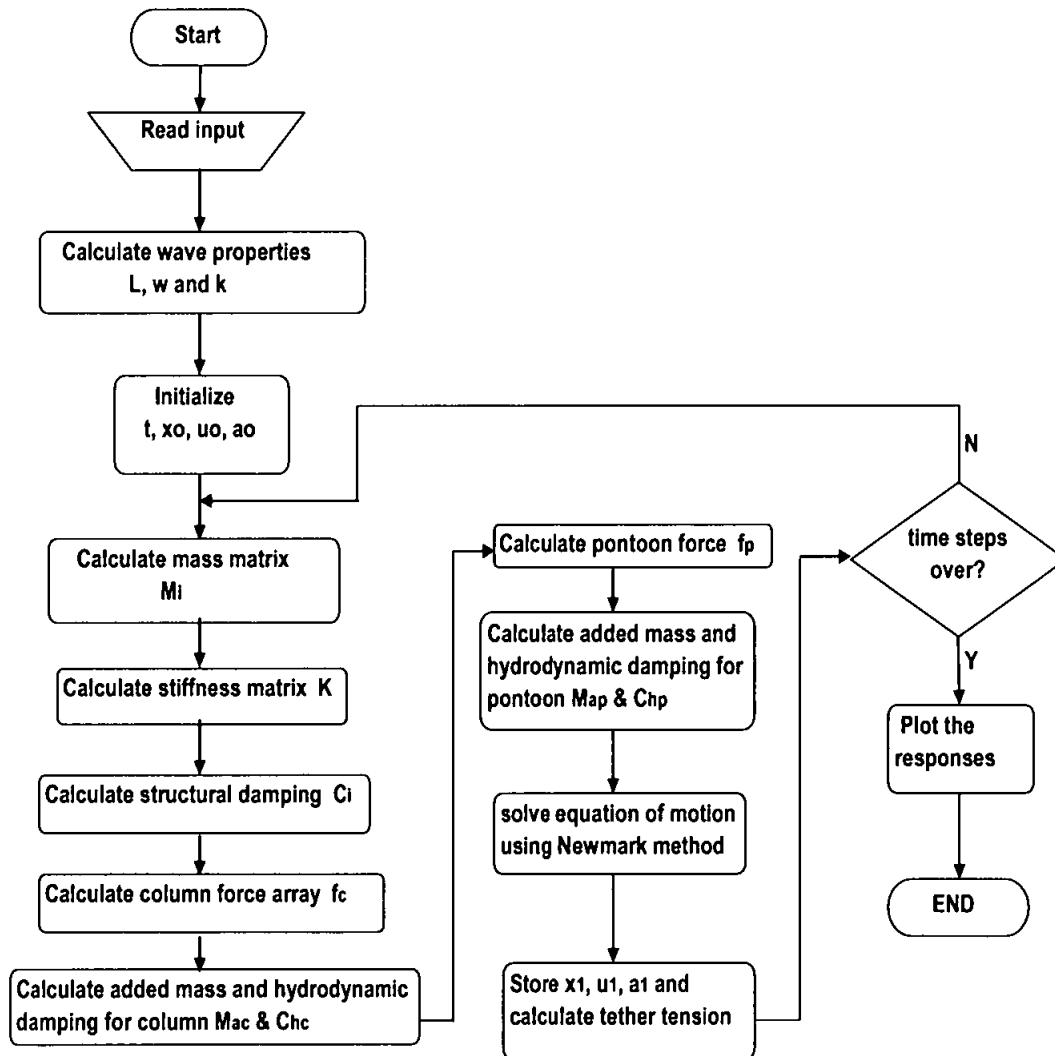


Figure 3.8: Program flow chart

CHAPTER FOUR

RESULTS AND DISCUSSIONS

4.1 Introduction

The discovery of giant fields for oil and gas in deep water has presented a major challenge to the industry, resulting in remarkable developments in the way of equipment, procedures, instrumentation and construction [52]. The dynamic behaviour (motions and tether tensions) of the deep water structures such as TLPs, when it is subjected to wave forces are needed for the design and maintenance of the structure. In this chapter comprehensive studies on the behaviour of TLP to determine the TLP responses are discussed. The main content of this chapter is predicting accurate responses for the platform under different parameters and load conditions by using different theories and approaches like varying hydrodynamic coefficients, different wave theories, frequency and time domain analysis. Limiting these responses forms the second part of this chapter by studying different TLP shapes square, triangular, and inclined tether TLP concept. Limiting the responses of the platform leads to better stability and safe drilling operations. The response amplitude operators (RAO) for typical TLPs have been compared with recorded results in the literature.

4.2 Selected data

The TLPs with the details given in Table 4.1 were selected for the numerical studies. Four square TLPs and one triangular TLP were chosen. TLP₁ is a square TLP. It was used to validate the results using studies reported in literature. TLP₂ is a square TLP and it was used as the main (reference) platform while the all other platforms were compared related to its behaviour. TLP₃ is the triangular TLP while TLP₄ and TLP₅ are inclined-tether TLPs. The last four TLPs were subjected to different load cases with

different parameters and their responses were determined and compared. A regular wave with 8 m height and 10 second period was applied with 45° incident angle to show the responses in all the six degrees of freedom due to regular wave in time series mode. A random wave of significant wave height 5 m using Pierson-Moskowitz (P-M) spectrum was chosen for the wave load calculations (Figure 4.1).

Table 4.1: Platforms details

Description	TLP ₁	TLP ₂	TLP ₃	TLP ₄	TLP ₅
length (m)	70	75.66	75.66	75.66	75.66
D _c (m)	17	14	19.42	14	13.85
d (m)	600	300	300	300	300
D _p (m)	12	12	12	12	12
ξ	0.04	0.05	0.05	0.05	0.05
F _b (kN)	521,600	465,500	465,500	465,500	463,441
G _i (kN/m)	84,000	34,000	34,000	34,000	34,000
h _c (m)	28.44	27.47	27.47	27.47	27.47
Tether length (m)	568	269	269	273.15	273.15
P _{ot} (kN)	170,000	135,500	135,500	137,590	135,500
r _x (m)	35.1	35.1	35.1	35.1	35.1
r _y (m)	35.1	35.1	35.1	35.1	35.1
r _z (m)	42.4	42.4	42.4	42.4	42.4
ρ (Kg/m ³)	1030	1030	1030	1030	1030
W(kN)	351,600	330,000	330,000	330,000	330,000

4.3 Discussion of the results

The analyses were conducted for twenty frequencies varying from 0.05 Hz to 0.25 Hz at interval of 0.01 Hz. The heights of response from the program were divided by corresponding wave height to obtain the Response Amplitude Operator (RAO). The RAOs were calculated and analyzed for all the above mentioned TLPs.

4.3.1 Square TLPs

Comprehensive studies were conducted on the square TLPs and responses determined as time series and in RAO form. The studies were conducted in frequency

and time domain. Different wave theories and varying hydrodynamic coefficients were used. Parametric studies were also conducted varying water depth, tether pretension, CG position and wave incident angle.

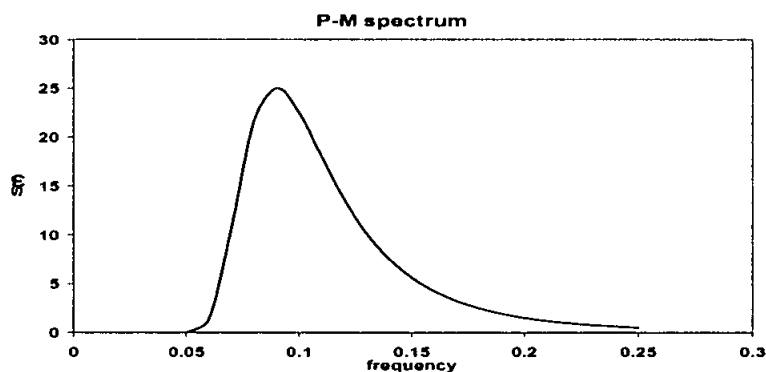


Figure 4.1: P-M spectrum

4.3.1.1 Frequency domain analysis

The Frequency Domain (FD) analysis is inherently linear, and in order to apply the approach to a nonlinear problem, all nonlinearities must be linearized. Due to the approximations made, the linearized frequency domain approach could not be expected to match the nonlinear time domain method exactly, and the expected degree of accuracy was not as well established due to the limited literature on the topic [53-54]. The frequency domain analysis results for TLP₂ have been briefly discussed in this chapter and its degree of accuracy established compared with time domain analysis.

Figures 4.2 to 4.5 show the responses for surge, heave, pitch and tether tension in RAO form. The highest value of RAO surge was 0.78 m/m at frequency 0.09 Hz which was the peak frequency of the P-M spectrum. The most effective period for heave response was between the frequencies 0.1 to 0.18 Hz with peak value 1.43 mm/m at 0.13 Hz. The pitch response had three similar peaks, the highest one being 4.3×10^{-5} (rad/m) at 0.14 Hz. The period between 0.1 to 0.23 Hz represented the most important frequencies in the tether tension while the peak value 74 kN/m occurred at 0.12 Hz. The surge, heave, pitch and tether tension responses spectra are shown in Figures 4.6 to 4.9.

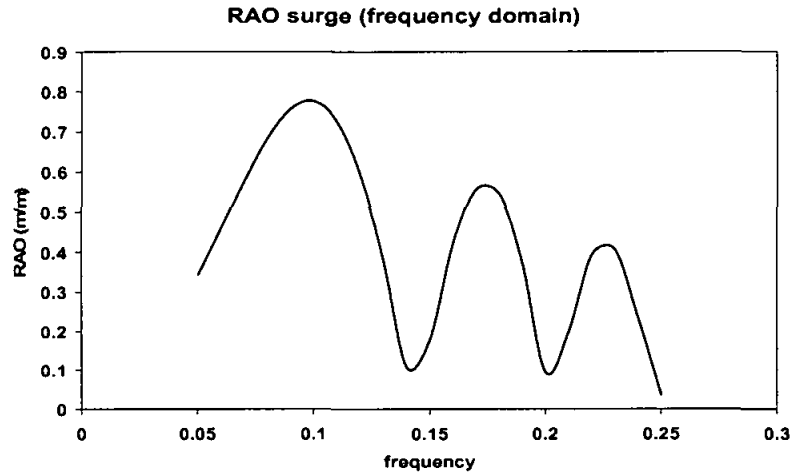


Figure 4.2: RAO surge.

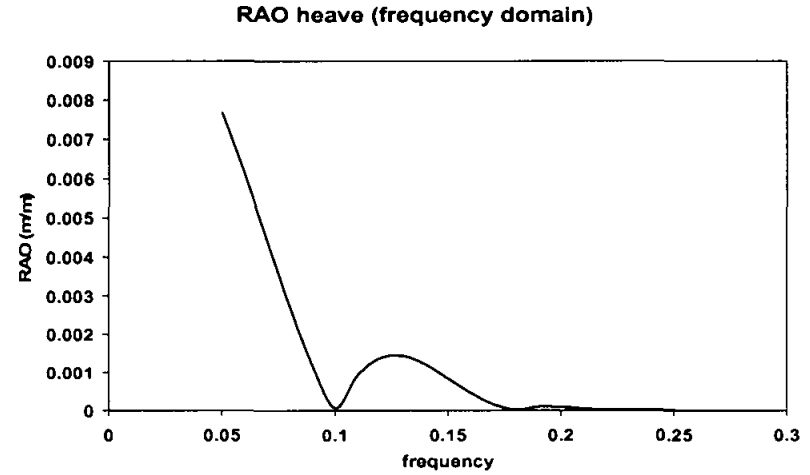


Figure 4.3: RAO heave.

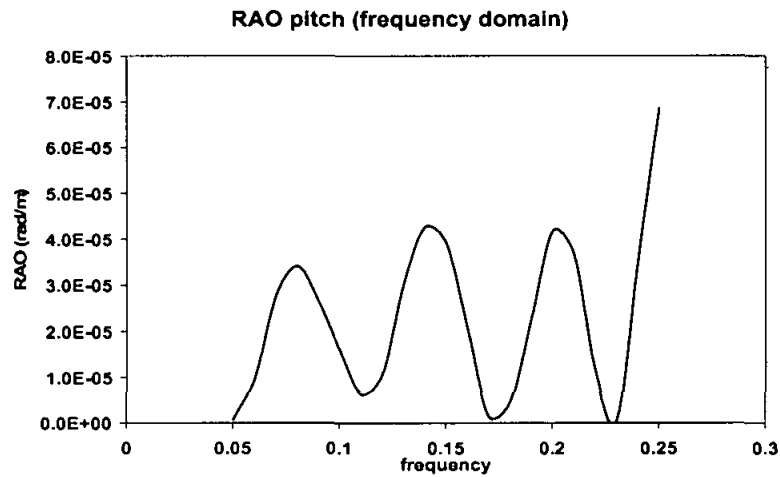


Figure 4.4: RAO pitch.

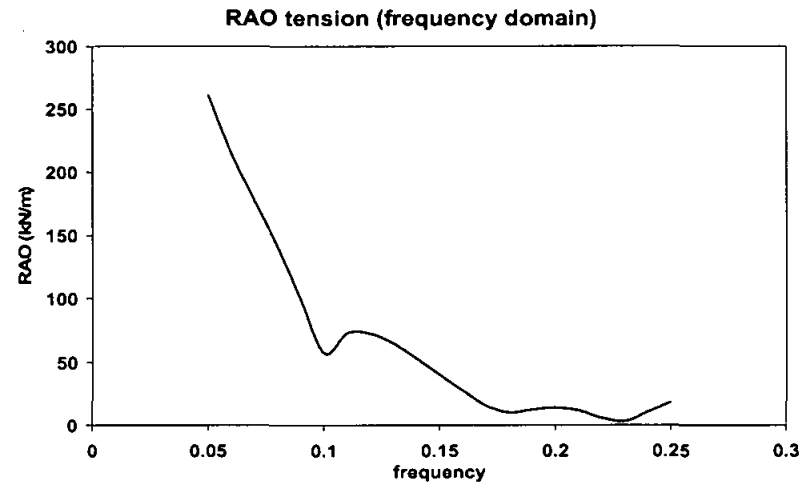


Figure 4.5: RAO tether tension.

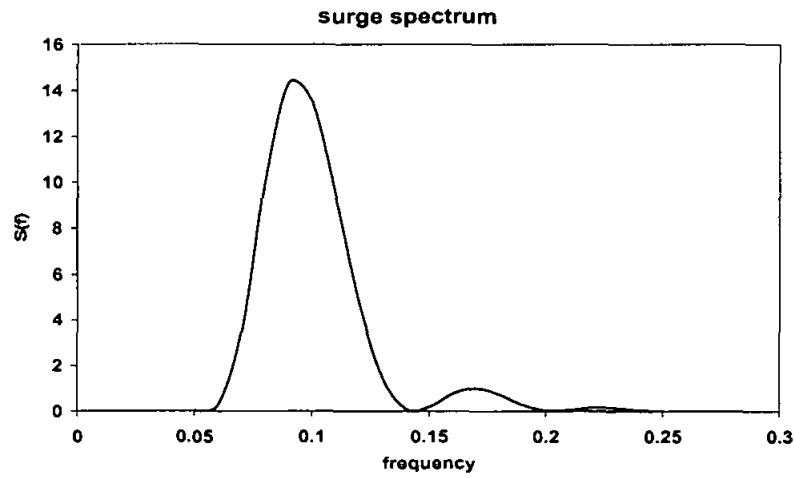


Figure 4.6: Surge spectrum

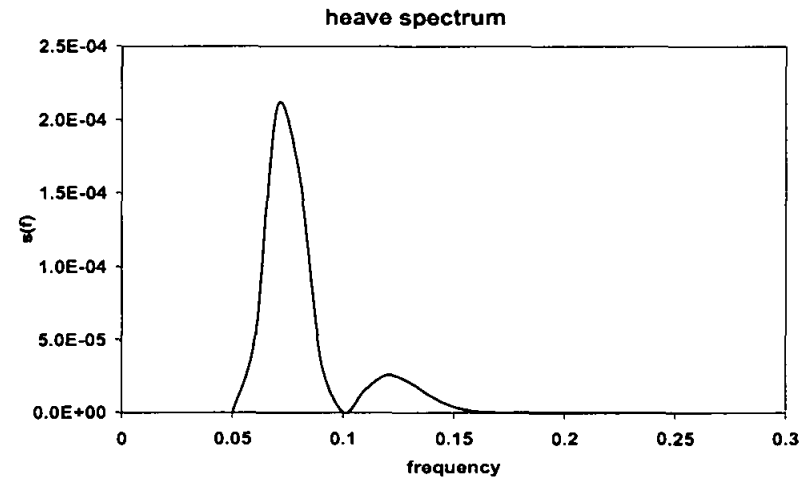


Figure 4.7: Heave spectrum

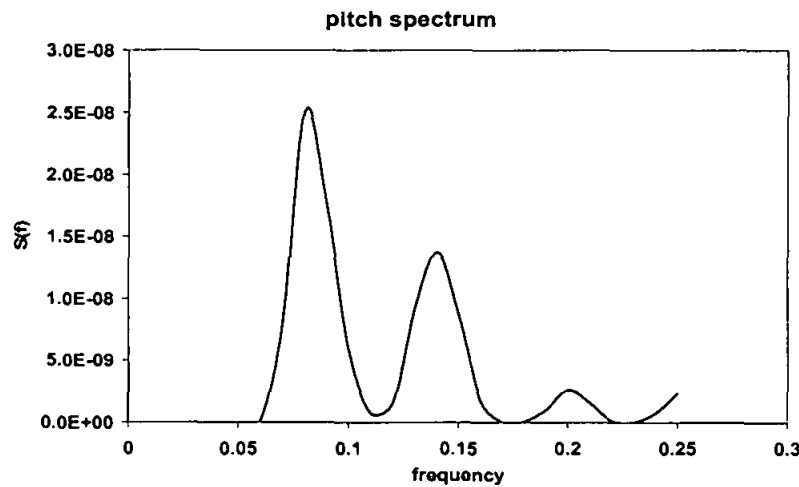


Figure 4.8: Pitch spectrum

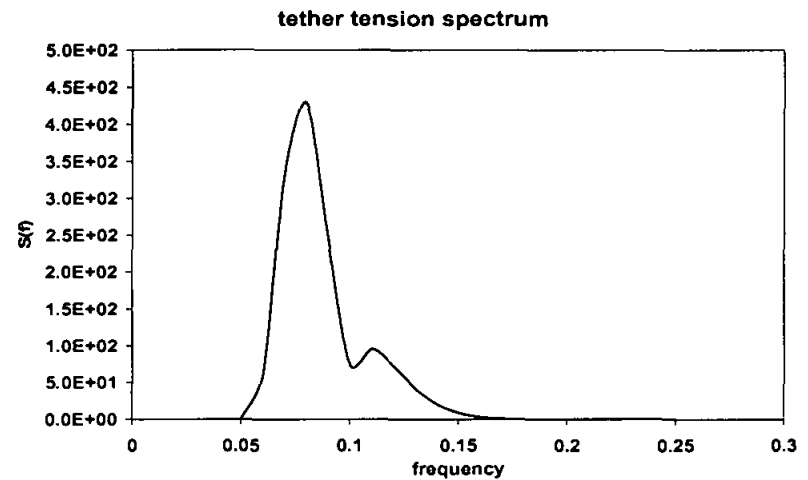


Figure 4.9: Tension spectrum

From the above spectra, the responses could be converted as time series shown in Figures 4.10 to 4.13 which represent the actual response of the platform. The surge response was following a random trend with 1.8 m as the maximum response. The maximum heave response was 5.9 mm. The maximum pitch maximum response was 8.2×10^{-4} rad and 354 kN was the maximum value for the tether tension.

4.3.1.2 Time domain analysis

The Time Domain (TD) analysis was inherently more stable than the frequency domain analysis and it took the nonlinear factors in to consideration. The time domain analysis is the most efficient dynamic analysis for solving the equation of motion by integrating in time applying the Newmark beta method.

The regular wave with details given in section 4.2 was applied to the platform TLP₂ and the responses are given in Figures 4.14 to 4.19. The responses had a transient period before reaching the final stable response as seen in the figures. The surge and sway responses were almost same in the trends and values. The roll and pitch responses were also similar in trends and in values.

4.3.1.2.1 Random wave results

The Response Amplitude Operator (RAO) has been the most accurate and common criterion to evaluate and compare the random responses. The results of the square TLP₂ were studied as RAO in time domain analysis for surge, heave, pitch and tether tension in Figures 4.20 to 4.23. Excluding the low wave frequencies (less than 0.07 Hz), the highest RAO for surge response was 1.26 m/m at 0.14 Hz with periodic peaks decreasing gradually with the higher wave frequencies. Due to the sensitivity of the heave response to the wave height, the meandrous RAO curve was obtained and the highest RAO for heave was 1.1 mm/m at 0.12 Hz. The period between 0.07 to 0.18 Hz represented the most effective period in pitch and tether tension life with peak values 1.7×10^{-4} rad/m and 218 kN/m respectively.

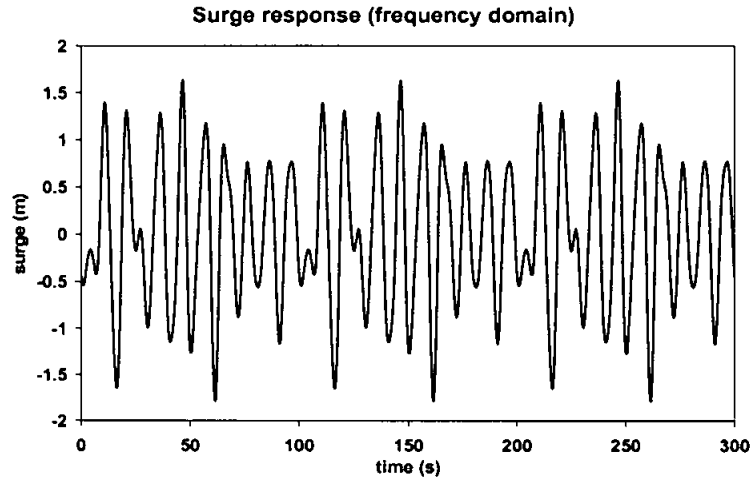


Figure 4.10: Surge response

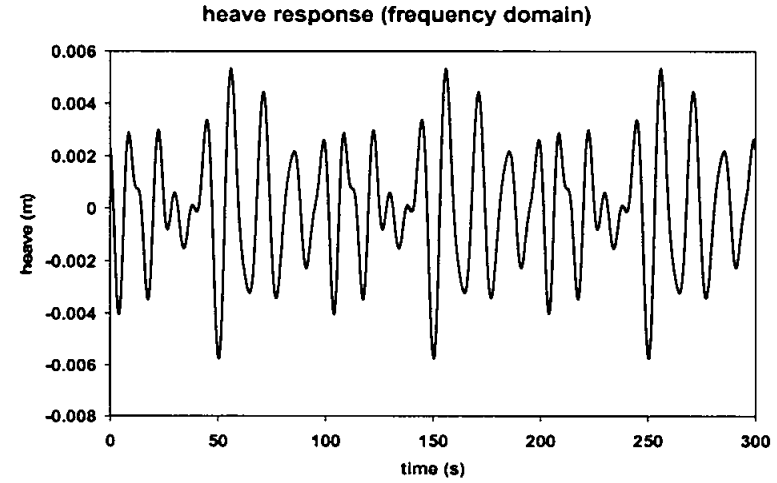


Figure 4.11: Heave response

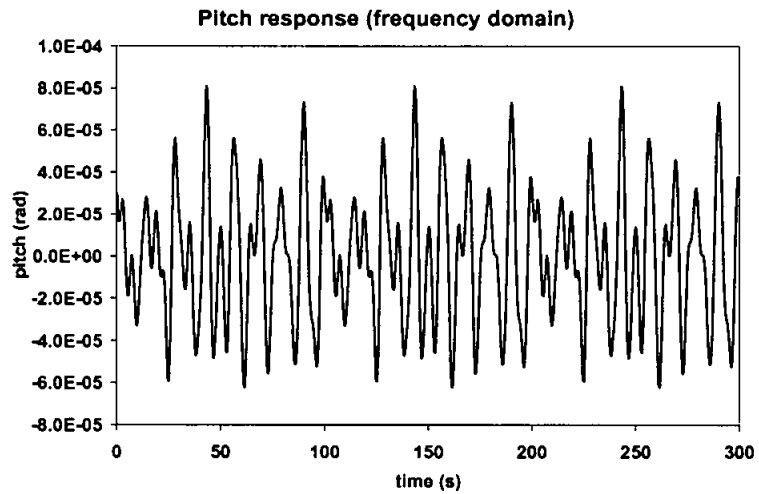


Figure 4.12: Pitch response

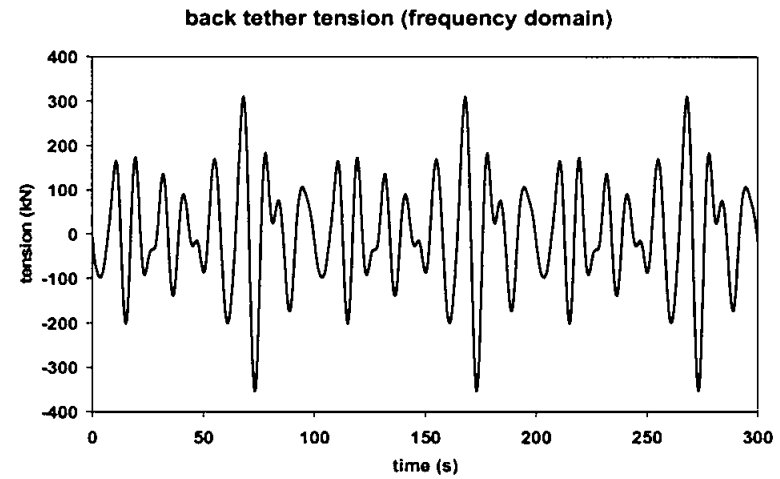


Figure 4.13: Tether tension

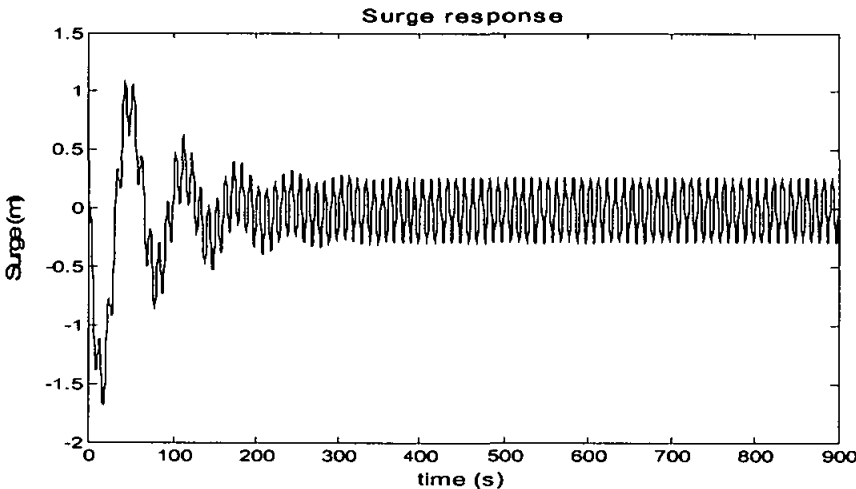


Figure 4.14: Surge responses in regular wave

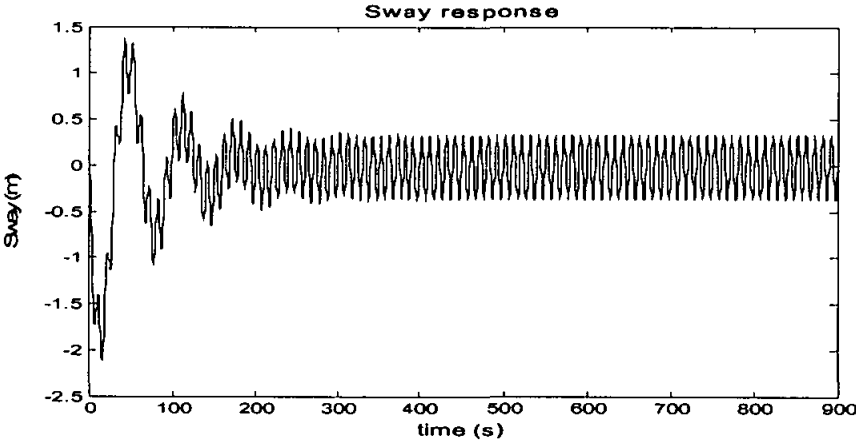


Figure 4.15: Sway responses in regular wave

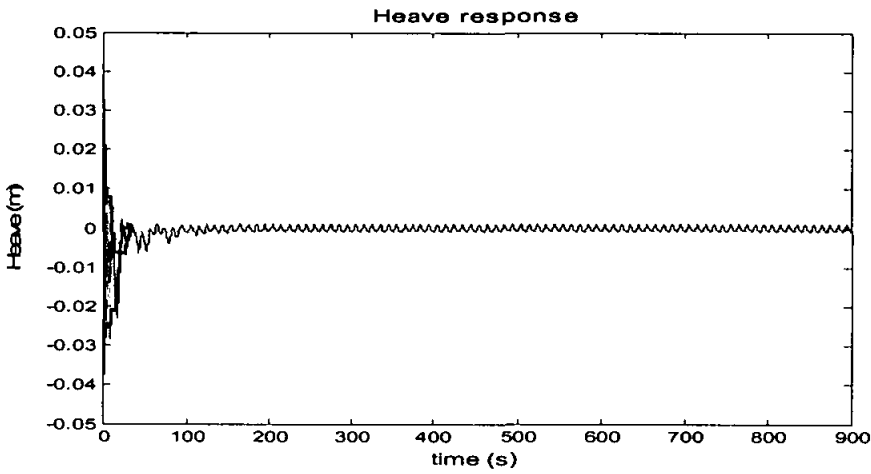


Figure 4.16: Heave responses in regular wave

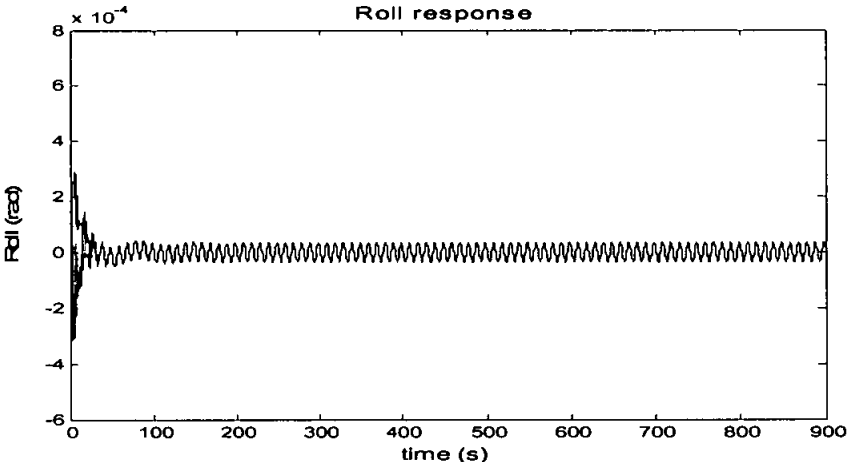


Figure 4.17: Roll responses in regular wave

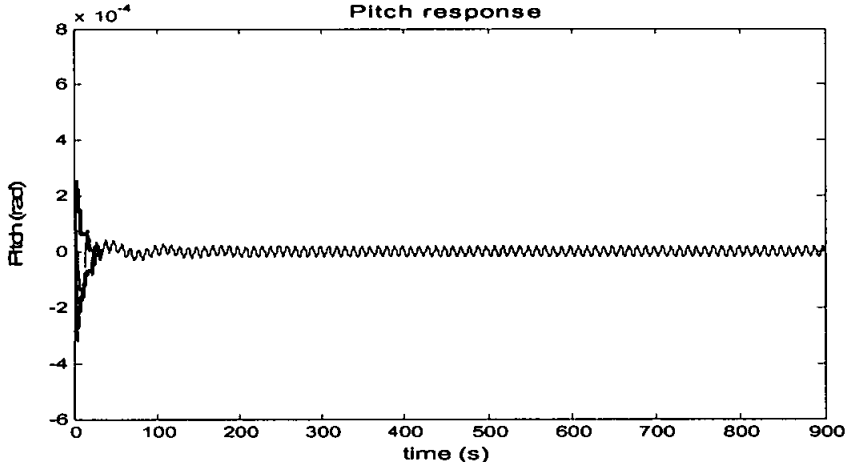


Figure 4.18: Pitch responses in regular wave

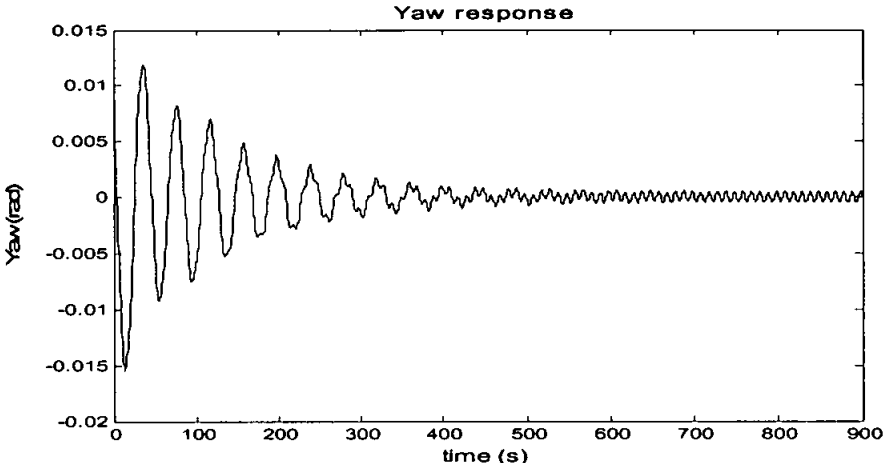


Figure 4.19: Yaw responses in regular wave

4.3.1.2.2 Typical responses

The typical responses in surge, heave, pitch and tether tension for the above mentioned platform, were determined by converting the RAOs to the time series. Figures 4.24 to 4.27 showed that the responses in surge, heave, pitch and tether tension and these follow a similar pattern as the input time series generated by the selected P-M spectrum.

The maximum responses were 2 m in surge, 2.5 mm in heave, 0.00036 radians in pitch and 420 kN for tether tension. These are within the permissible limits.

4.3.1.2.3 Results validation

The square TLP₁ was used to compare and validate the results with the results reported in the literature. Figure 4.28 compared the results in surge and tether tension, obtained on TLP₁ for the University College London (UCL), results in Indian institute of technology, Madras (reported by Kurian V. John. [39]) with MATLAB computer program which was developed in this study.

The surge RAO for the current study followed same trend for UCL and Kurian results with slight more or less values. The program showed a bit higher values for the period between 0.10 to 0.15 Hz probably because of the effects of recalculated hydrodynamic coefficients in the program. These will be discussed in detail for the three degrees of freedom in the coming paragraphs.

The results obtained for tension RAO fluctuated between the lower and higher values of Kurian and UCL results. The period between 0.11 to 0.134 Hz recorded a bit higher RAO values and the period between 0.07 to 0.11 Hz recorded a bit lower RAO values probably because of the effects of recalculated hydrodynamic coefficients as mentioned before.

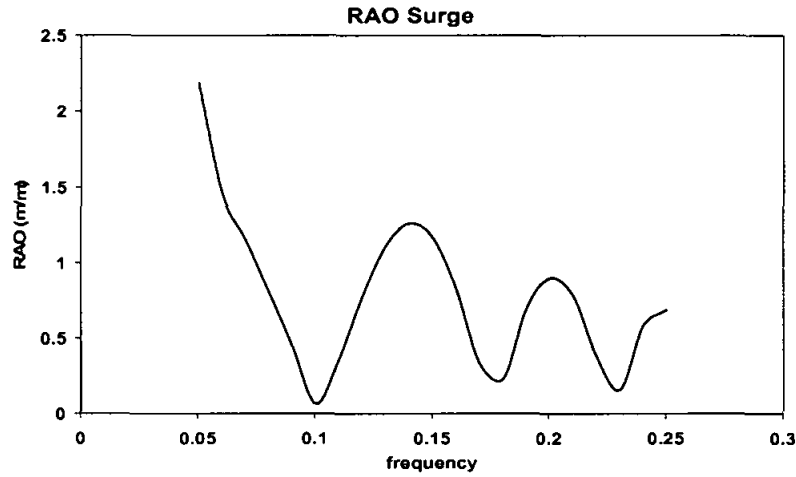


Figure 4.20: RAO Surge in time domain for TLP₂

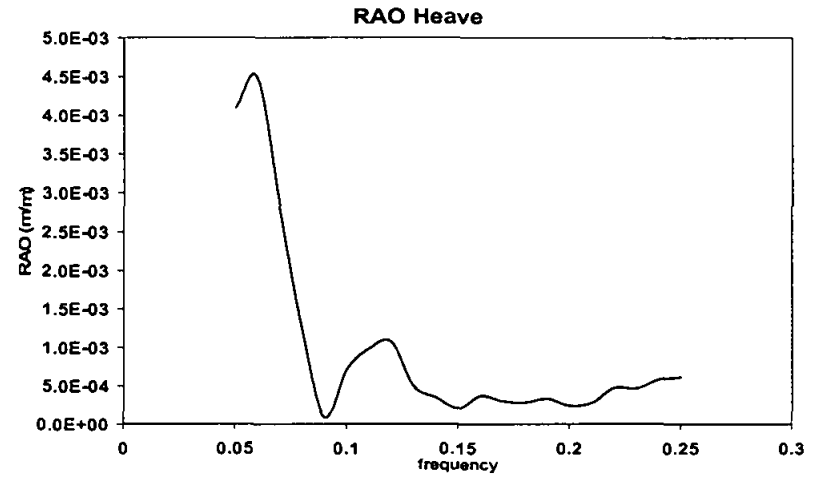


Figure 4.21: RAO Heave in time domain for TLP₂

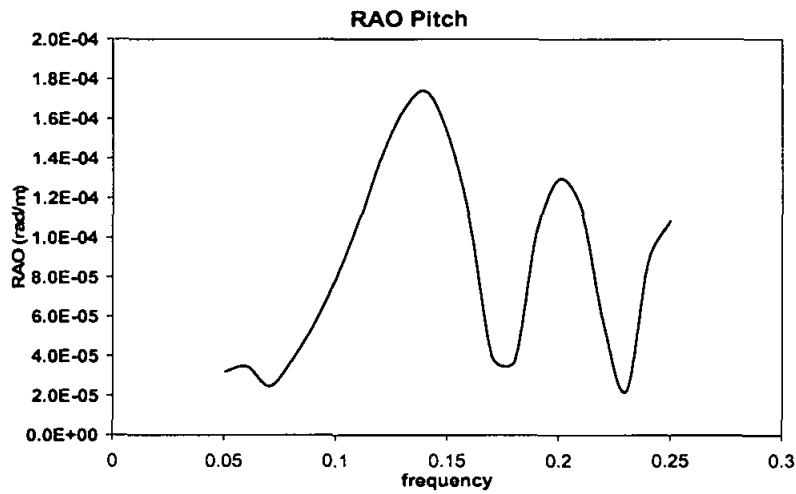


Figure 4.22: RAO Pitch in time domain for TLP₂

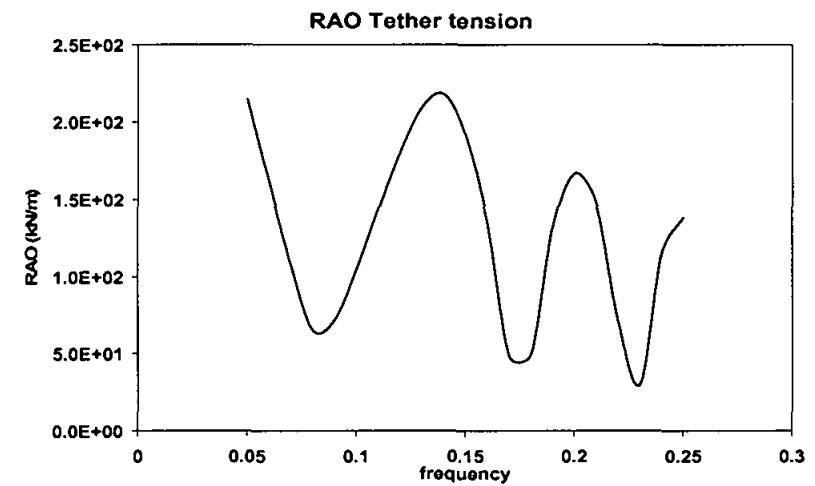


Figure 4.23: RAO tension in time domain for TLP₂

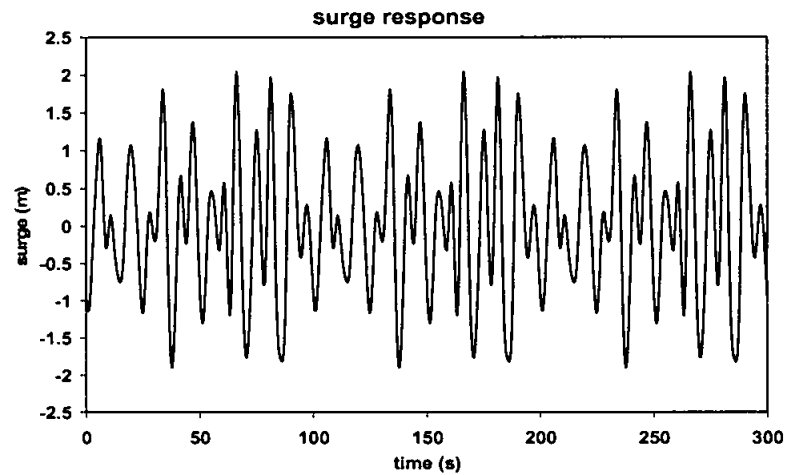


Figure 4.24: Surge response in time domain for TLP₂

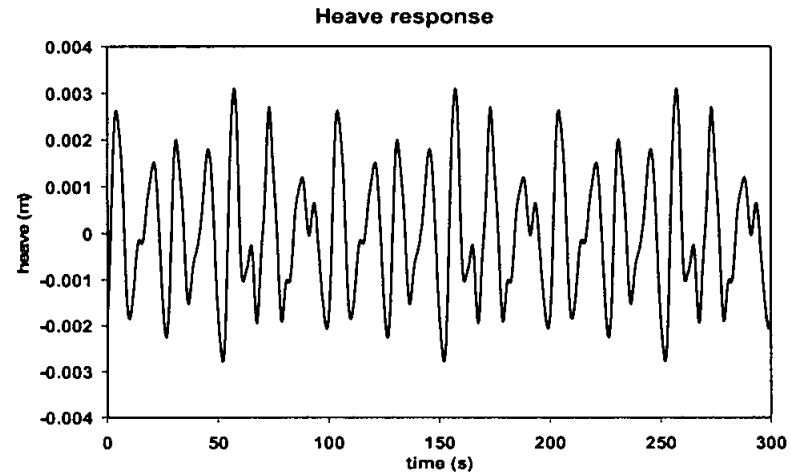


Figure 4.25: Heave response in time domain for TLP₂

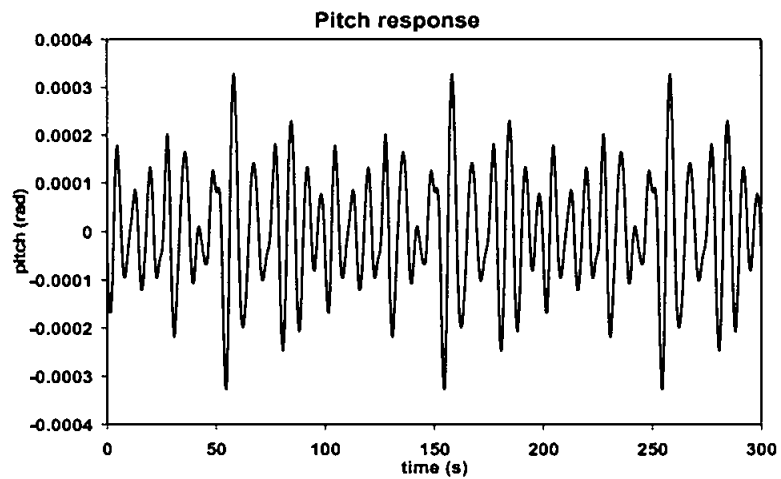


Figure 4.26: Pitch response in time domain for TLP₂

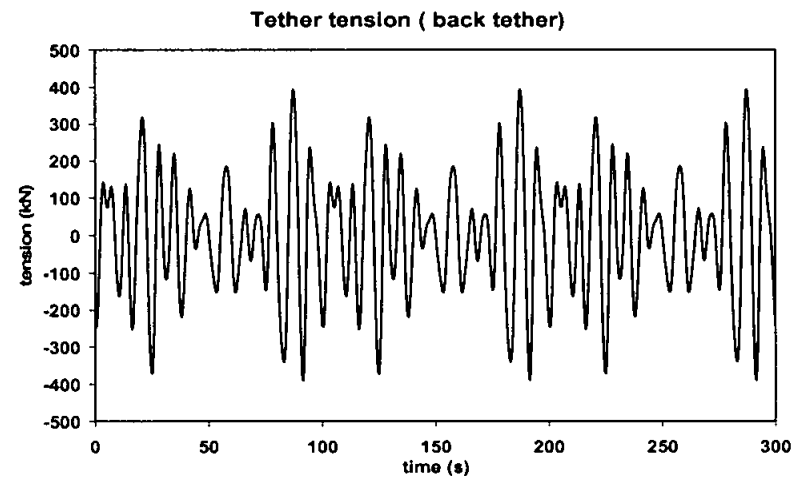


Figure 4.27: Tether tension in time domain for TLP

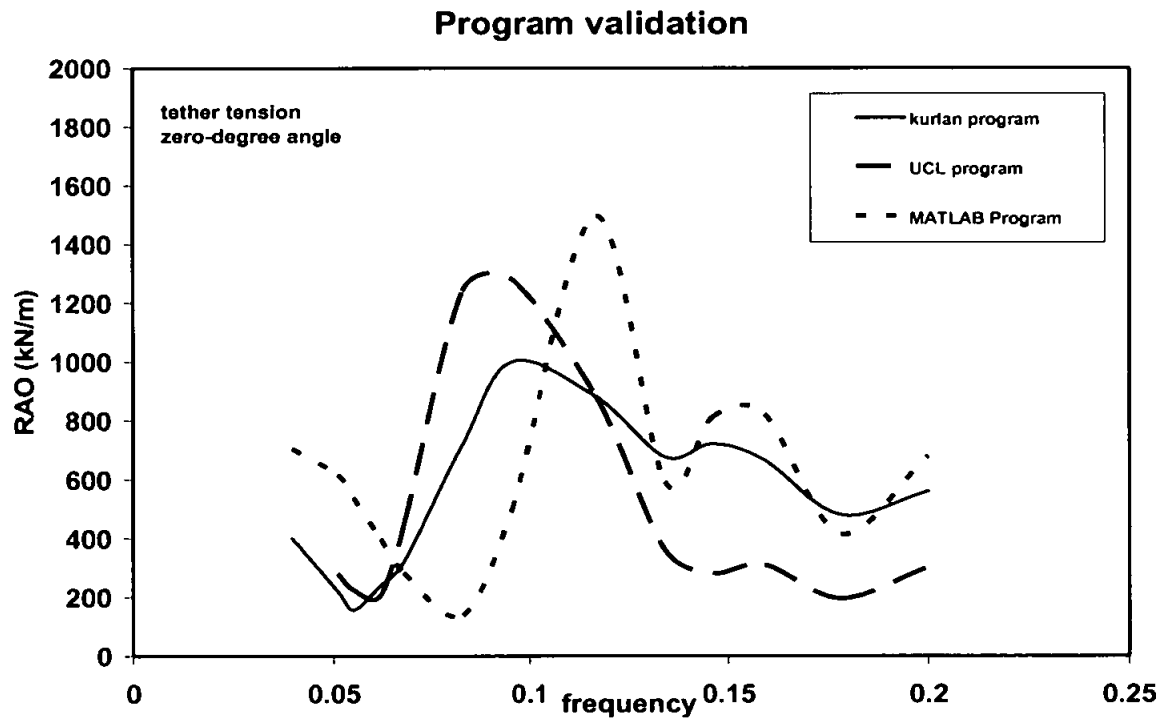
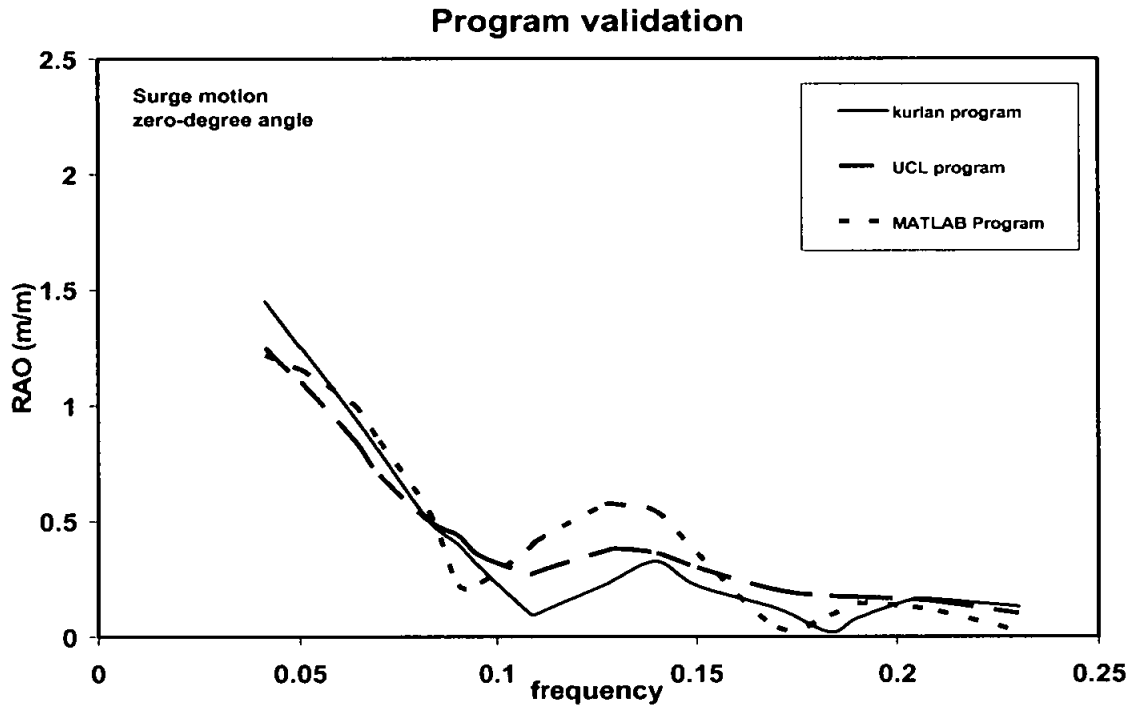


Figure 4.28: Results validation for surge and tether tension

4.3.1.2.4 Comparison of Frequency and time domain results

Due to the differences in approaches and approximations, the comparisons between time and frequency domain is not fair. Yet these comparisons are shown in this work to assess the degree of accuracy for the frequency domain analysis. Figures 4.29 to 4.32 summarized the comparisons of responses as RAO for surge, heave, pitch and tether tension.

RAO surge in frequency domain was less than that for time domain, with a shift of frequency for peak values. The surge response calculated using frequency domain analysis was smaller than the equivalent surge response calculated by time domain analysis by about 19%

RAO heave in frequency and time domain were same in trend and near in values with bit higher values for the frequency domain between the frequencies 0.12 to 0.16 Hz. Heave response of frequency domain was higher than the heave response of time domain by about 35%.

The RAO calculated using the frequency domain analysis showed the inaccuracy of the frequency domain analysis in the prediction of the pitch response. Although the trends of the RAOs were same, the values of time domain were more the double of the frequency domain response.

Excluding the period less than 0.07 Hz, tether tension RAO by TD was higher than FD. The tether tension of TD was more than FD by 25%. According to the above comparisons, the frequency domain analysis was less accurate, because of the elimination of nonlinearities in the drag term, thereby underestimating the wave forces on the platform. Moreover the FD depends on the uncoupled analysis and hence is not preferred to be used in the design of real projects.

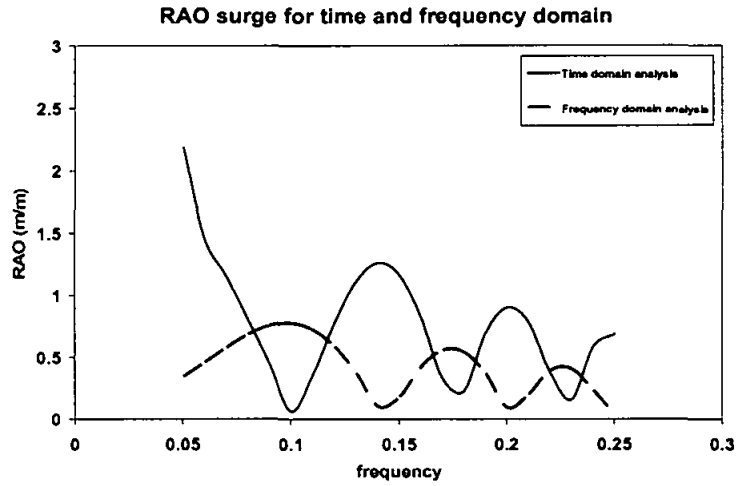


Figure 4.29: RAO surge for TD and FD

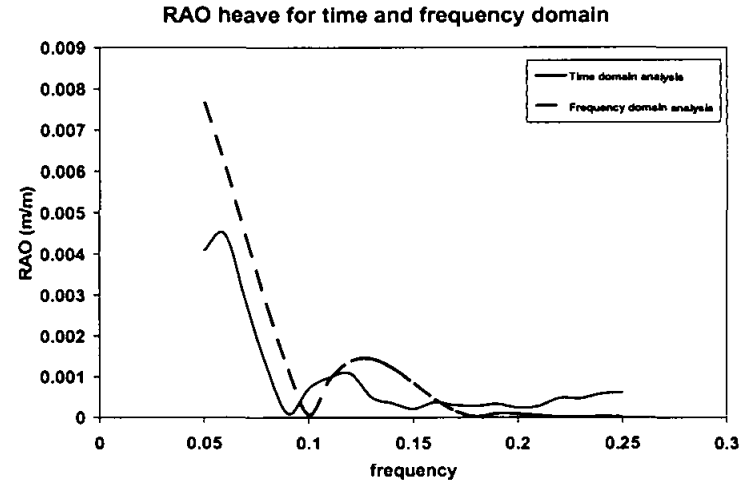


Figure 4.30: RAO heave for TD and FD

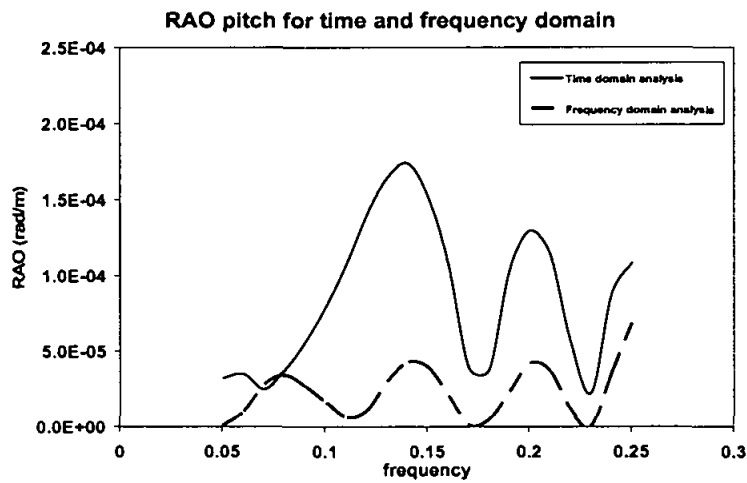


Figure 4.31: RAO pitch for TD and FD

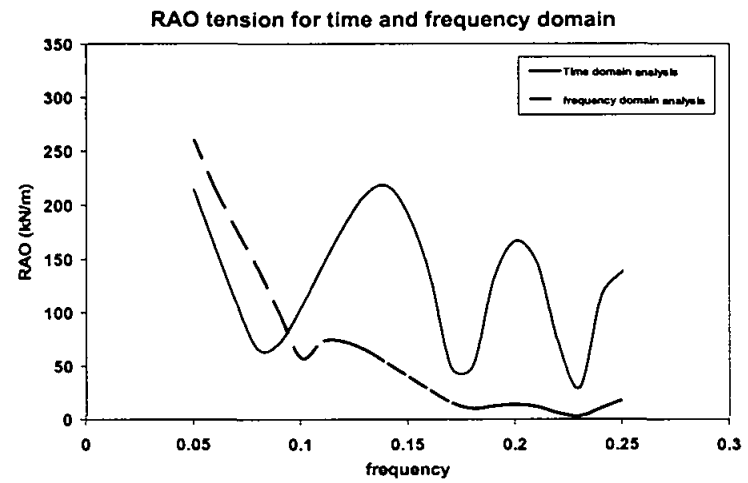


Figure 4.32: RAO tension for TD and FD

4.3.1.3 Square TLP Parametric studies

The square platform TLP₂ was used for the parametric studies. Water depth, tether pretension, center of gravity (CG) position, wave angle and hydrodynamic coefficients were varied and studied. The above mentioned parameters were important for study because of the possibility for them to change during installation and operation procedures.

4.3.1.3.1 Water depth

Figures 4.33 to 4.35 showed that water depth affected only surge response mainly. It could be observed that raising water depth from 300 m to 900 m increased the maximum surge RAO by about 47%. The effect on heave and pitch responses were only very little.

4.3.1.3.2 Tether pretension

Three values of pretension were used namely 101000, 135500 and 170000 kN. Figures 4.36 to 4.38 showed that, for a 25% increase of pretension, the surge response decreased by about 10% and there was no considerable effect on heave and pitch response. Similarly, for a 25% decrease of pretension, the surge response increased by about 10%, and there was no considerable effect on heave and pitch response. These agree with the fact that increasing the pretension increased the restraint on the platform and thereby decreased the responses.

4.3.1.3.3 Center of gravity position

Figures 4.39 to 4.41 showed that the change in center of gravity (CG) had no effect in surge and heave degrees of freedom, but the pitch response decreased by about 33% when the CG was decreased by 4 m downward. The reason of decreasing pitch response due to decreased CG position was that reducing CG position reduced the balancing moment that affected pitch response.

4.3.1.3.4 Wave angle

The change of wave angle generated responses in all the six degrees of freedom. The surge response at 45° wave angle was about 65% of that at zero wave angles. The heave and pitch responses at 45° wave angle were about 55% of that at zero wave angle. The sway response at 45 degree wave angle was three times that at 15 degree angle. The 45 degree wave angle increased the roll response by 59% from that at 15 degree wave angle. The yaw responses at all the 3 inclinations were nearly the same. Increasing wave angle decreased the x axis components and increased the y axis components. Figures 4.42 to 4.47 gave the wave angle effects.

4.3.1.3.5 Second order wave theory and hydrodynamic coefficients

It was decided to check the results of our study by comparing Airy linear wave theory and second order wave theory to see the degree of convergence between the results.

The hydrodynamic coefficients (inertia and drag) were taken at each point on the platform according to its position (case one) and refreshed at each time step to give more accuracy in response calculation. The fixed hydrodynamic coefficients (case two) approach was compared with case one and their effects were compared for surge heave and pitch responses. Figures 4.48 to 4.50 compared the responses by Airy linear wave theory, second order wave theory and varied hydro dynamic coefficients. The Figures showed that in the current study there were no changes in responses whether Airy linear wave theory or second order wave theory were used. The responses by using varied hydrodynamic coefficients were more than that due to fixed hydrodynamic coefficient by about 15% in surge, 21% in heave and 22% in pitch.

4.3.2 Triangular TLP

The triangular TLP₃ with the details given in Table 4.1 was selected for the study. The studies were conducted in time domain and it included random wave

applications, parametric studies and comparisons between square and triangular TLPs in all degrees of freedom under random wave excitation.

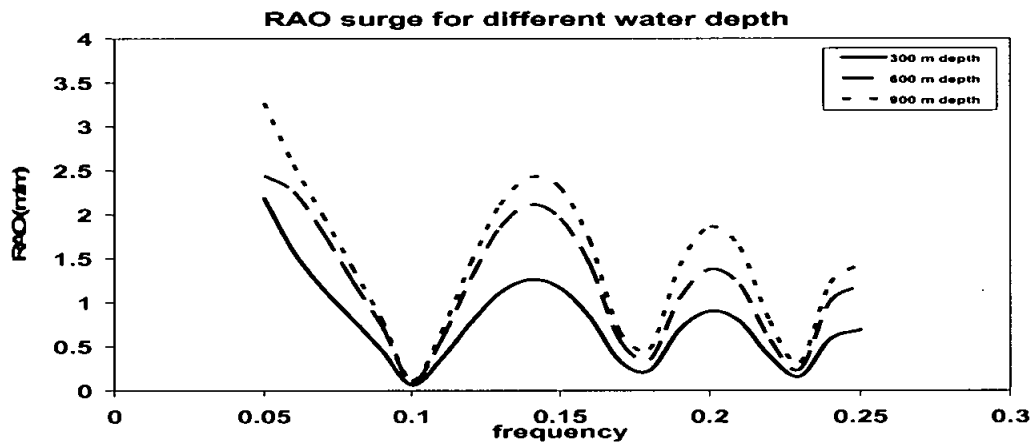


Figure 4.33: RAO surge for different depths

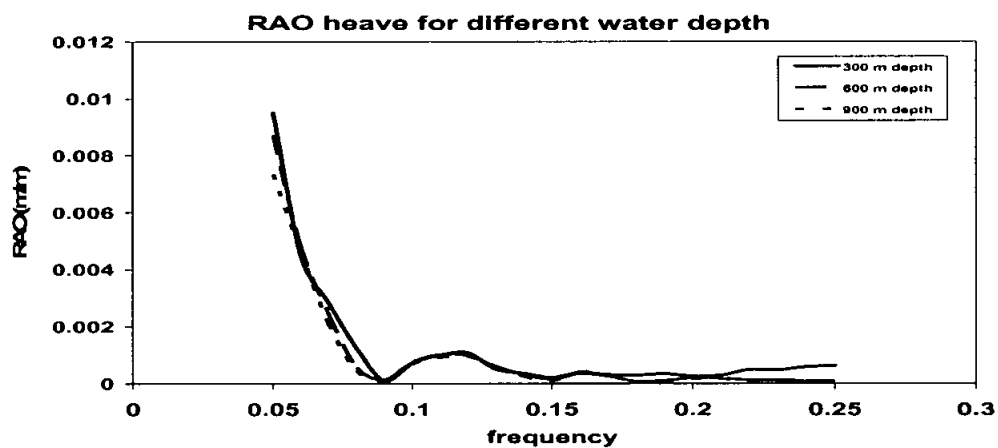


Figure 4.34: RAO heave for different depths

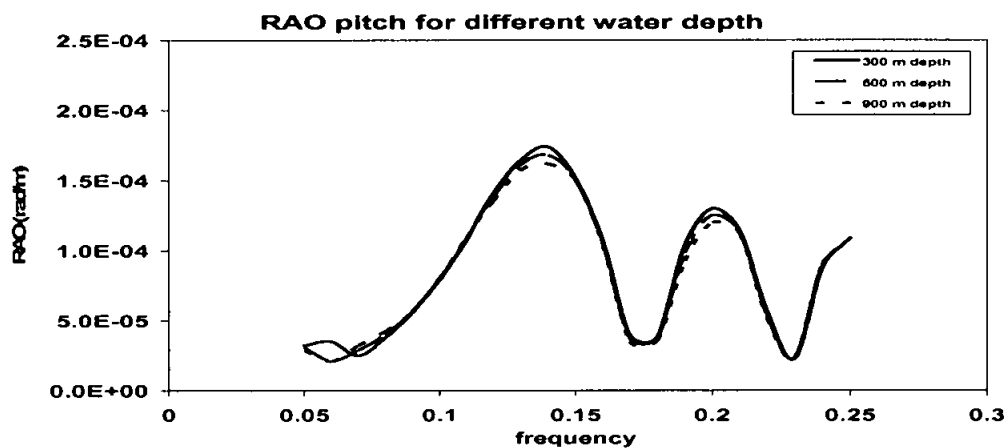


Figure 4.35: RAO pitch for different depths

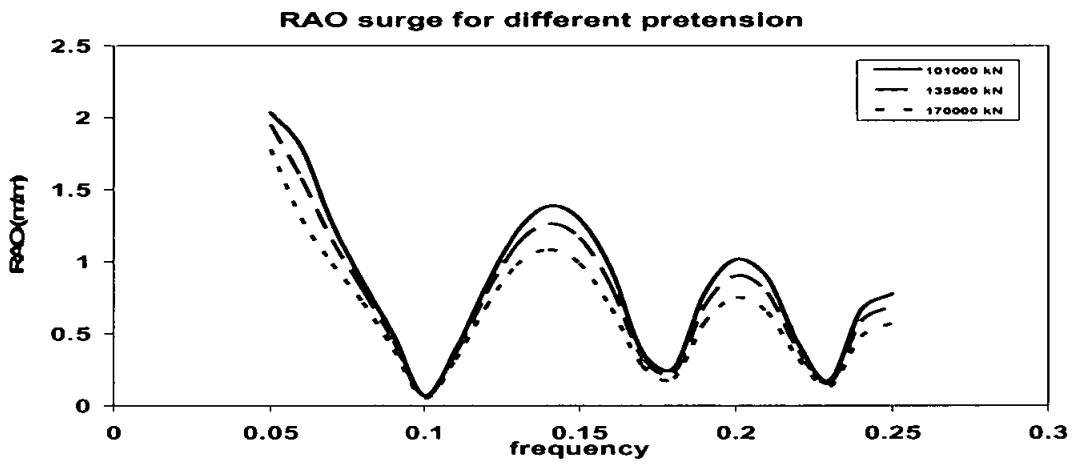


Figure 4.36: RAO surge for different pretension

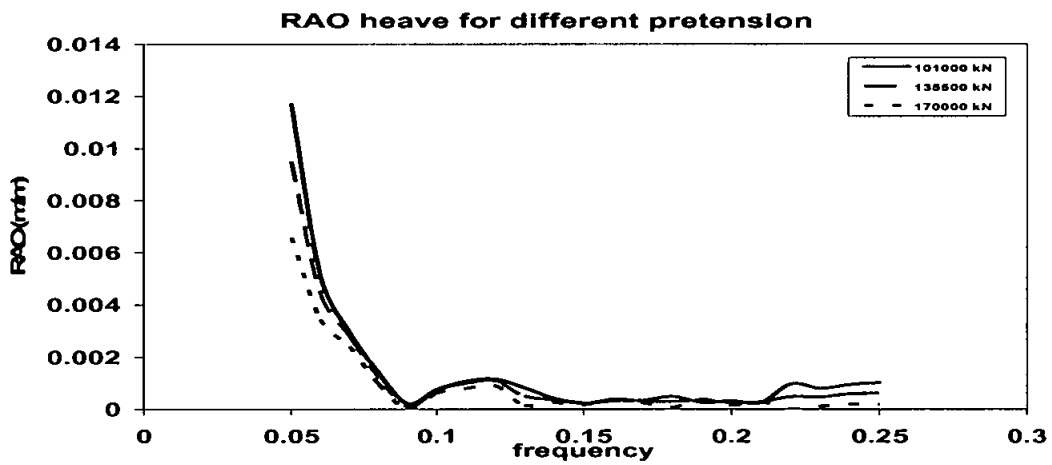


Figure 4.37: RAO heave for different pretension

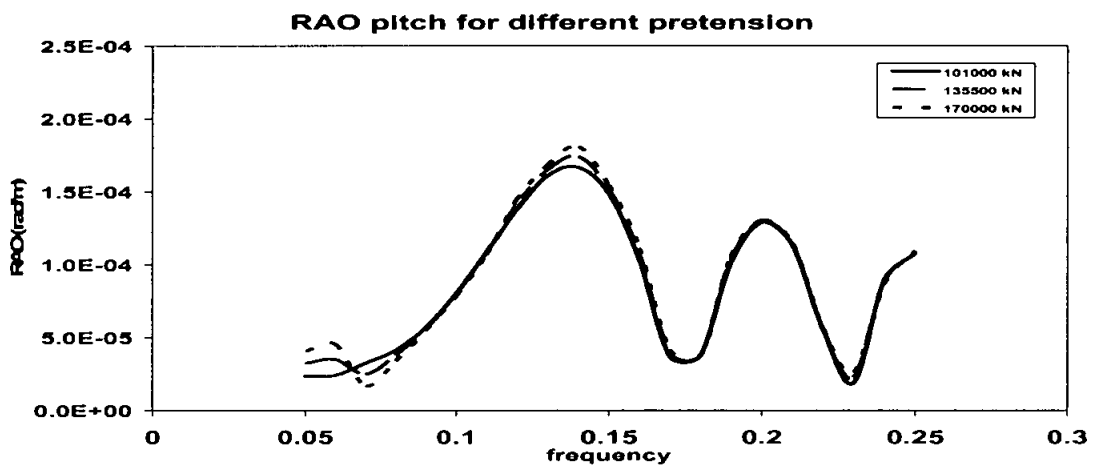


Figure 4.38: RAO pitch for different pretension

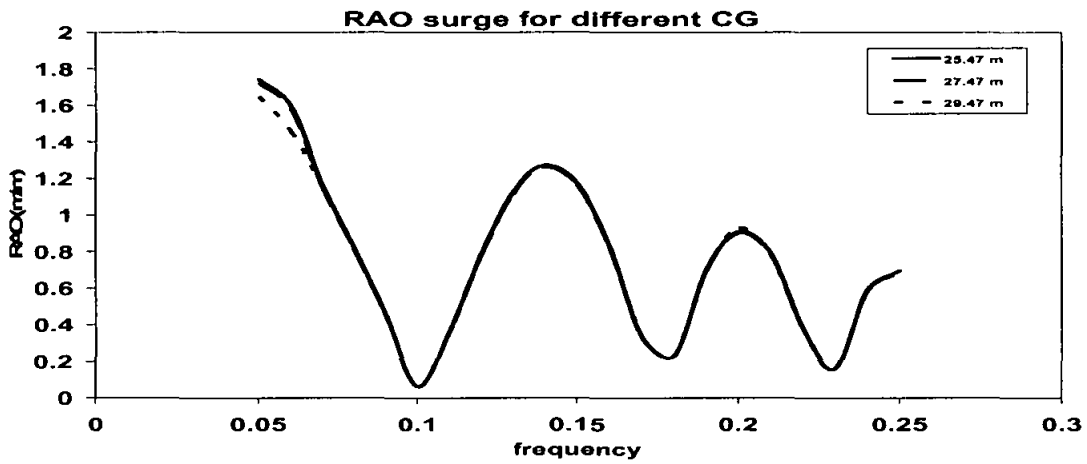


Figure 4.39: RAO surge for different CG position

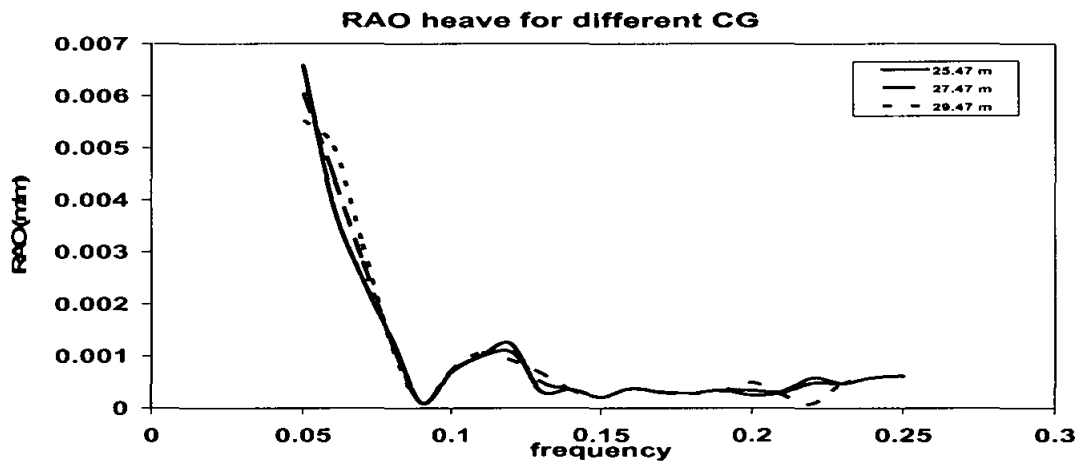


Figure 4.40: RAO heave for different CG position

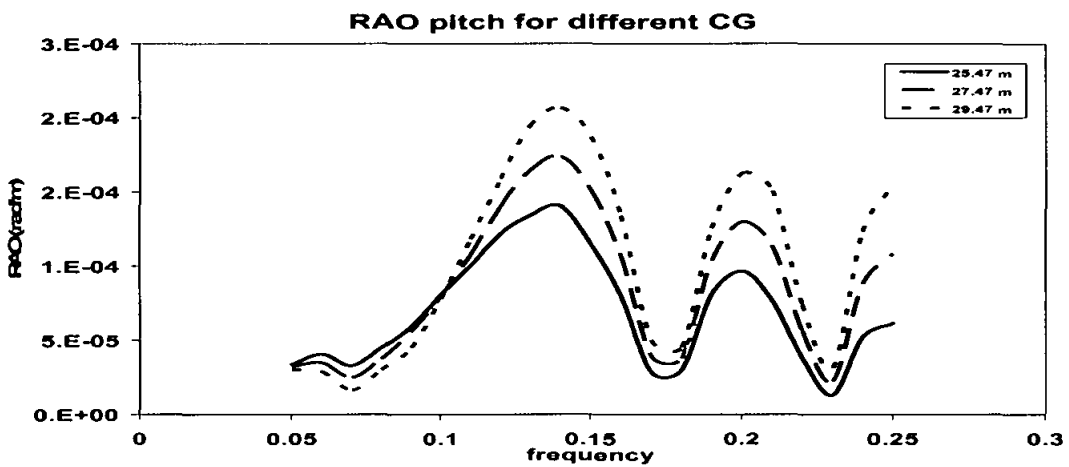


Figure 4.41: RAO pitch for different CG position

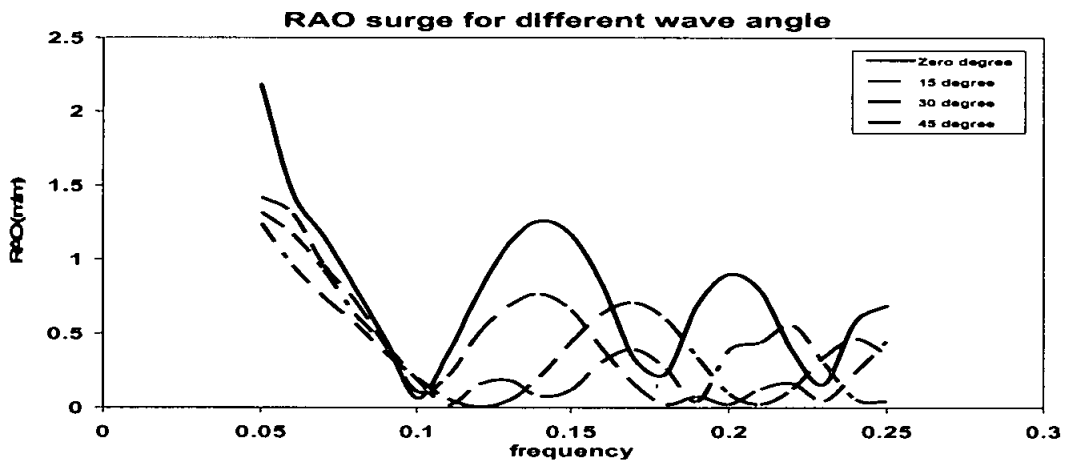


Figure 4.42: RAO surge for different wave angle

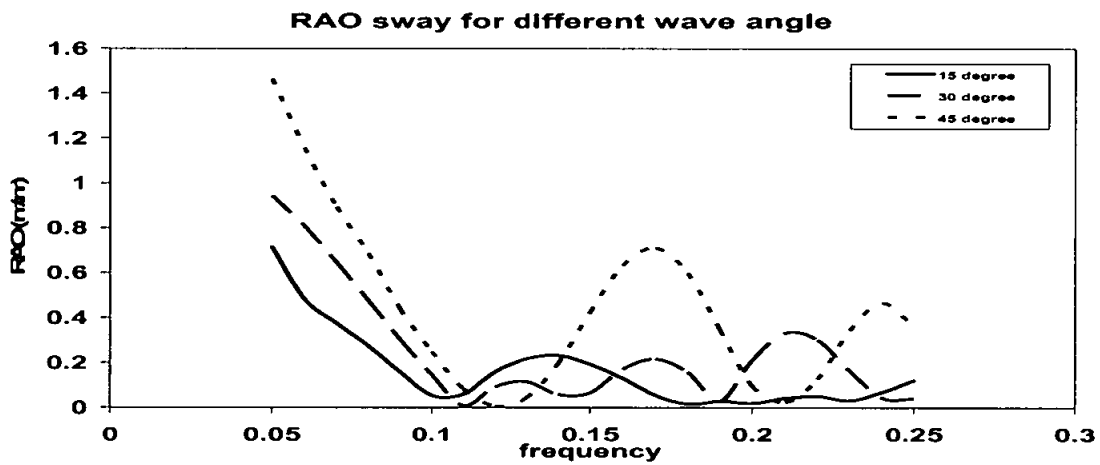


Figure 4.43: RAO sway for different wave angle

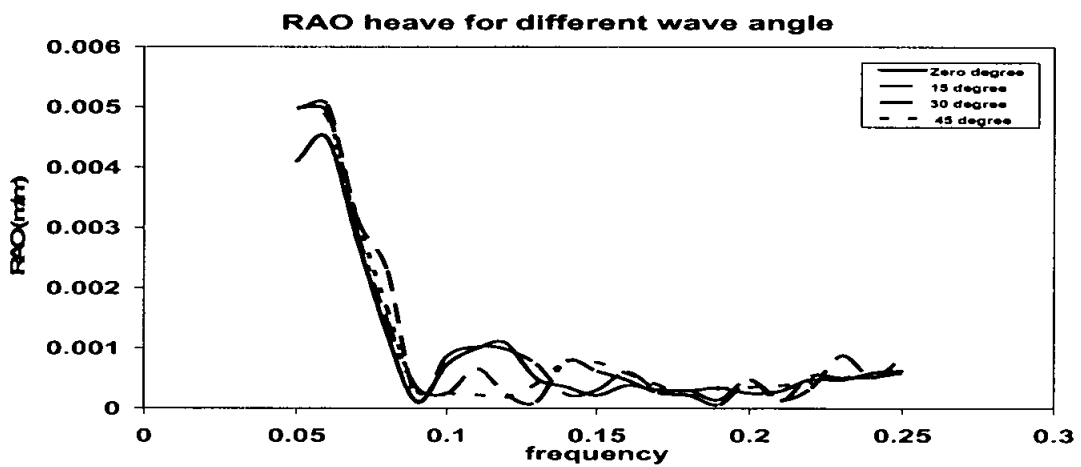


Figure 4.44: RAO heave for different wave angle

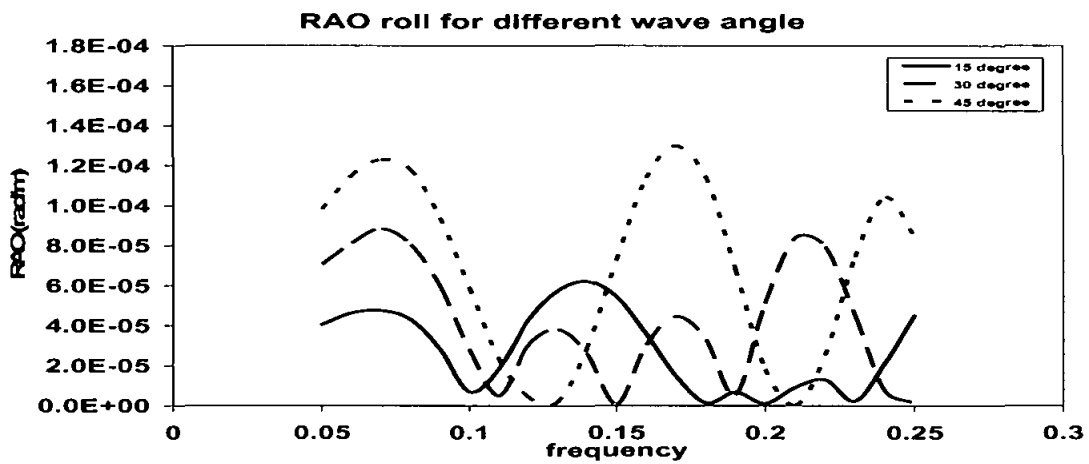


Figure 4.45: RAO roll for different wave angle

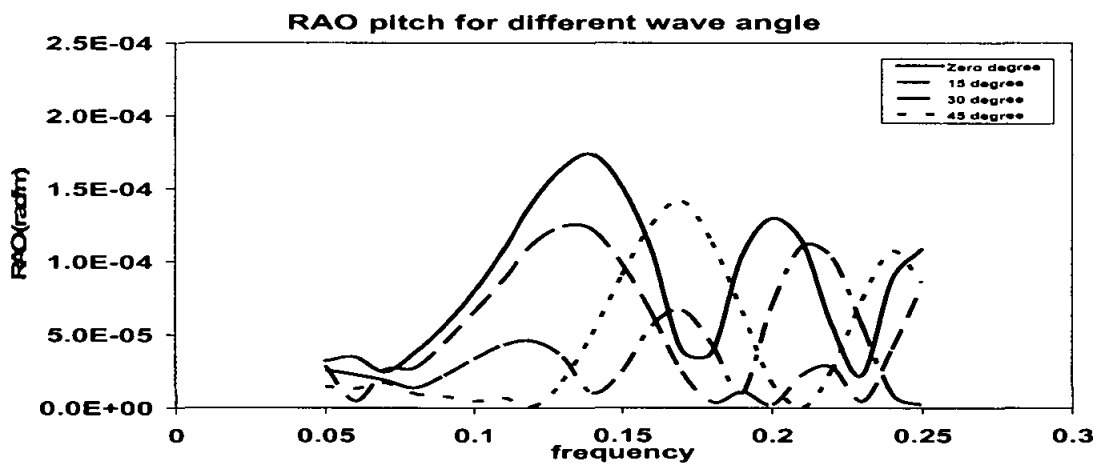


Figure 4.46: RAO pitch for different wave angle

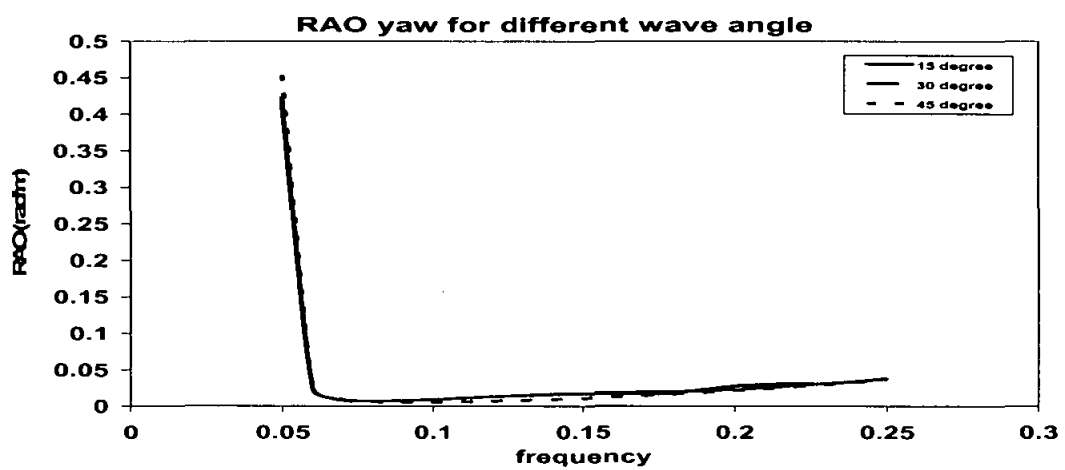


Figure 4.47: RAO yaw for different wave angle

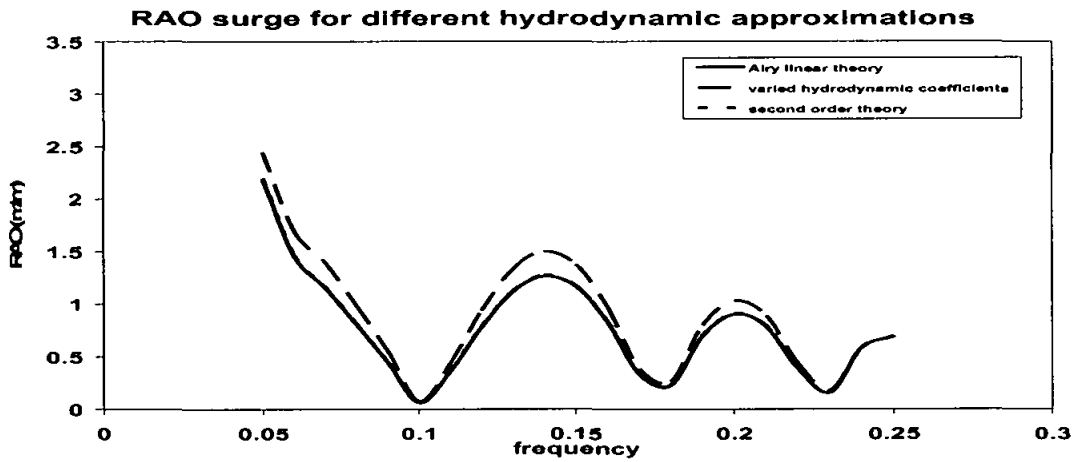


Figure 4.48: RAO surge for different hydrodynamic approximations

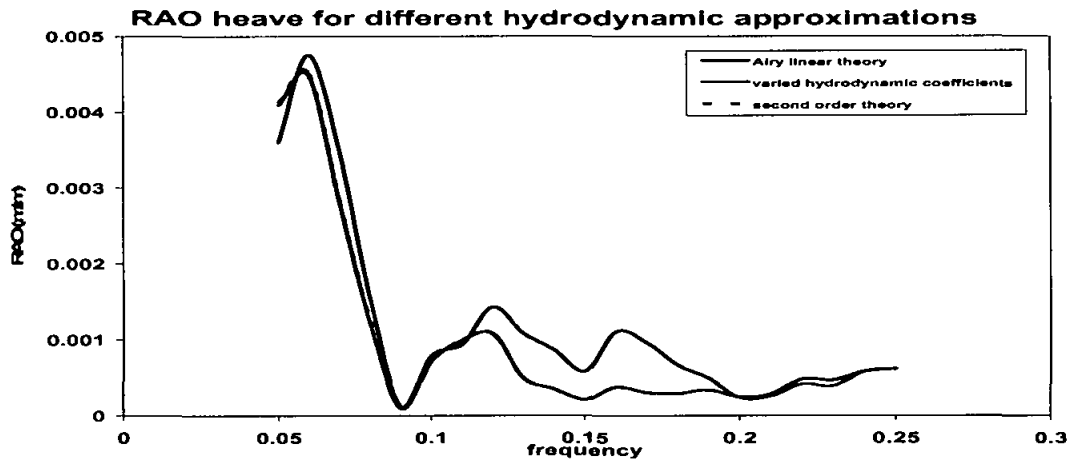


Figure 4.49: RAO heave for different hydrodynamic approximations

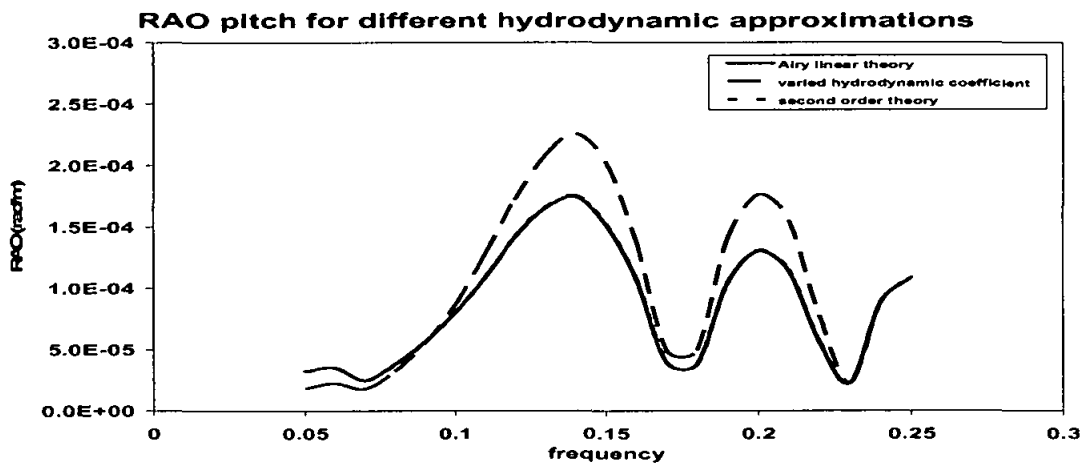


Figure 4.50: RAO pitch for different hydrodynamic approximations

4.3.2.1 Random wave results

The results of the triangular TLP₃ were studied in RAO form in time domain analysis for surge, heave, pitch and tether tension in Figure 4.51 to 4.54. Excluding the low wave frequencies (less than 0.07 Hz) the highest RAO for surge response was 0.884 m/m at 0.22 Hz with periodic peaks decreasing gradually with the higher wave frequencies.

The highest RAO for heave was 3.5 mm/m at 0.10 Hz. The period between 0.07 to 0.22 Hz represented the most effective period in pitch and tether tension when the highest pitch RAO was 0.0028 rad/m at 0.15 Hz while the highest tether tension RAO was 2724 kN/m at 0.12 Hz.

4.3.2.2 Typical responses

The typical responses in surge, heave, pitch and tether tension for the above mentioned platform, were determined by converting the RAOs to the time series. Figures 4.55 to 4.58 showed that the responses in surge, heave, pitch and tether tension follow a similar pattern as the input time series generated by the selected P-M spectrum.

The maximum responses were 2.18 m in surge, 6.3 mm in heave, 0.00786 radians in pitch and 6000 kN for tether tension. These are within the permissible limits [6].

4.3.2.3 Square and Triangular TLPs comparisons

The comparisons between the square and triangular TLPs were conducted in Figures 4.59 to 4.62. These comparisons aimed to clarify the effects of the platform shapes in the behavior of the structure. The platform TLP₂ was the square TLP while TLP₃ was the triangular TLP. The comparisons were made for surge, heave, pitch and tether tension in RAO terms.

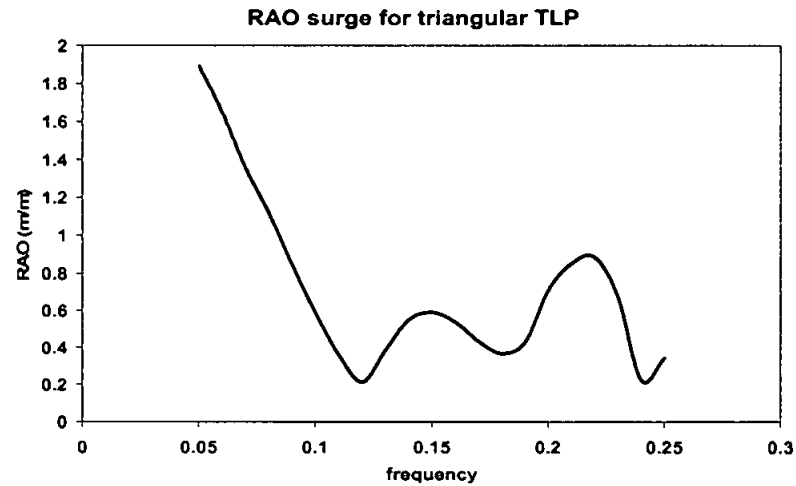


Figure 4.51: RAO surge for triangular TLP

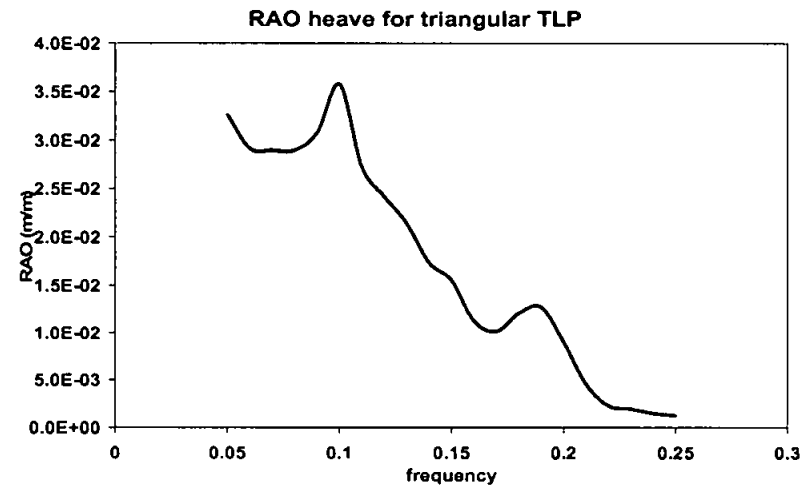


Figure 4.52: RAO heave for triangular TLP

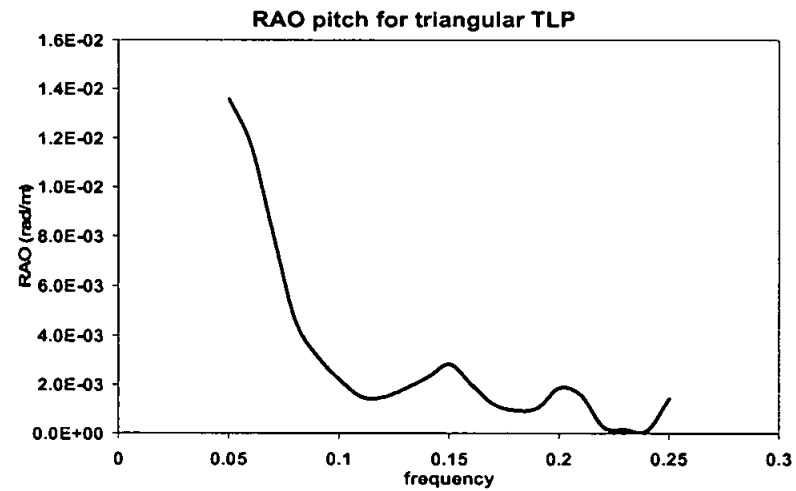


Figure 4.53: RAO pitch for triangular TLP

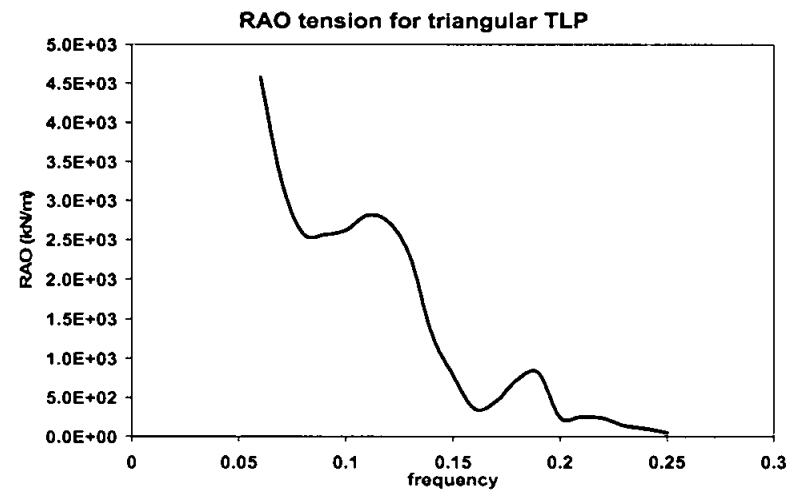


Figure 4.54: RAO tension for triangular TLP

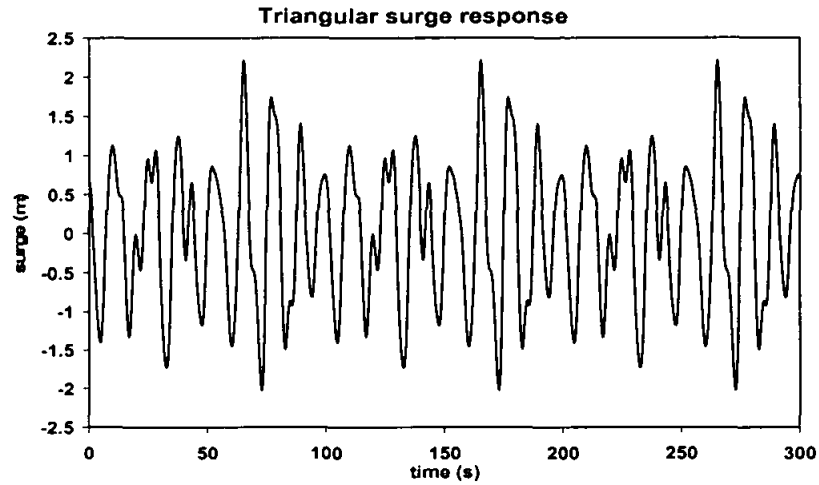


Figure 4.55: Triangular surge response

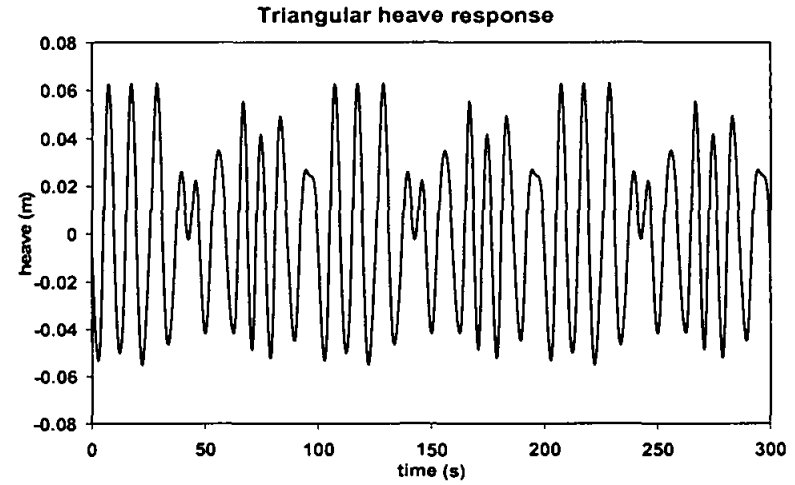


Figure 4.56: Triangular heave response

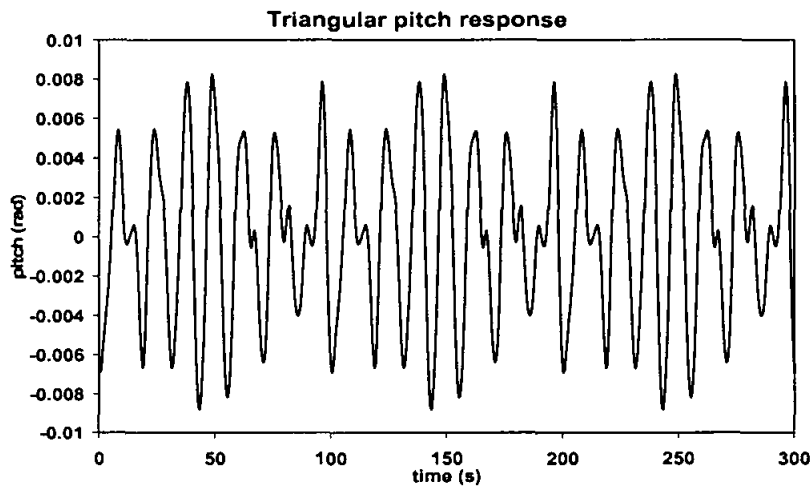


Figure 4.57: Triangular pitch response

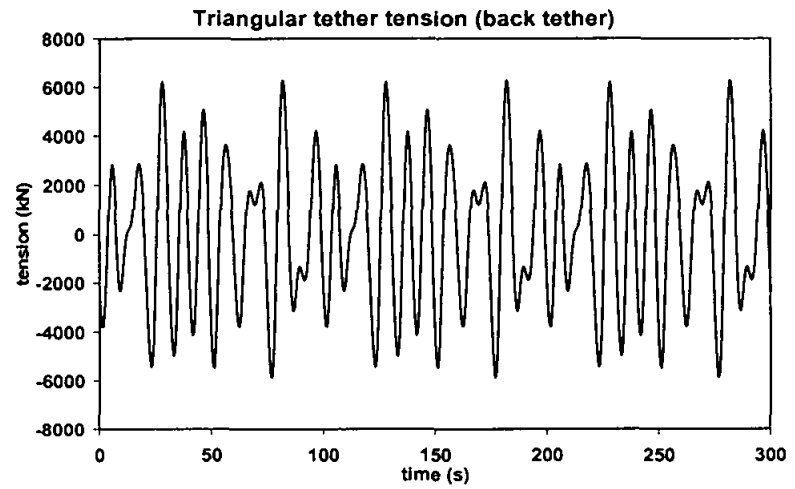


Figure 4.58: Triangular tether tension

The comparison in RAO surge showed that the highest square RAO value was at 0.14 Hz and the highest triangular RAO was at 0.22 Hz. The wave frequencies for the worst surge responses were not same for the square and triangular TLPs. The maximum surge response for triangular TLP was higher than the maximum surge response for square TLP by 8.2% (Figure 4.59).

RAO heave showed remarkable difference between square and triangular TLP in the values and the trends. Triangular TLP gave higher heave response with 60% higher values compared to the square one. That difference may be attributed to the tether system. While the square TLP resisted the displacements by four tether groups, the triangular had only three groups and the heave response was affected by the tether number and stiffness.

The comparison of pitch responses showed the clear superiority of the square TLP that gave a better pitch performance.

Except for frequencies above 0.24 Hz, the triangular tether tension RAO was higher than the rectangular one. The tether tension was affected by the responses of the platform specially the vertical motion (heave, roll, pitch). As the triangular TLP had higher responses in all degrees of freedom, the tether tension was much higher than the square one.

4.3.2.4 Triangular TLP parametric studies

The triangular platform TLP₃ was used for the parametric studies. Water depth, tether pretension, center of gravity (CG) position and wave angle were studied.

4.3.2.4.1 Water depth

Figures 4.63 to 4.65 showed that unlike the square TLP the water depth affected all the degrees of freedom. It could be observed that raising water depth from 300 m to 900 m increased the maximum surge RAO by about 47%. The heave response increased by 42% and the pitch response increased by 53%.

4.3.2.4.2 Tether pretension

Three values of pretension were used namely 101000, 135500 and 170000 kN. Figures 4.66 to 4.68 showed that, for a 25% increase of pretension, the surge response decreased by about 41%, the pitch response decreased by about 22.5% and there was no considerable effect on heave response. Similarly, decreasing the pretension by 25% increased the responses vice versa.

4.3.2.4.3 Center of gravity position

Figures 4.69 to 4.71 showed that the change in center of gravity (CG) had no effect in surge and heave degrees of freedom, but the pitch response increased by 64% when the CG was raised by 4 m. The reason of increase in the pitch response due to lowering CG position was that reducing CG position reduced the balancing moment which affected the pitch response.

4.3.2.4.4 Wave angle

The change of wave angle generated responses in all the six degrees of freedom. The surge response at 45° wave angle was about 70% less than that at zero wave angles. The heave response at 45° wave angle showed a jump between the periods 0.08 to 0.18 Hz with amount 92% higher than that at zero degree angle. The pitch response was fluctuating between lower and higher with maximum difference 51% than that at zero wave angle.

The sway response by 45 degree wave angle was three times that at 15 degree angle. The highest RAO roll occurred at 30 degree wave angle and the difference of values between 15 and 30 degree was 62%. The yaw responses for 15 and 45 degree inclinations were nearly same and less than that at 30 degree by 31%. Increasing wave angle decreased the x axis components and increased the y axis components. Figures 4.72 to 4.77 gave the wave angle effects.

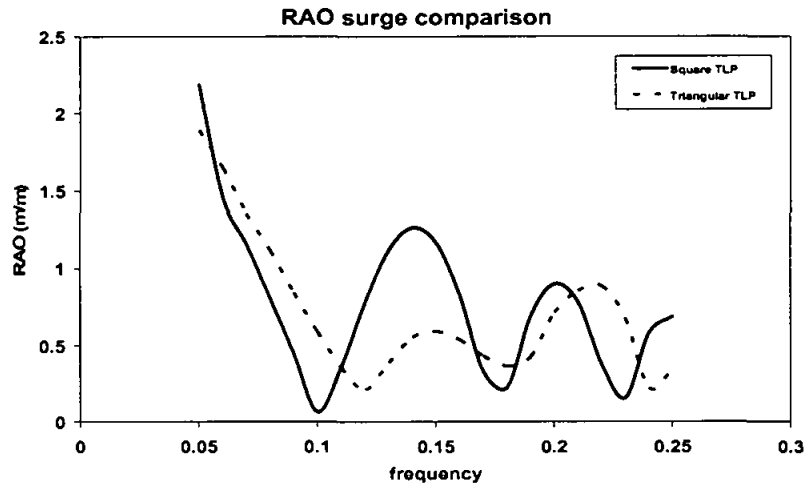


Figure 4.59: RAO surge for TLP₂ and TLP₃

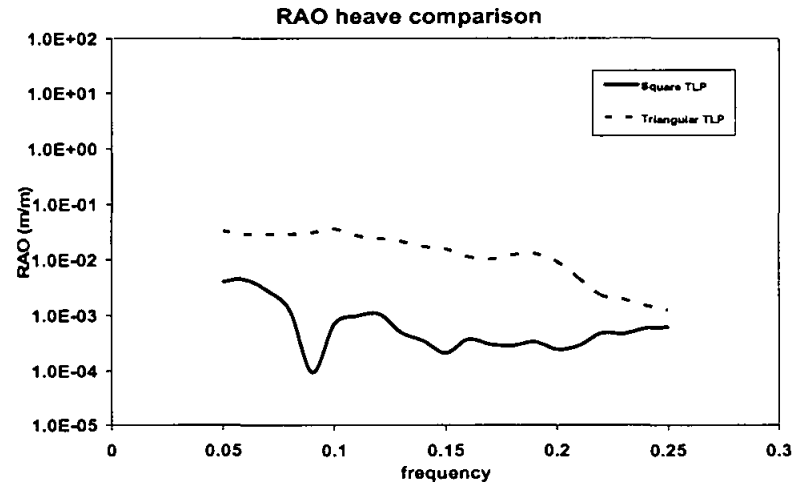


Figure 4.60: RAO heave for TLP₂ and TLP₃

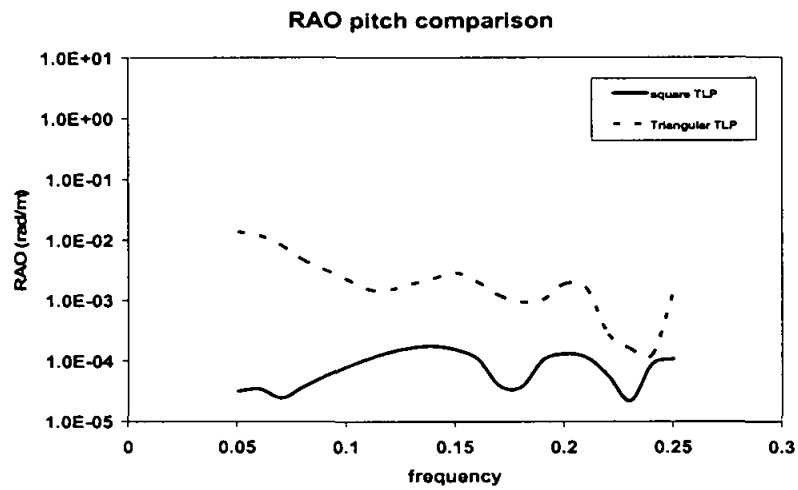


Figure 4.61: RAO pitch for TLP₂ and TLP₃

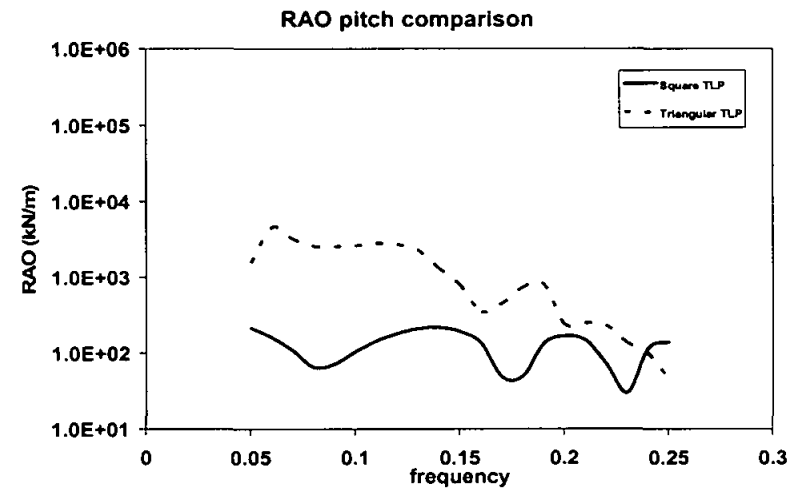


Figure 4.62: RAO tension for TLP₂ and TLP₃

4.3.3 Inclined tether TLP

Mooring system design is to make the system stiff enough to avoid damage to drilling or production risers, caused by excessive offsets [54]. The tension leg platform is vertically restrained precluding motions vertically (heave) and rotationally (pitch and roll) but it is compliant in the horizontal direction permitting lateral motions. The inclined tether TLP concept is introduced to increase the restraint in the horizontal degrees of freedom. The tethers were formed at angle with the three axes (x, y and z). The pretension and the stiffness components of the particular axis restrain the motion along that axis, which will distribute the restriction between horizontal and vertical axis.

4.3.3.1 Inclined tether TLP behavior

Inclined tether TLP was a normal square TLP with an inclination in the mooring system. The TLP₄ and TLP₅ in Table 4.1 were inclined tether TLP. The tethers were inclined by 10 degrees with the vertical z axis and 45 degree with x and y axis after solving it in x, y plane. The difference between TLP₄ and TLP₅ was that, TLP₄ kept the buoyancy same with the normal tether TLP while TLP₅ kept the pretension same.

4.3.3.2 Inclined tether TLP RAOs

Figures 4.78 to 4.81 showed the inclined tether TLP₄ RAOs in surge, heave, pitch and tether tension. The RAO surge gave 0.292 m/m at 0.14 Hz as maximum value followed by smaller crests in the higher wave frequency. The maximum heave RAO was 2 mm/m at frequency 0.13 Hz. RAO pitch and tether tension had almost same trend with values 0.00042 rad/m and 450 kN/m respectively at 0.14 Hz.

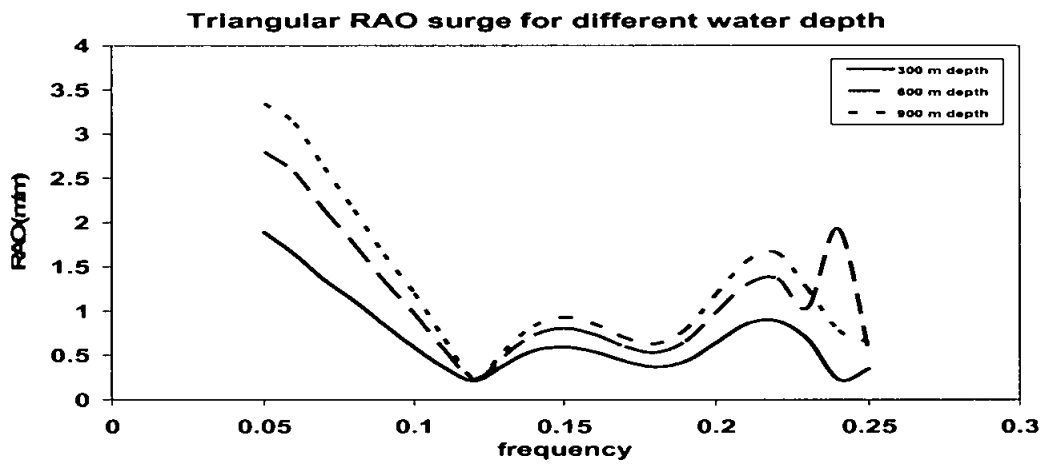


Figure 4.63: Triangular RAO surge for different depths

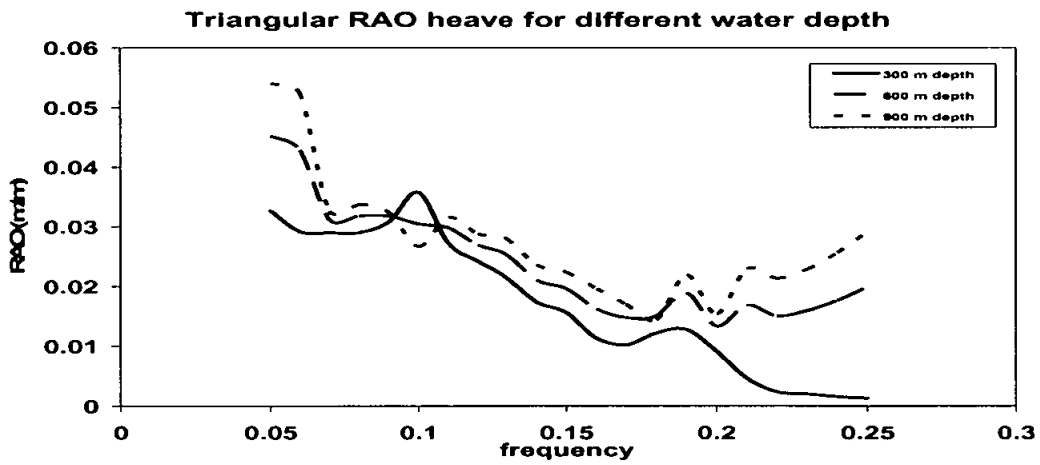


Figure 4.64: Triangular RAO heave for different depths

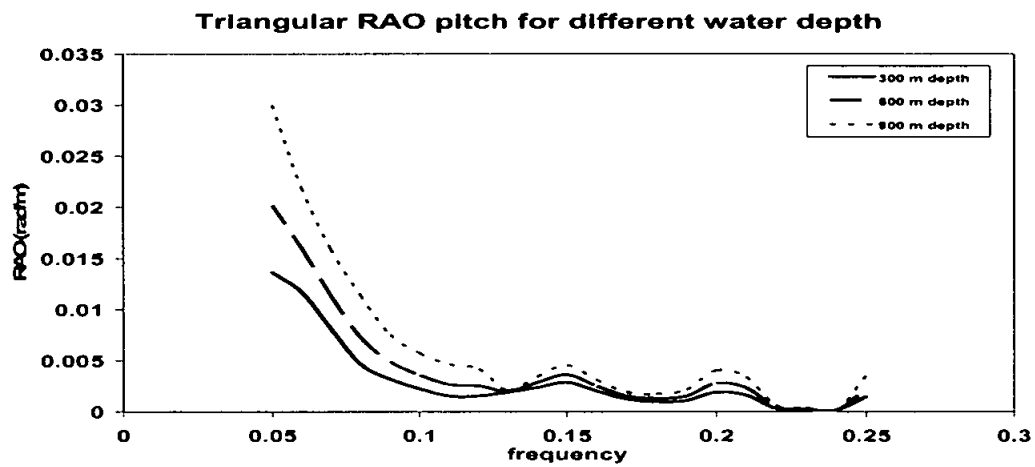


Figure 4.65: Triangular RAO pitch for different depths

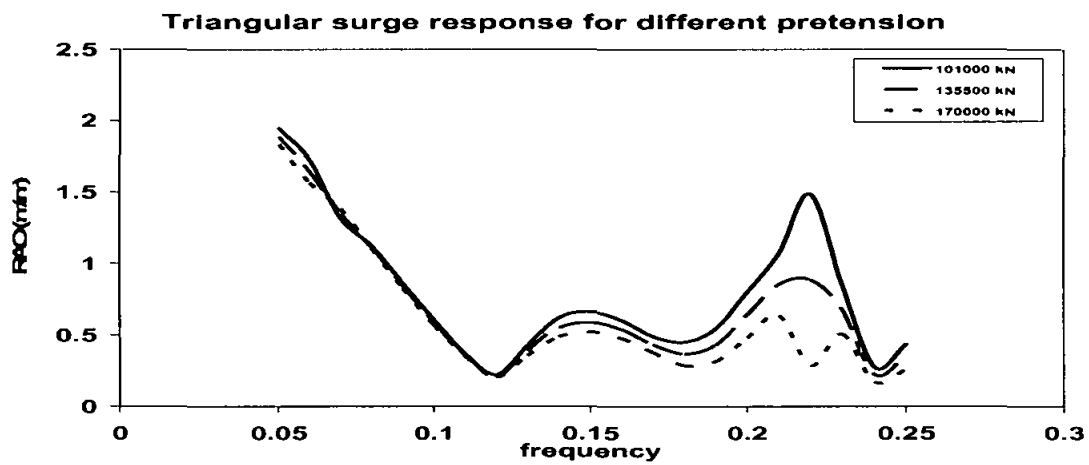


Figure 4.66: Triangular RAO surge for different pretension

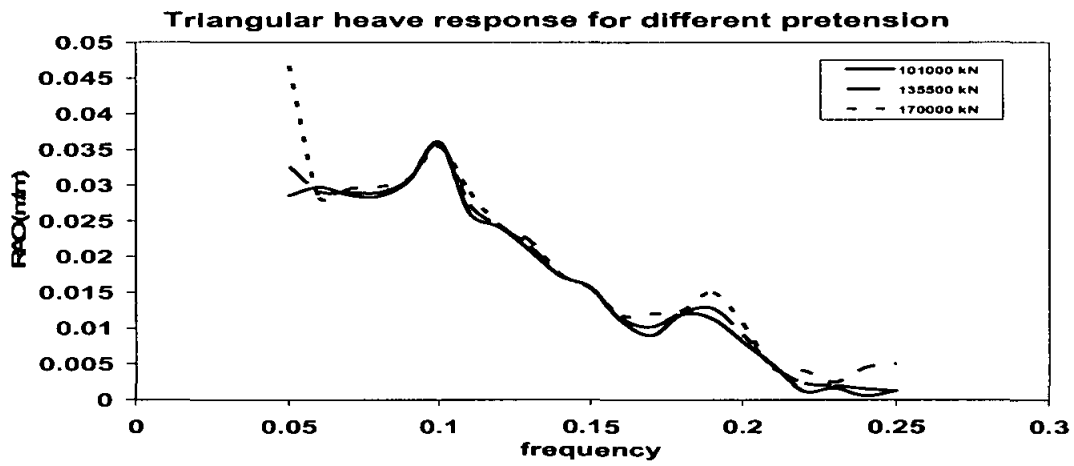


Figure 4.67: Triangular RAO heave for different pretension

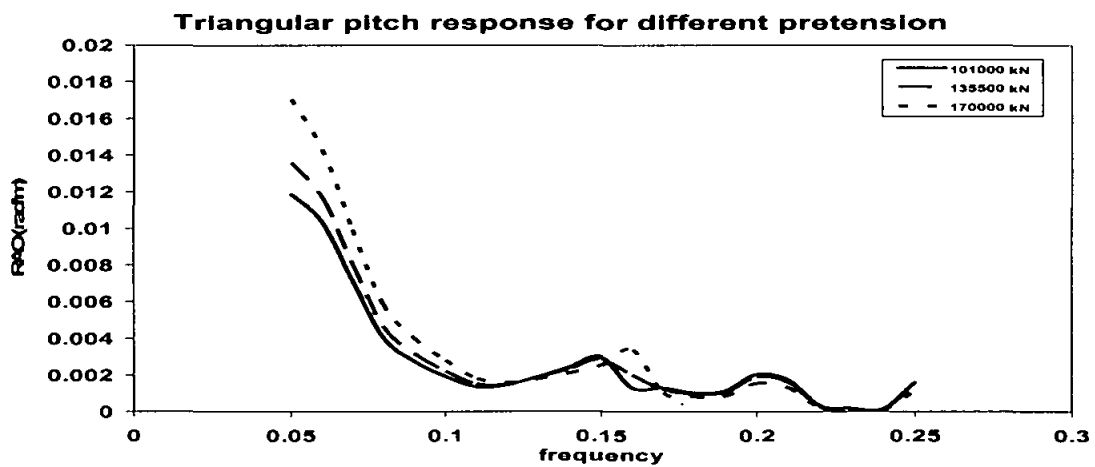


Figure 4.68: Triangular RAO pitch for different pretension

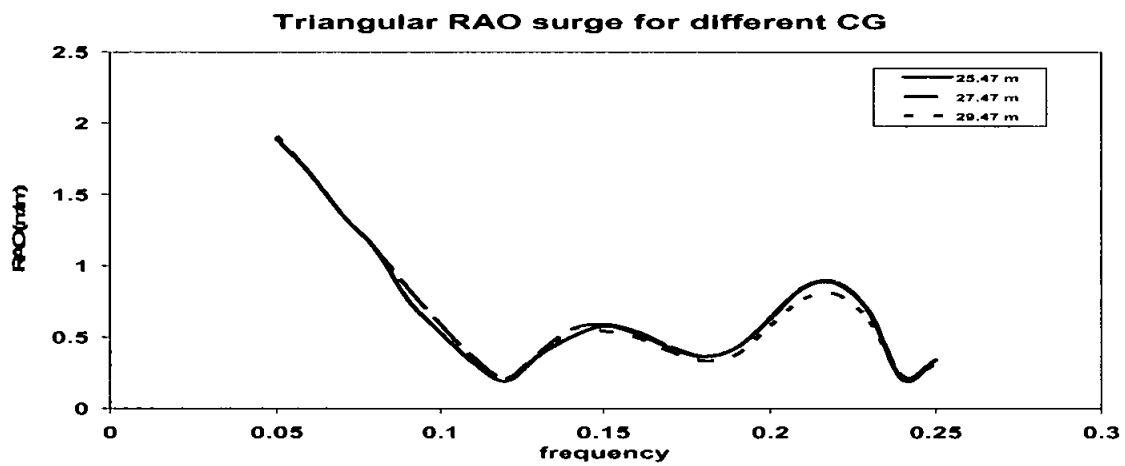


Figure 4.69: Triangular RAO surge for different CG position

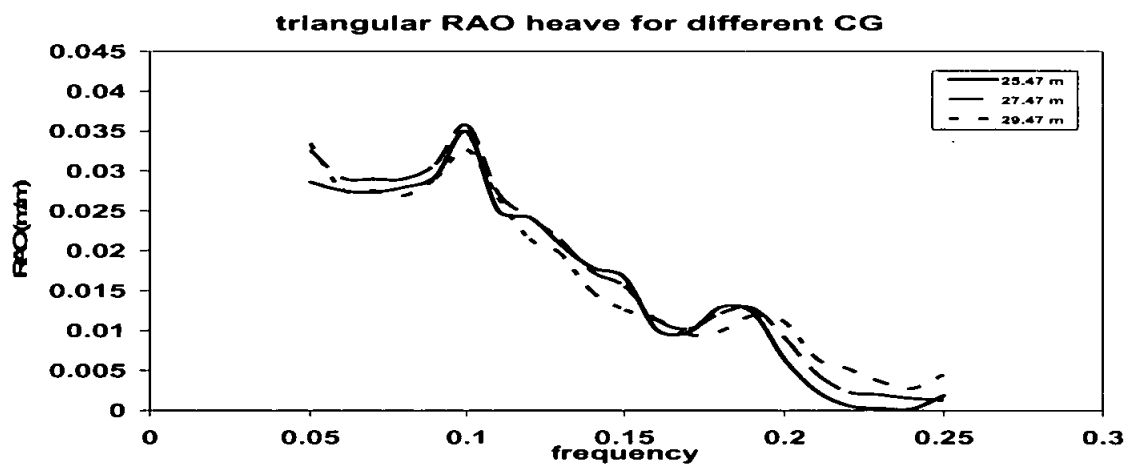


Figure 4.70: Triangular RAO heave for different CG position

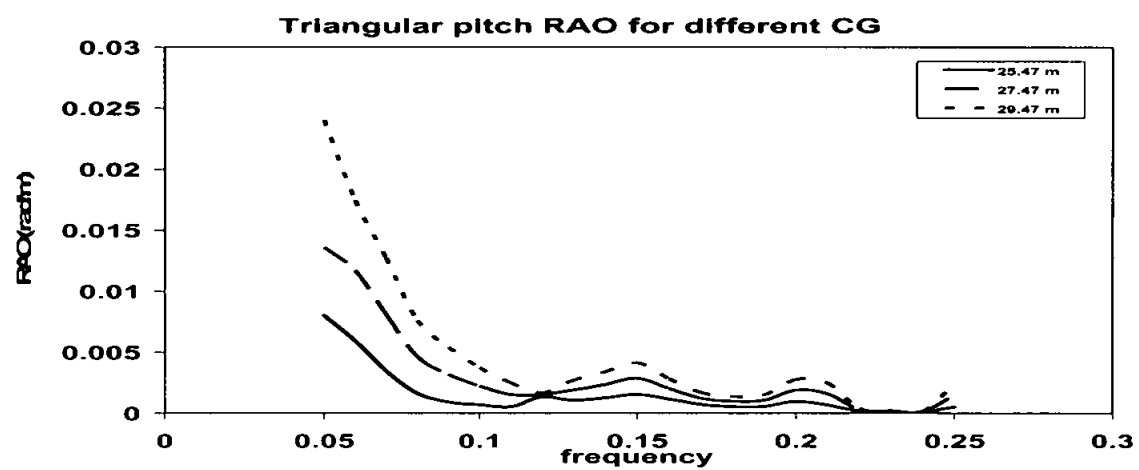


Figure 4.71: Triangular RAO pitch for different CG position

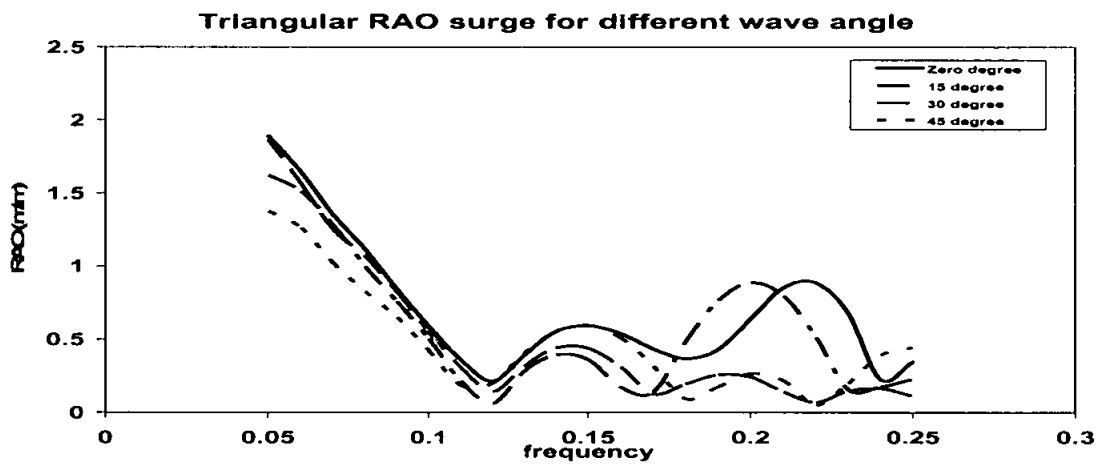


Figure 4.72: Triangular RAO surge for different wave angle

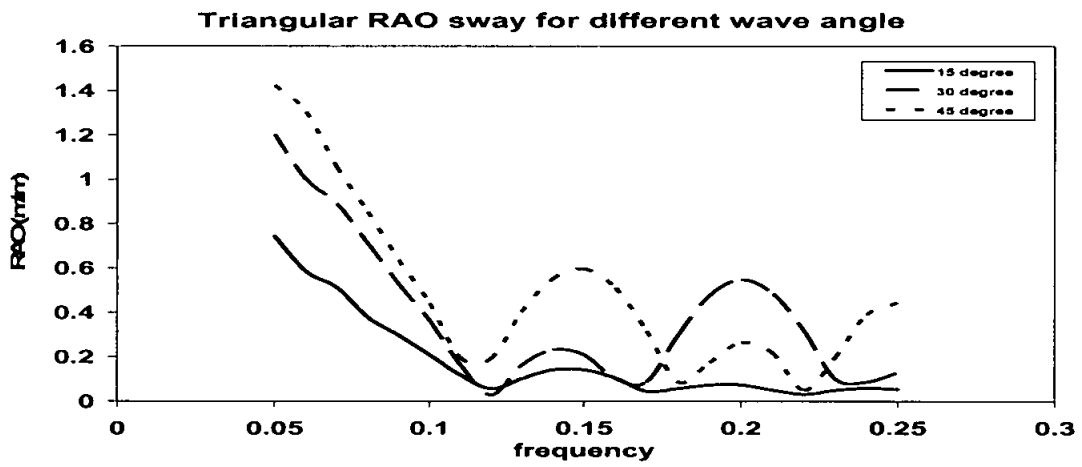


Figure 4.73: Triangular RAO sway for different wave angle

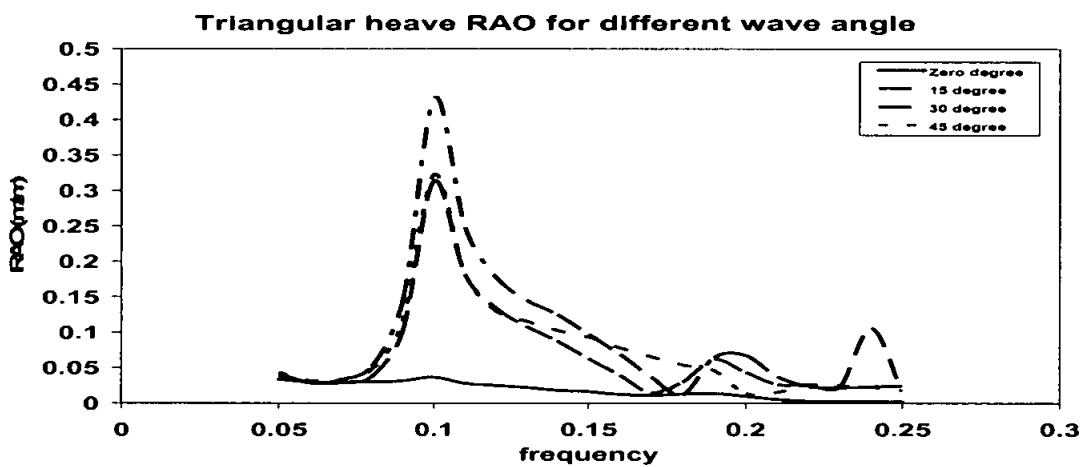


Figure 4.74: Triangular RAO heave for different wave angle

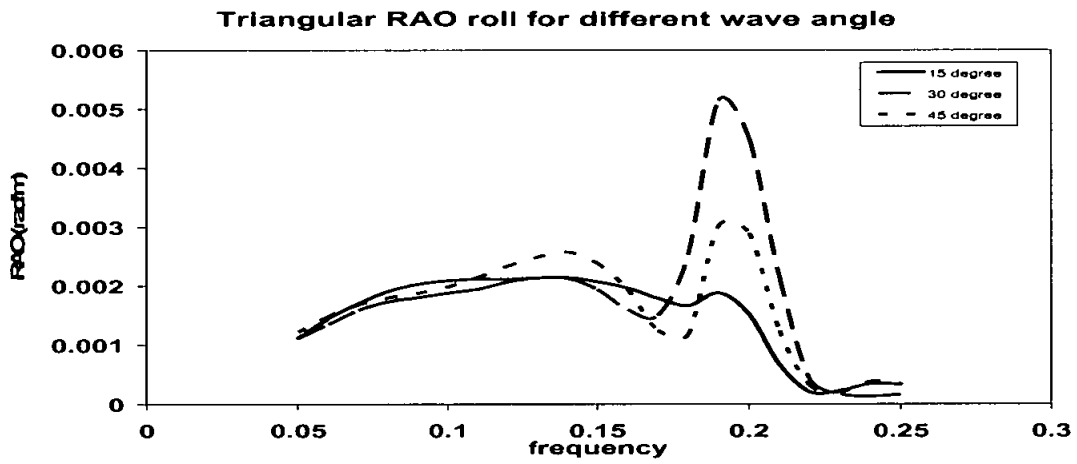


Figure 4.75: Triangular RAO roll for different wave angle

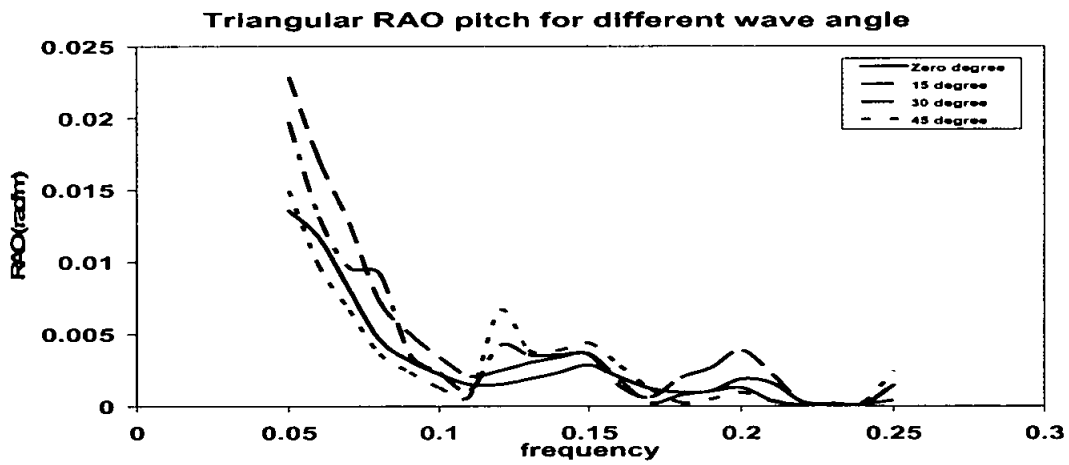


Figure 4.76: Triangular RAO pitch for different wave angle

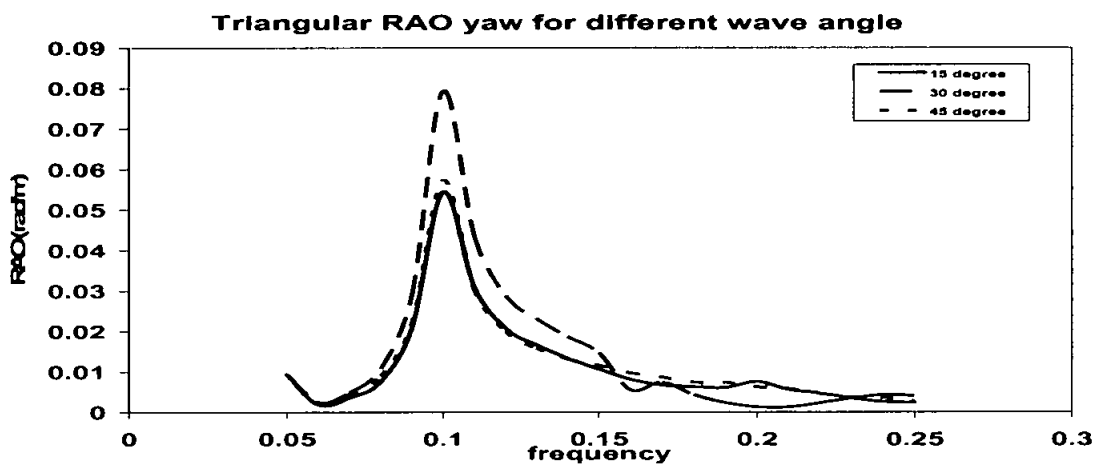


Figure 4.77: Triangular RAO yaw for different wave angle

4.3.3.3 Typical responses

Figures 4.82 to 4.85 showed the responses in surge, heave, pitch and tether tension. The maximum responses were 1.024 m in surge, 6 mm in heave, 8.9×10^{-4} radians in pitch and 850 kN for the tether tension. These agreed with actual practical values.

4.3.3.4 Inclined tether TLP comparisons

The comparisons demonstrated in Figures 4.86 to 4.89 were between square (TLP₂), triangular (TLP₃) and inclined tether (TLP₄ and TLP₅). These comparisons were conducted to study the various shapes effects on the behavior of TLPs and to compare the inclined tether TLPs with the square and triangular TLPs to conclude the optimum selection under the existing condition.

Inclined tether TLP had the smallest RAO surge with remarkable difference with square and triangular TLPs. The inclined tether TLP₄ and TLP₅ had very little difference in RAO surge. RAO surge for inclined TLP was 79% less than the square one and 87% less than the triangular one. TLP₄ followed same square TLP trend which were different from the triangular one. The horizontal pretension and stiffness components precluded the surge motion which made that difference. This insured that the inclined tether TLP reduced a great part of surge motion.

Heave motion for inclined tether TLP was different in trend compared to square and triangular TLPs. The fixed buoyancy (TLP₄) was lower in the responses than fixed pretension (TLP₅) by 20% and lower than the triangular TLP₃ by 43%. Although the

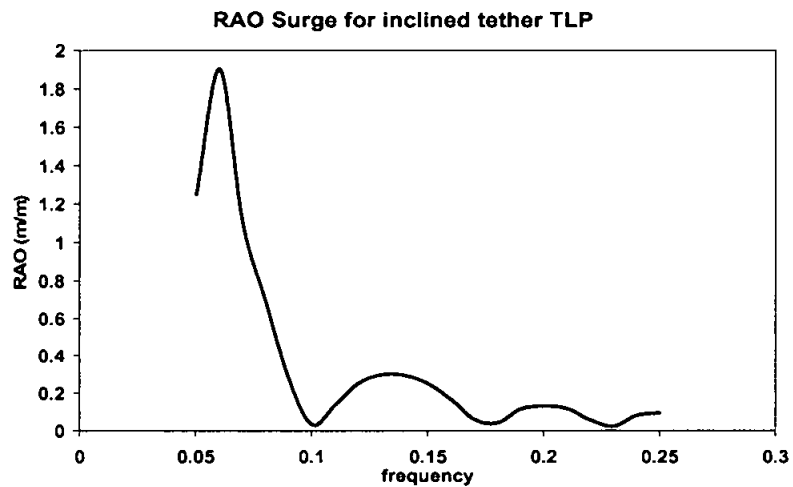


Figure 4.78: RAO surge for inclined TLP

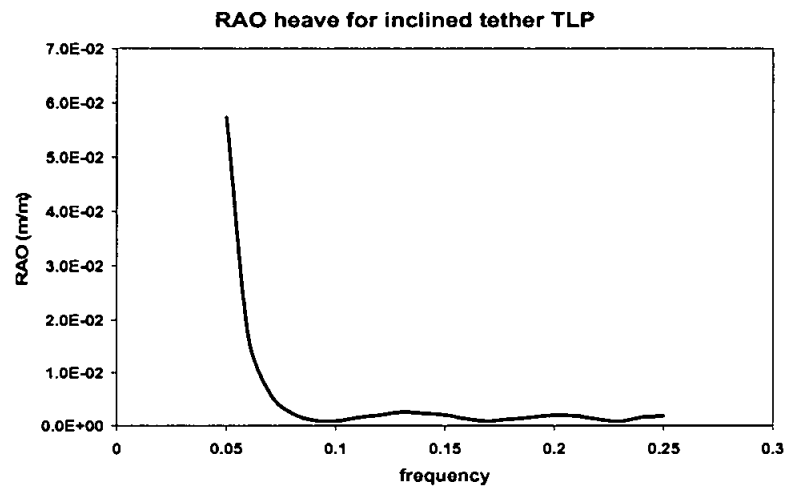


Figure 4.79: RAO heave for inclined TLP

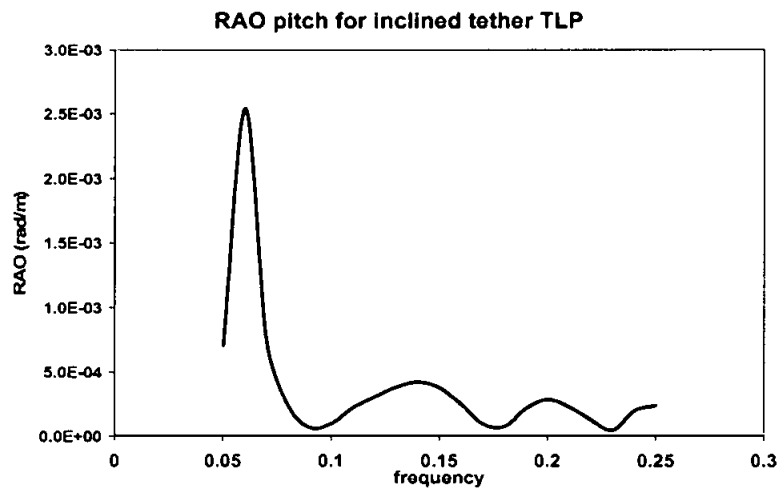


Figure 4.80: RAO pitch for inclined TLP

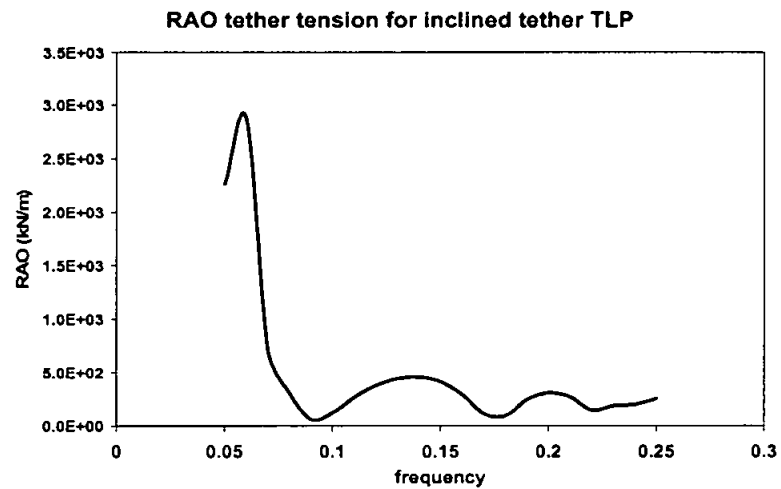
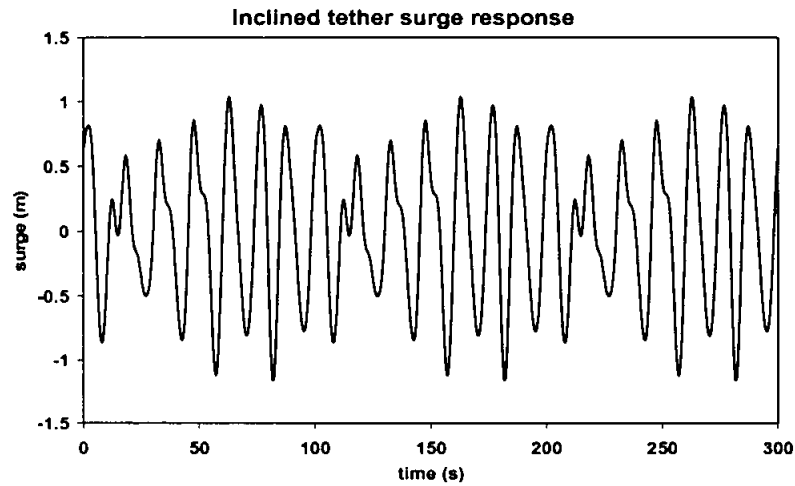
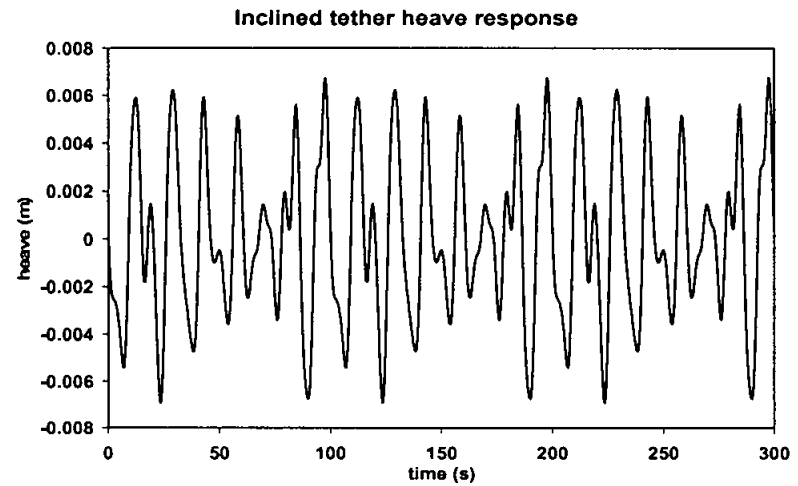
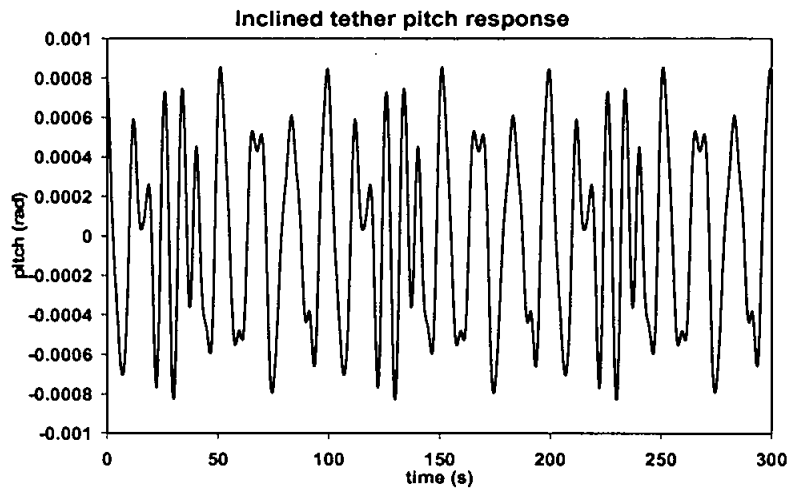
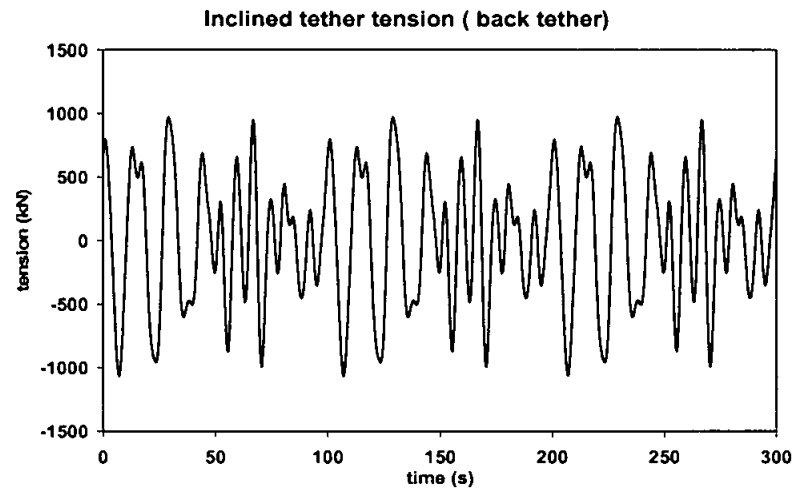


Figure 4.81: RAO tension for inclined TLP

Figure 4.82: Surge response for TLP₄Figure 4.83: Heave response for TLP₄Figure 4.84: Pitch response for TLP₄Figure 4.85: Tether tension for TLP₄

inclined TLP₄ was higher than square TLP₂ by 45%, the difference was very small. The reason of higher inclined TLP response is that unlike the normal TLP which resist the heave motion by almost full tether pretension and stiffness, the inclined tether TLP resisted the heave motion by the vertical components of pretension and stiffness.

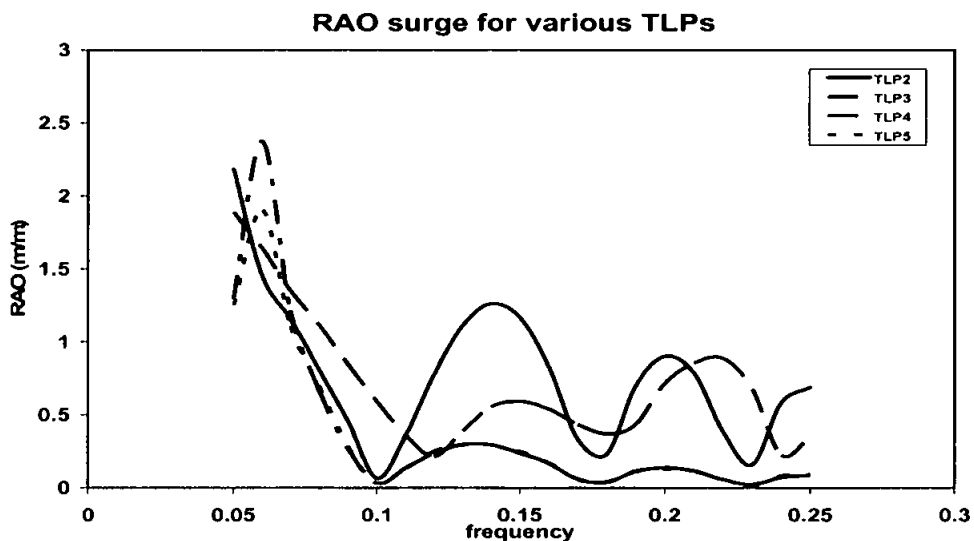


Figure 4.86: RAO surge for various types of TLPs

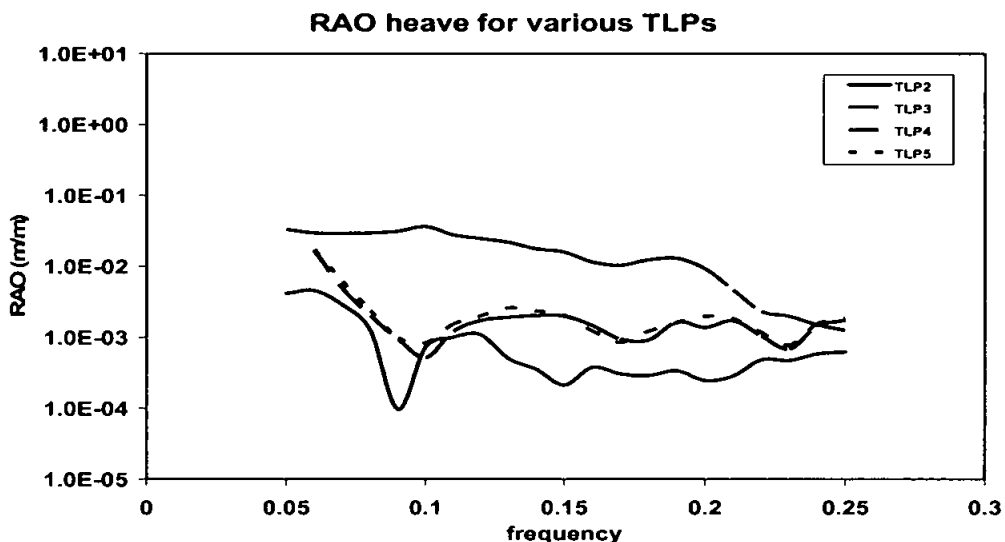


Figure 4.87: RAO heave for various types of TLPs

Pitch RAO for inclined and normal TLPs had same trend and different values. The pitch RAO for TLP₄ was lower 7% than TLP₅ and 86% lower than the triangular TLP₃. The difference between the square TLP₂ and the Inclined TLP₄ was 52% higher which could be considered as small because of the small pitch values.

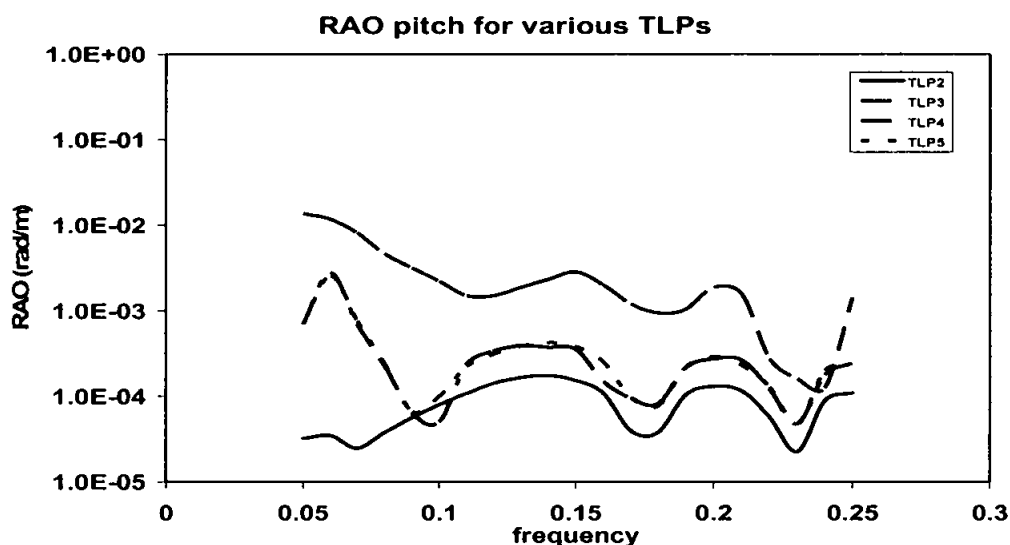


Figure 4.88: RAO pitch for various types of TLPs

RAO tether tension for inclined TLP₄ was a little higher than inclined TLP₅ by 7%. The triangular TLP₃ was higher in tension than TLP₄ by 83%. The difference between inclined TLP₄ and square TLP₂ was 52% (inclined was higher), because of the additional tension caused by restraining the surge response. Table 4.2 gave the values of the RAO for TLP₂, TLP₃, TLP₄ and TLP₅ in surge, heave, pitch and tether tension.

4.3.3.5 Inclined Tether TLP advantages

- According to the above studies, inclined tether TLP has much lower surge response that is the most important criterion for platform stability.
- Unlike other compliant platforms, the TLP pile foundation experience tension rather than compression. The pile tension in case of the inclined TLP is reduced because of the inclination.

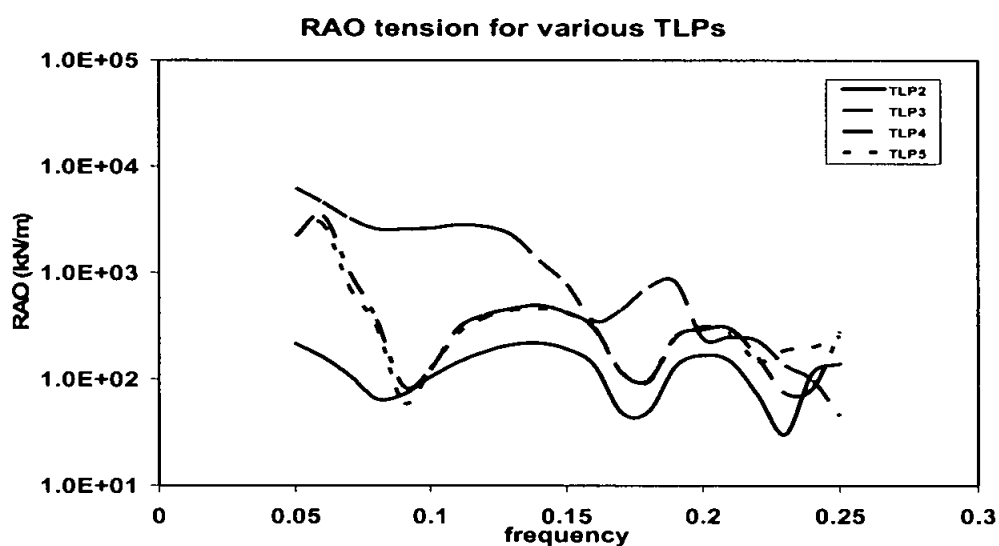


Figure 4.89: RAO tension for various types of TLPs

- The horizontal components of the tether tension increases the friction force between the soil and pile skin thereby reducing the pile perimeter and thus the pile cost.
- The vertical pretension in the inclined tether TLPs is less than that of the normal TLP. Decreasing the pretension decreases the buoyancy this leading to small hull sizes and hence smaller cost of platform.

Table 4.2: RAOs for various Tension leg Platform

Description	RAO surge (m/m)	RAO heave (mm/m)	RAO pitch (rad/m)	RAO tension (kN/m)
TLP2	1.26	1.1	1.7×10^{-4}	218
TLP3	0.880	3.5	2.8×10^{-3}	2724
TLP4	0.292	2.0	4.2×10^{-4}	450
TLP5	0.290	2.3	4.2×10^{-4}	458

CHAPTER FIVE

CONCLUSIONS AND FURTHER STUDIES

5.1 Introduction

In this work an elaborate study on the dynamic analysis of different types of Tension Leg Platforms were conducted in time and frequency domain using MATLAB language. The results were validated with available results in the literature. Using this programmer, it was possible to conduct an accurate time domain dynamic analysis of any type of TLP. The response in all the degrees of freedom and the tether tension could be determined at any time. As these responses form the major criterion for the stability of a TLP during operation, this program will help in a great way for preliminary design, conceptual design, analysis and research for developing TLP technology for deep water. The dynamic responses of the various TLP configurations subjected to random waves were analyzed and compared. Parametric studies and hydrodynamic approximations were analyzed. The following conclusions were drawn.

5.2 Conclusions

1. The responses due to the varying hydrodynamic coefficients showed higher values than the responses taking constant hydrodynamic coefficients in surge, heave and pitch degrees of freedom by amounts ranging from 15 % to 22%.
2. The comparison between the frequency and time domain analysis showed that the frequency domain analysis was not accurate and could be used only for some preliminary analysis.

3. Increasing water depth increased the surge response, but there were no remarkable effects on the heave and pitch responses.
4. The increase in the pretension decreased the surge and there was no considerable effect on heave and pitch response. The same was true vice versa also.
5. The change in position of centre of gravity affected only the pitch responses. Raising the CG increased the pitch response.
6. When the wave was incident at an inclination, there were responses in all the six degrees of freedom. Increasing wave angle with surge direction decreased x axis components and increased y axis components.
7. When the square and triangular TLPs were compared, the surge responses of both square and triangular were nearly same and followed almost the same trend. The responses in heave, pitch, and tether tension for triangular TLPs were higher compared to square TLPs. Based on this study, it could be concluded that square TLPs have better performance criteria compared to triangular TLPs in random waves.
8. The inclined-tether square TLP which was proposed by the author, had better performance compared with vertical-tethered rectangular and triangular TLPs. More over the inclined tether TLP decreased the cost by decreasing pile and hull sizes.

5.3 Further studies

Based on the present study, the following works are proposed for the future studies.

- Detailed Finite Element Analysis of TLP can be conducted dividing the platform and tether into different types of elements.
- The wave force calculations can be improved by using diffraction theory instead of Morison Equation.
- Detailed studies on the pile of the inclined tether TLPs can be incorporated in the analysis.
- The comparisons between inclined tether for square, triangular and extended tension leg platforms can be investigated

REFERENCES

- [1]. S. K. Chakrabarti. Handbook of offshore engineering, Volume I, Offshore structure analysis, Inc. Plainfield, Illinois, USA (2005). Elsevier 0-08-044568-3.
- [2]. Zhihuang Ran. Coupled dynamic analysis of floating structures in waves and current. Texas A&M University (2000). UMI 9994319.
- [3]. Jun Zhao. Nonlinear surge response statistics of compliant offshore structures. Department of Civil and Environmental Engineering, University of Houston (1993). UMI 9619071.
- [4]. Basim Behnam Mekha. Non-linear dynamic response of Tension Leg Platform. Faculty of the Graduate School of the University of Texas at Austin (1994). UMI 9519350.
- [5]. John W. Chianis. Advancement in Tension Leg Platform technology. PETRONAS International Research and Development (R&D) Forum, Kuala Lumpur, Malaysia (2004).
- [6]. Zeki Demirebilek. TLP- A State of the Art Review. American Society of Civil Engineers (ASCE), New York (1989), 0-87262-683-0.
- [7]. S. K. Chakrabarti. Hydrodynamics of Offshore structures. CBI Industries, Inc. Plainfield, Illinois 60544-8929, USA (1987). 0-925451-66-X.
- [8]. Seon Mi Han and Hayam Benaroya. Nonlinear and Stochastic Dynamics of Compliant Offshore Structures. Department of Civil Engineering, University of Waterloo, Ontario, Canada (2002). Kluwer Academic Publishers 1-4020-0573-3.
- [9]. James F. Wilson. Dynamics of Offshore Structures, Second Edition. Department of Civil and Environmental Engineering, Duke University, USA (2003). Published by John Wiley 0-471-26467-9.
- [10]. A. K. Jain. Nonlinear coupled response of offshore Tension Leg Platforms to regular wave force. Department of Civil Engineering, Indian Institute of Technology, India (1995). Ocean Engineering 0029-8018(95)00059-3.
- [11]. Hsien Hua Lee, Pei-Wen Wang, Chung-Pan Lee. Dragged surge motion of Tension Leg Platforms and strained elastic tethers. Department of Marine

- Environment, National Sun Yat-sen University, Kaohsiung, Taiwan (1999). *Ocean Engineering* 575–594.
- [12]. M.S. Turnbull, A.G.L. Borthwick, R. Eatock Taylor, Wave–structure interaction using coupled structured–unstructured finite element meshes, HR Wallingford Ltd, Howbery Park, Wallingford, Oxon OX10 8BA, UK (2003), *Applied Ocean Research* 63–77.
- [13]. Zeng Xiao-hui, Shen Xiao-peng, WU Ying-xiang. Governing equations and numerical solutions of tension leg platform with finite amplitude motion. Division of Engineering Sciences, Institute of Mechanics, Chinese Academy of Sciences (2007). Editorial Committee of *Appl. Math* 0253-4827.
- [14]. Y.M. Lova, R.S. Langleyb. Time and frequency domain coupled analysis of deepwater floating production systems. Nanyang Technological University, School of Civil and Environmental Engineering, Nanyang Avenue, Singapore (2007). Elsevier 371–385.
- [15]. A.Naess, O. Gaidai, P.S. Teigen, Extreme response prediction for nonlinear floating offshore structures by Monte Carlo simulation, Centre for Ships and Ocean Structures, Norwegian University of Science and Technology, NO-7491 Trondheim, Norway (2007), *Applied Ocean Research* 221–230.
- [16]. S. Ahmad. Stochastic TLP Response Under Long Crested Random Sea. Department of Applied Mechanics, Indian Institute of Technology, Delhi, India (1996). Elsevier 0045-7949(96)00188-5.
- [17]. J.L.B. Carvalho, C.E. Parente, Directional wave measurements using a slope array system, Laboratory of Physical Oceanography, University of Vale do Itajai', Rua Uruguai,458, Itajai'-SC 88.302-202, Brazil (2000), *Applied Ocean Research* 95–101.
- [18]. M.R. Tabeshpour, A.A. Golafshani, M.S. Seif. Comprehensive study on the results of tension leg platform responses in random sea. Department of Civil Engineering, Sharif University of Technology, Tehran, Iran (2006). *J.Zhejiang Univ SCIENC* 1305-1317.

- [19]. S. Chandrasekaran, A.K. Jain, A. Gupta, A. Srivastava. Response behaviour of triangular tension leg platforms under impact loading. Department of Civil Engineering, Institute of Technology, India (2007). *Ocean Engineering* 45–53.
- [20]. A. Ertas and S. Ekwardo-Osire. Effects of damping and wave parameters on offshore structure under random excitation. Texas Tech University, Department of Mechanical Engineering, Lubbock, Texas 79409, U.S.A (1991).
- [21]. V. Vengatesan, K. S. Varyani, N. Barltrop, An experimental investigation of hydrodynamic coefficients for a vertical truncated rectangular cylinder due to regular and random waves, Department of Naval Architecture and Ocean Engineering, University of Glasgow, Glasgow, G12 8QQ Scotland, UK (2000), *Ocean Engineering* 291–313.
- [22]. S. Chandrasekaran, A.K. Jain , N.R. Chandak, Influence of hydrodynamic coefficients in the response behavior of triangular TLPs in regular waves. Department of Civil Engineering, Institute of Technology, Banaras Hindu University Varanasi 221 005, India (2004), *Ocean Engineering* 2319–2342.
- [23]. S. Chandrasekaran, A.K. Jain, Anupam Gupta. Influence of wave approach angle on TLP's response. Department of Civil Engineering, IT BHU, Varanasi 221005, Uttar Pradesh, India (2007). *Elsevier* 1322–1327.
- [24]. S. Chandrasekaran, A.K. Jain. Dynamic behaviour of square and triangular offshore tension leg platforms under regular wave loads. Rao Tula Ram College of Technical Education, New Delhi, India(2002). *Ocean Engineering* 279–313.
- [25]. S. Chandrasekaran, A.K. Jain. Triangular Configuration Tension Leg Platform behaviour under random sea wave loads. Department of Civil Engineering, I.I.T. Delhi, Haus Khas, New Delhi 110016, India (2002). *Ocean Engineering* 1895–1928.
- [26]. Xiaohong Chen, Yu Ding, Jun Zhang, Pierre Liagre, John Niedzwecki, Per Teigen, Coupled dynamic analysis of a mini TLP: Comparison with measurements, Department of Civil Engineering, Texas A&M University, College Station, TX 77843-3136, USA (2006), *Ocean Engineering* 93–117.
- [27]. N.A. Siddiqui, S. Ahmad, Reliability analysis against progressive failure of TLP tethers in extreme tension, Department of Civil Engineering, Jamia Millia

- Islamia, New Delhi 110025, India (2000), *Reliability Engineering and System Safety* 195–205
- [28]. N.A. Siddiqui, Suhail Ahmad, Fatigue and fracture reliability of TLP tethers under random loading, Department of Civil Engineering, Aligarh Muslim University, Aligarh 202002, India (2001), *Marine Structures* 331-352.
- [29]. S. Chandrasekaran, N.R. Chandak, Gupta Anupam, Stability analysis of TLP tethers, Department of Civil Engineering, Institute of Technology, Banaras Hindu University, Varanasi-05, India (2006), *Ocean Engineering* 471–482.
- [30]. Mangala M. Gadagi, Haym Benaroya, Dynamic response of an axially loaded tendon of a tension leg platform, Department of Mechanical and Aerospace Engineering, Rutgers University, 98 Brett Road, Piscataway, NJ 08854, USA (2006), *Journal of Sound and Vibration* 38–58.
- [31]. R.A. Khan, N.A. Siddiqui, S.Q.A.Naqvi and S. Ahmad. Reliability analysis of TLP tethers under impulsive loading. Department of Civil Engineering, Aligarh Muslim University, India (2006). Elsevier 73-83.
- [32]. Claes-Goran Gustafson , Andreas Echtermeyer. Long-term properties of carbon fibre composite tethers. Department of Engineering Design and Materials, Norwegian University of Science and Technology, N-7491, Norway (2007). Elsevier 1353–1362.
- [33]. F. Barranco-Cicilia , E.C.P. Lima, L.V.S. Sagrilo, Reliability-based design criterion for TLP tendons, Instituto Mexicano del Petroleo, Deep Waters Exploitation Department, Eje Central Lázaro Cárdenas 152, Gustavo A Madero 07730, D.F., Mexico (2008), *Applied Ocean Research*.
- [34]. Ivar Holand, ove T. Gudmestad and Erik Jersin. Design of Offshore concrete structures. Spon Press 11 New Fetter Lane, London (2000) 0-419-24320-8.
- [35]. R. Adrezin and H Benaroya. Non-Linear Stochastic dynamics of Tension Leg Platforms. Department of Mechanical Engineering, University of Hartford, West Hartford, USA (1999), *Journal of Sound and Vibration*, 27-65.
- [36]. S. Chandrasekaran¹, A. K. Jain and N. R. Chandak. Response Behavior of Triangular Tension Leg Platforms under Regular Waves Using Stokes Nonlinear

- Wave Theory. Dept. of Civil Engineering, Indian Institute of Technology, Hauz Khas, New Delhi-16, India (2007). *Journal of Waterway* 0733-950X
- [37]. Inyeol Palk and Jose Roesset. Use of Quadratic Transfer Function to Predict Response of Tension Leg Platform. Department of Civil Engineering Kyungwon University, Korea (1996). *Journal of Engineering Mechanics*.
- [38]. Anne M. Rustad, Carl M. Larsen, Asgeir J. Sørensen. FEM modeling and automatic control for collision prevention of top tensioned risers. Department of Marine Technology, Norwegian University of Science and Technology, Norway (2007). Elsevier.
- [39]. V. J. Kurian. Analytical and Experimental investigations on the behavior of Tension Leg Platform. Ocean Engineering Center Indian Institute of Technology, Madras, India (1993).
- [40]. Bhaskar Sengupta and Suhail Ahmad. Reliability assessment of tension leg platform tethers under nonlinearly coupled loading. Department of Applied Mechanics, IIT Delhi, Hauz Kaus, New Delhi 110016, India (1996). Elsevier 47-60.
- [41]. M.R. Tabeshpour, A.A. Golafshani, M.S. Seif. Second-order perturbation added mass fluctuation on vertical vibration of tension leg platforms. Department of Civil Engineering, Sharif University of Technology, Tehran, Iran (2007). *Marine Structures* 271–283.
- [42]. Joseph W. Tedesco, William G. McDougal and C. Allen Ross. *Structural Dynamics “Theory and Applications”*. Civil Engineering Department, Auburn University. Addison Wesley Longman 0-673-98052-9.
- [43]. Dia Aref Malaeb. Dynamic Analysis of Tension Leg Platform. Civil Engineering Department, Texas A&M University (1982). UMI 48106.
- [44]. Chuel-Hyun Kim, Chang-Ho Lee, Ja-Sam Goo. A dynamic response analysis of tension leg platforms including hydrodynamic interaction in regular waves. Department of Naval Architecture and Marine Systems Engineering, Pukyong National University, Korea (2007). *Ocean Engineering* 1680–1689.

- [45]. John M. Biggs. Introduction to Structural Dynamics. Civil Engineering Department, Massachusetts Institute of Technology (1964). McGraw-Hill 07-005255-7.
- [46]. Mario Paz and William Leigh. Structural Dynamic “Theory and Computation”, Fifth Edition (2004). Kluwer Academic Publishers 1-4020-7667-3.
- [47]. A. J. Kappos. Dynamic Loading and Design of Structures. Department of Civil Engineering, Aristotle University of Thessaloniki, Greece (2002). Spon press 0-203-30195-1.
- [48]. Xiaohong Chen. Studies on dynamic interaction between deep-water floating structures and their mooring/tendon systems. Texas A&M University (2002). UMI 48 106-1346.
- [49]. Hsien Hua Lee, Wang Pei-Wen. Dynamic behavior of tension-leg platform with net-cage system subjected to wave forces. Department of Marine Environment and Engineering, National Sun Yat-sen University, Kaoshiung Taiwan (1999). Ocean Engineering 179–200.
- [50]. Anil K. Chopra. Dynamics of structures “Theory and applications to earthquake Engineering”, Second Edition. University of California at Berkeley (2001). Prentice Hall 0-13-086973-2.
- [51]. Ray W. Clough, Joseph Penzien. Dynamics of structures, Second Edition. University of California, Berkeley (1993). McGraw-Hill 0-07-011394-7.
- [52]. Ben C. Gerwick. Construction of Marine and Offshore Structures, Second Edition. University of California, Berkeley (2000). CRC Press 0-8493-7485-5.
- [53]. Xing Jian Jinga, Zi Qiang Langa, Stephen A. Billingsa, Geoffrey R. Tomlinson. Frequency domain analysis for suppression of output vibration from periodic disturbance using nonlinearities. Department of Automatic Control and Systems Engineering, University of Sheffield, UK (2008). Elsevier 536–557.
- [54]. S. K. Chakrabarti. Handbook of offshore engineering, Volume II, Offshore structure analysis, Inc. Plainfield, Illinois, USA (2005). Elsevier 0-08-044569-1.

PUBLICATIONS

A: Published papers

1. **M.A. Gasim**, V.J. Kurian, Effects of Varying Hydrodynamic Coefficients on the Behaviour of TLP, NPC 2008, UTP, March 2008.
2. **M.A. Gasim**, V.J. Kurian, S.P. Narayanan, V. Kalaikumar, *Responses of Square and Triangular TLPs Subjected to Random Waves*, pp 133-140, ICCBT 2008, Kuala Lumpur, June 2008.
3. V.J. Kurian, **M.A. Gasim**, S.P. Narayanan, V. Kalaikumar, *Parametric Studies on the Behaviour of TLP under Regular and Random Waves*, pp 213-222, ICCBT 2008, Kuala Lumpur, June 2008.

B: Papers under preparation.

1. V.J. Kurian, **M.A. Gasim**, S.P. Narayanan, Parametric Studies of Triangular TLPs, Abstract submitted, *ENCON 08*, Kuching, December 2008.
2. V.J. Kurian, **M.A. Gasim**, S.P. Narayanan, Frequency and Time Domain Analyses for TLP Responses, Abstract submitted, *ICSTIE* 2008, Penang, December 2008.
3. V.J. Kurian, **M.A. Gasim**, S.P. Narayanan, Inclined Tether TLPs for Better Stability, Under preparation, Platform, *UTP Journal*, July – December 2008.
4. **M. A. Gasim**, V. J. Kurian, S. P. Narayanan, Dynamic behavior for various TLPs configurations, under preparation, *IJOPE*, October - December 2008.

APPENDICES

Relationships between KC and hydrodynamic coefficients [7]:

Drag coefficient vs. KC

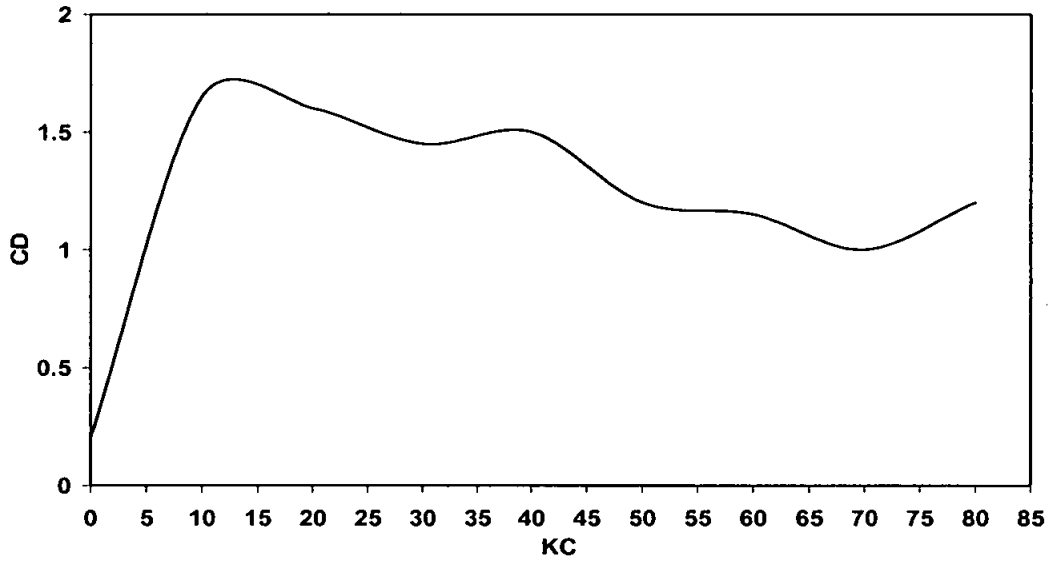


Figure A-1: KC and Drag coefficient relationship

Inertia coefficient vs. KC

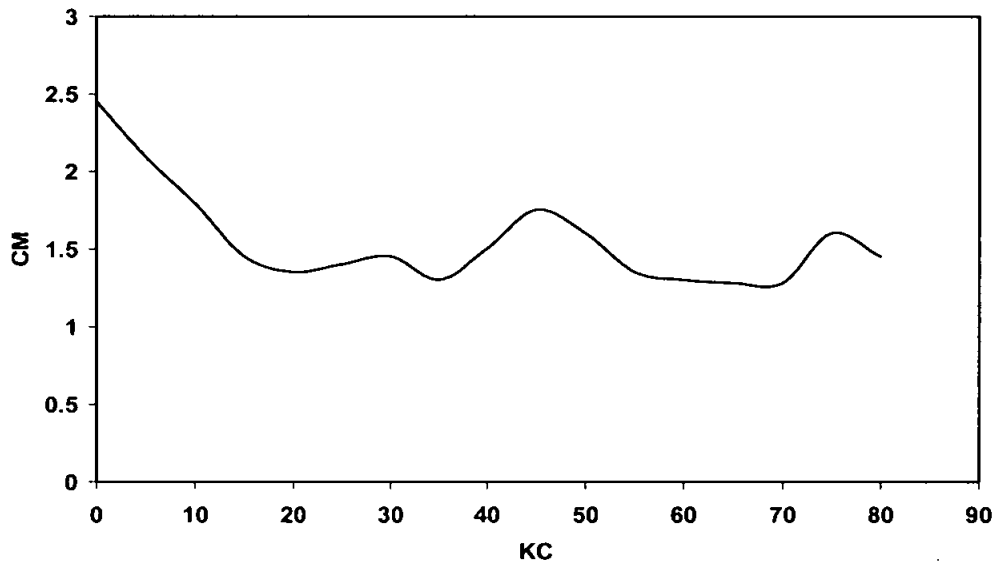


Figure A-2: KC and Inertia coefficient relationship

RAOs for various Tension Leg Platforms:

Table A-1:. RAOs for square TLP

Frequency (Hz)	Surge (m)	Heave (m)	Pitch (rad)	Tension (N)	Tension (kN)	RAO _s (m/m)	RAO _H (m/m)	RAO _P (rad/m)	RAO _T (kN/m)
0.05	0.03802	7.13E-05	5.57E-07	3738	3.738	2.183008	0.004092	3.2E-05	214.6261
0.06	0.4588	0.001413	1.09E-05	50650	50.65	1.453523	0.004477	3.46E-05	160.4642
0.07	1.0429	0.002544	2.22E-05	97460	97.46	1.153914	0.002815	2.46E-05	107.8344
0.08	1.0491	0.001601	4.87E-05	84700	84.7	0.806784	0.001231	3.74E-05	65.13637
0.09	0.6289	0.000133	7.82E-05	101020	101.02	0.447883	9.45E-05	5.57E-05	71.94323
0.1	0.08292	0.000956	0.000106	139870	139.87	0.062158	0.000716	7.93E-05	104.8483
0.11	0.4304	0.001178	0.000129	172050	172.05	0.360138	0.000985	0.000108	143.9633
0.12	0.8096	0.00112	0.000146	188460	188.46	0.776333	0.001074	0.00014	180.7161
0.13	1.0014	0.000447	0.000148	188750	188.75	1.111898	0.000496	0.000164	209.5773
0.14	0.9778	0.00027	0.000135	169100	169.1	1.260028	0.000348	0.000174	217.9082
0.15	0.7806	0.00014	0.000101	128060	128.06	1.165283	0.000209	0.000151	191.1685
0.16	0.4806	0.000215	6.22E-05	78470	78.47	0.827862	0.000371	0.000107	135.1692
0.17	0.16768	0.000152	1.98E-05	24470	24.47	0.331667	0.000301	3.91E-05	48.40104
0.18	0.09992	0.000126	1.66E-05	21990	21.99	0.225751	0.000286	3.75E-05	49.68249
0.19	0.2694	0.00013	4.02E-05	51720	51.72	0.691547	0.000333	0.000103	132.7647
0.2	0.31	8.36E-05	4.47E-05	57560	57.56	0.899445	0.000243	0.00013	167.0067
0.21	0.2403	8.64E-05	3.49E-05	44900	44.9	0.784138	0.000282	0.000114	146.5159
0.22	0.10445	0.00013	1.54E-05	19436	19.436	0.381523	0.000475	5.62E-05	70.99359
0.23	0.03854	0.000115	5.47E-06	7394	7.394	0.156879	0.000466	2.23E-05	30.09762
0.24	0.12864	0.000128	1.94E-05	25510	25.51	0.581104	0.00058	8.78E-05	115.2361
0.25	0.137717	0.000123	2.17E-05	27780	27.78	0.687685	0.000615	0.000108	138.7184

Table A-2. RAOs for triangular TLP

Frequency (Hz)	Surge (m)	Heave (m)	Pitch (rad)	Tension (N)	Tension (kN)	RAO _s (m/m)	RAO _H (m/m)	RAO _P (rad/m)	RAO _T (kN/m)
0.05	0.032912	0.000568	0.000237	109559.8	109.56	1.88972	0.032619	0.013579	6290.634
0.06	0.51904	0.009202	0.00369	1446656.4	1446.7	1.64437	0.029152	0.011689	4583.149
0.07	1.222	0.026181	0.00731	2928340.8	2928.3	1.352079	0.028968	0.008088	3240.056
0.08	1.44936	0.037692	0.005999	3350467.12	3350.5	1.114593	0.028986	0.004613	2576.591
0.09	1.18328	0.043254	0.004419	3604147.68	3604.1	0.842694	0.030804	0.003147	2566.759
0.1	0.7836	0.047682	0.002931	3501632.4	3501.6	0.587397	0.035743	0.002197	2624.868
0.11	0.42888	0.032535	0.001784	3365023.2	3365	0.358866	0.027224	0.001493	2815.692
0.12	0.22104	0.0252	0.00155	2840770.8	2840.8	0.211957	0.024165	0.001486	2724.043
0.13	0.34936	0.019251	0.001671	2053808.4	2053.8	0.38791	0.021375	0.001856	2280.433
0.14	0.42776	0.013456	0.001792	1020856.03	1020.9	0.551227	0.01734	0.002309	1315.511
0.15	0.39544	0.010409	0.00189	526198.4	526.2	0.590314	0.015538	0.002822	785.511
0.16	0.31176	0.006554	0.001151	205186.24	205.19	0.537025	0.011289	0.001983	353.4455
0.17	0.21888	0.005142	0.000604	226420.992	226.42	0.432939	0.01017	0.001194	447.855
0.18	0.16264	0.005365	0.000415	324094.624	324.09	0.367456	0.012121	0.000937	732.2341
0.19	0.16728	0.004963	0.000401	316808.8	316.81	0.429406	0.012739	0.00103	813.2451
0.2	0.245016	0.003127	0.000642	82759.488	82.759	0.710898	0.009072	0.001862	240.1214
0.21	0.2612	0.001405	0.000478	76252.064	76.252	0.852338	0.004584	0.001559	248.8228
0.22	0.24208	0.000626	0.000075	62801.312	62.801	0.884242	0.002287	0.000274	229.3934
0.23	0.16592	0.000478	3.89E-05	33253.248	33.253	0.675385	0.001945	0.000158	135.3589
0.24	0.049448	0.000328	2.74E-05	21605.2704	21.605	0.223371	0.001483	0.000124	97.59727
0.25	0.069088	0.000248	0.000284	9002.196	9.0022	0.344988	0.001237	0.001419	44.95212

Table A-3. RAOs for inclined tether TLP

Frequency (Hz)	Surge (m)	Heave (m)	Pitch (rad)	Tension (N)	Tension (kN)	RAO _s (m/m)	RAO _H (m/m)	RAO _P (rad/m)	RAO _T (kN/m)
0.05	0.021718	0.001	1.2E-05	39450	39.45	1.246984	0.057394	0.000705	2265.115
0.06	0.600533	0.005432	0.0008	905600	905.6	1.902549	0.01721	0.002541	2869.03
0.07	1	0.005467	0.00068	653500	653.5	1.106448	0.006049	0.000754	723.0635
0.08	0.9	0.00306	0.00031	403900	403.9	0.692122	0.002353	0.000238	310.609
0.09	0.3852	0.00137	9.3E-05	84120	84.12	0.274327	0.000976	6.62E-05	59.90759
0.1	0.04047	0.0011	0.00013	162360	162.36	0.030337	0.000825	9.92E-05	121.7071
0.11	0.1629	0.0018	0.00026	319800	319.8	0.136307	0.001506	0.000221	267.5935
0.12	0.2605	0.002049	0.00032	394800	394.8	0.249796	0.001964	0.000306	378.5776
0.13	0.2669	0.002295	0.00034	399500	399.5	0.296351	0.002548	0.000382	443.5822
0.14	0.2272	0.001796	0.00033	355800	355.8	0.292778	0.002314	0.00042	458.4964
0.15	0.16607	0.00135	0.00025	277900	277.9	0.24791	0.002015	0.000376	414.8502
0.16	0.095	0.000708	0.00014	171350	171.35	0.163643	0.001219	0.000249	295.1606
0.17	0.02959	0.000424	4.8E-05	57390	57.39	0.058528	0.000838	9.56E-05	113.516
0.18	0.017624	0.000533	3.4E-05	41753	41.753	0.039818	0.001204	7.64E-05	94.33347
0.19	0.04431	0.000615	8.5E-05	95690	95.69	0.113743	0.001578	0.000217	245.6353
0.2	0.0446	0.000674	9.9E-05	106400	106.4	0.129404	0.001956	0.000286	308.7129
0.21	0.03551	0.000552	7E-05	82750	82.75	0.115875	0.001802	0.000228	270.0266
0.22	0.015255	0.000317	3.5E-05	40056	40.056	0.055722	0.001156	0.000127	146.312
0.23	0.005516	0.000189	1.2E-05	45910	45.91	0.022453	0.00077	4.77E-05	186.8788
0.24	0.017723	0.00034	4.4E-05	44191	44.191	0.08006	0.001534	0.000198	199.6236
0.25	0.018719	0.000364	4.8E-05	50762	50.762	0.093473	0.001819	0.000239	253.4781